UNIVERSITÀ
DI SIENA
1240

Department of Medical Biotechnologies

PhD Programme in Genetics, Oncology and Clincal Medicine

Cicle XXXVIII

Coordinator: Prof. Ilaria Meloni

3D CT-based pre-operative planning and intraoperative navigation for glenoid component fixation in reverse shoulder arthroplasty: an in vivo impact study

Candidate
Elisa Troiano
University of Siena

Supervisor
Prof. Stefano Giannotti
University of Siena

Co-supervisor
Prof. Alessandra Renieri
University of Siena

ELISA TROIANO
02/03/2026 09:42:17

Academic year
2024/25

INDICE

ABSTRACT (IT)

La protesi inversa di spalla (RSA) rappresenta una soluzione chirurgica consolidata per il trattamento dell'artrosi gleno-omerale associata a lesione irreparabile della cuffia dei rotatori. Tuttavia, il successo dell'intervento dipende in larga misura dalla corretta gestione del bone loss glenoideo, elemento chiave per ottimizzare stabilità dell'impianto e gli outcome clinici e funzionali. In questo contesto, le tecnologie computer-assistite, quali la pianificazione tridimensionale su TC, la navigazione intraoperatoria e, più recentemente, i sistemi di intelligenza artificiale, hanno assunto un ruolo sempre più rilevante. Questo lavoro di dottorato integra quattro studi complementari per valutare il ruolo delle nuove tecnologie – pianificazione 3D TC, navigazione intraoperatoria e intelligenza artificiale – nel percorso decisionale e terapeutico della RSA.

Il primo studio (Capitolo 6) analizza l'affidabilità inter-osservatore della pianificazione preoperatoria di 81 casi valutati da 9 chirurghi esperti italiani. I risultati evidenziano un'elevata variabilità individuale (ICC singole 0.13-0.33, Fleiss' κ -0.093÷0.325) bilanciata da un consenso collettivo affidabile (ICC medie 0.58-0.82) e pattern decisionali razionali e difetto-specifici (Kruskal-Wallis $H=48.079$, $p<0.001$). Emergono protocolli condivisi, quali l'uso preferenziale di augment posteriori in caso di retroversione (55%) e superiori nei difetti di inclinazione (68%).

Il secondo studio (Capitolo 7) valuta la validità del software di intelligenza artificiale Predict® in una coorte di 10 pazienti. Le predizioni aggregate mostrano una buona accuratezza (MAE VAS 1.4 < MCID), a fronte di una limitata specificità individuale ($\rho=0.15–0.33$), suggerendo attuali limiti nella personalizzazione paziente-specifica.

Il terzo studio (Capitolo 8) quantifica l'impatto clinico della pianificazione e navigazione intraoperatoria in 158 casi consecutivi eseguiti da un singolo chirurgo, documentando un aumento dell'83% nell'utilizzo di baseplate augment, un incremento della lunghezza delle viti (+25%; 36.5 vs 29.1 mm) e una riduzione del numero medio di viti (-13%; 2.1 vs 2.4), con una conseguente standardizzazione dell'esecuzione chirurgica.

Infine, il quarto studio (Capitolo 9) confronta gli outcome clinici a medio termine (follow-up medio 42 mesi) tra 80 pazienti trattati con tecnica navigata e convenzionale, mostrando risultati

funzionali sovrapponibili (Constant 67±16; DASH 20±19; $p>0.05$) e confermando la non inferiorità della navigazione rispetto alla tecnica tradizionale.

Nel loro insieme, questi studi dimostrano che le tecnologie avanzate nella RSA non eliminano la variabilità decisionale, ma ne rendono visibili i meccanismi sottostanti, favorendo strategie correttive coerenti e riproducibili. La pianificazione 3D consente di identificare principi biomeccanici condivisi nella gestione della perdita ossea glenoidea, mentre la navigazione intraoperatoria contribuisce a standardizzare l'esecuzione chirurgica senza compromettere gli outcome clinici. I sistemi di intelligenza artificiale mostrano un potenziale promettente come supporto decisionale aggregato, sebbene siano necessari ulteriori sviluppi per una reale personalizzazione paziente-specifica. Nel complesso, queste tecnologie rappresentano strumenti complementari che, se correttamente integrati, possono migliorare la qualità del processo decisionale e costituire una base solida per l'evoluzione futura della RSA verso modelli più predittivi, standardizzati e personalizzati.

ABSTRACT (EN)

Reverse shoulder arthroplasty (RSA) is an established surgical option for the treatment of glenohumeral osteoarthritis associated with an irreparable rotator cuff tear. However, procedural success hinges largely on the appropriate management of glenoid bone loss, a key determinant for optimizing implant stability and clinical and functional outcomes. Within this framework, computer-assisted technologies—including 3D CT-based preoperative planning, intraoperative navigation, and, more recently, artificial intelligence (AI) systems—have assumed an increasingly prominent role. This doctoral thesis integrates four complementary studies to assess the role of these emerging technologies—3D CT planning, intraoperative navigation, and AI—across the decision-making and therapeutic pathway of RSA.

The first study (Chapter 6) investigates the interobserver reliability of preoperative planning in 81 cases assessed by nine experienced Italian surgeons. The findings demonstrate substantial individual variability (single-measure ICC 0.13–0.33; Fleiss' κ −0.093 to 0.325), balanced by reliable collective consensus (average-measure ICC 0.58–0.82) and rational, defect-specific decision patterns (Kruskal–Wallis $H = 48.079$, $p < 0.001$). Shared planning strategies emerge, including the preferential use of posterior augments in cases of retroversion (55%) and superior augments for inclination defects (68%).

The second study (Chapter 7) evaluates the validity of the AI-based Predict® software in a cohort of 10 patients. Aggregate predictions show good accuracy (MAE VAS 1.4 < MCID), but limited patient-specific performance ($\rho = 0.15$–0.33), suggesting current constraints in achieving true personalization.

The third study (Chapter 8) quantifies the clinical impact of preoperative planning and intraoperative navigation in 158 consecutive cases performed by a single surgeon, documenting an 83% increase in the use of augmented baseplates, the use of longer screws (+25%; 36.5 vs 29.1 mm), and a reduction in the mean number of screws (−13%; 2.1 vs 2.4), thereby supporting the standardization of surgical execution.

Finally, the fourth study (Chapter 9) compares mid-term clinical outcomes (mean follow-up 42 months) between 80 patients treated with navigated versus conventional techniques, showing

comparable functional results (Constant 67±16; DASH 20±19; $p > 0.05$) and confirming the non-inferiority of navigation relative to the traditional approach.

Taken together, these studies indicate that advanced technologies in RSA do not eliminate decision-making variability, but rather render its underlying mechanisms quantifiable, facilitating coherent and reproducible corrective strategies. Three-dimensional planning helps identify shared biomechanical principles in the management of glenoid bone loss, while intraoperative navigation contributes to standardizing surgical execution without compromising clinical outcomes. AI-based systems appear promising as an aggregate decision-support tool, although further development is required to achieve robust patient-specific accuracy. Overall, these technologies should be regarded as complementary tools that—when appropriately integrated—may improve the quality of the decision-making process and provide a solid foundation for the future evolution of RSA toward more predictive, standardized, and personalized care.

CHAPTER 1 – Clinical anatomy of the shoulder

The shoulder is a complex functional unit connecting the trunk to the upper limb. It comprises three bones—the clavicle, scapula, and humerus—integrated with a coordinated system of muscles and ligaments. This architecture facilitates extreme mobility, making it the most mobile joint in the human body. However, this flexibility also increases susceptibility to pathological changes that distort normal anatomy.

Modern prosthetic surgery increasingly integrates digital technologies to manage these anatomical alterations. Tools such as 3D preoperative planning and intraoperative navigation do not replace anatomical knowledge; rather, they enhance clinical interpretation. This chapter outlines essential anatomical landmarks. These concepts form the foundation for understanding how technological innovation overcomes the limits of "free-hand" surgery to personalize the treatment of complex deformities.

1.1 Bones

The glenohumeral joint is a ball-and-socket articulation. It consists of the shallow glenoid cavity and the larger humeral head[1]. Significant incongruence exists between these surfaces: the humeral head's articular area is roughly three times larger than the glenoid's. This disparity is the primary driver of the shoulder's extensive range of motion[2–4]. Key morphometric parameters include:

- Humeral cervico-diaphyseal angle: Approximately 135°.
- Humeral head retroversion: Roughly 25° relative to the epicondylar axis.

Following the Neer classification[5] the proximal humerus comprises four main fragments: the greater tuberosity, lesser tuberosity, humeral head, and humeral shaft. Anatomically, the anatomical neck separates the head from the tuberosities, while the surgical neck separates the tuberosities from the shaft. The bicipital groove—a dense cortical region—runs between the tuberosities and houses the long head of the biceps tendon. The glenoid, the scapula's articular surface, typically faces laterally with a slight superior tilt (5–6°) and anterior orientation (30° in the sagittal plane). Its pear-shaped configuration features a wider inferior base[6]. High morphologic variability is common, and degenerative disease further accentuates these

features. Consequently, accurate assessment of glenoid orientation and bone stock remains a critical surgical challenge.

1.2 Soft tissues and ligaments

The glenoid labrum encircles the glenoid, deepening the socket and expanding the articular surface. It also provides an attachment site for the capsuloligamentous structures[7]. The superior, middle, and inferior glenohumeral ligaments reinforce the joint capsule and contribute to shoulder stability across different positions of the arm in space[8]. The superior glenohumeral ligament originates from the superior glenoid tubercle and merges with the anterior rotator cuff fibers and the coracohumeral ligament to form the biceps pulley near the bicipital groove[8,9]. The middle glenohumeral ligament extends from the anterior labrum to the lesser tuberosity, whereas the inferior glenohumeral ligament spans from the inferior glenoid to the humerus[8,10,11].

1.3 Muscles

The muscles inserting on the scapular girdle play a direct role in glenohumeral motion.

1.3.1 Deltoid

The deltoid muscle is composed of three distinct portions—anterior, lateral, and posterior—separated by fibrous septa. Proximally, it originates from the lateral third of the clavicle (anterior fibers), the acromion (lateral fibers), and the spine of the scapula (posterior fibers). Distally, it inserts on the deltoid tuberosity of the lateral humerus[8]. It is innervated by branches of the axillary nerve, and its primary actions include humeral abduction, flexion, and extension[12,13].

1.3.2 Coracobrachialis and pectoralis major

The coracobrachialis and pectoralis major lie medial to the deltoid. The two heads of the pectoralis major originate from the clavicle and sternum and converge laterally to insert on the bicipital groove of the humerus[14]. The pectoralis major is innervated by the medial and lateral pectoral nerves and functions primarily as a powerful humeral adductor. The coracobrachialis and the short head of the biceps lie deep to both the pectoralis major and the deltoid[14]. They originate from the coracoid process and are innervated by the musculocutaneous nerve.

Together, they form the conjoined tendon, an important surgical landmark due to the fact that the brachial plexus and major vascular structures lie immediately medial and deep to it.

1.3.3 Rotator cuff

The rotator cuff lies deep to the deltoid and envelops the glenohumeral joint[12,14]. It consists of four fundamental muscles for glenohumeral motion and dynamic stabilization[14–16]. Its coordinated action depresses the humeral head, preventing superior migration and impingement during deltoid activation. The subscapularis originates from the anterior surface of the scapula and inserts on the lesser tuberosity of the humerus. It is innervated by the upper and lower subscapular nerves and acts as the primary internal rotator of the humerus[15]. The supraspinatus arises from the supraspinous fossa and inserts on the greater tuberosity[15–17]. It is innervated by the suprascapular nerve[17] and initiates shoulder abduction, enabling more efficient deltoid activation[18]. The infraspinatus and teres minor, innervated respectively by the suprascapular and axillary nerves, originate from the posterior aspect of the scapula just below the scapular spine and insert on the greater tuberosity posterior to the supraspinatus[15–17]. Their primary role is external rotation of the humerus at varying degrees of abduction.

1.4 Vascular and nervous structures

The subclavian and axillary arteries provide the primary blood supply to the shoulder [12,13]. The suprascapular artery follows the suprascapular nerve but passes over the transverse scapular ligament. Surgeons must protect this vessel during nerve decompression. The thoracoacromial artery follows the coracoacromial ligament and is at risk during surgical dissection. Deep to the deltoid, the anterior and posterior circumflex humeral arteries encircle the humerus[12,13]. The anterior branch, encountered during the deltopectoral approach, requires ligation before subscapularis mobilization.

Shoulder innervation derives from the brachial plexus. The axillary nerve innervates the deltoid and teres minor. It originates from the posterior cord, travels anterior to the subscapularis, and exits through the quadrangular space. Clinically, the nerve lies approximately 5–7 cm distal to the acromion[12,13,18]. The musculocutaneous nerve enters the coracobrachialis muscle 4–8 cm distal to the coracoid process. It then travels between the biceps and brachialis muscles. While rarely encountered in standard glenohumeral approaches, it remains at risk from excessive traction on the conjoined tendon[19]. The suprascapular nerve originates from the upper trunk. It

then passes deep to the trapezius and through the suprascapular notch[20]. The nerve segment skirting the superior glenoid margin before the infraspinous fossa is particularly vulnerable to surgical or traumatic injury[21].

1.5 Concept of anatomical layers

The surgical anatomy of the shoulder is organized into four distinct layers, a framework established by Cooper et al.[22]. This layered approach is fundamental for surgical dissection and the preservation of neurovascular structures.

- Layer 1 (Superficial): Comprises the large muscle bellies of the deltoid and pectoralis major.
- Layer 2 (Intermediate): Formed anteriorly by the clavipectoral fascia, the conjoined tendon, and the coracoacromial ligament. Posteriorly, this layer continues as the scapular fascia covering the infraspinatus and teres minor.
- Layer 3 (Deep): Consists of the subdeltoid bursa's deep surface and the rotator cuff muscles.
- Layer 4 (Articular): Represented by the glenohumeral joint capsule itself.

CHAPTER 2 – Reverse shoulder arthroplasty

A solid understanding of clinical anatomy is an essential prerequisite for shoulder surgery, and reverse shoulder arthroplasty represents one of the most significant paradigm shifts in the field. Originally developed to overcome the limitations of anatomic total shoulder arthroplasty in the setting of rotator cuff insufficiency, reverse shoulder arthroplasty (RSA) does more than replace articular surfaces: it fundamentally alters glenohumeral biomechanics, creating a functionally stable construct even in the absence of an intact rotator cuff. This biomechanical revolution, however, has introduced new critical variables—component positioning, the balance between implant medialization and lateralization, and the management of procedure-specific complications. These factors provide a strong rationale for integrating advanced technological tools to support both preoperative planning and intraoperative execution.

2.1 Historical evolution

Shoulder arthroplasty was initially regarded as a salvage procedure for severely damaged and functionally compromised joints[23]. Traditional prosthetic replacement relied on anatomic total shoulder arthroplasty (TSA), which aims to replicate native shoulder anatomy. The humeral component could be an unconstrained monoblock implant or, alternatively, a modular design available in various shapes and sizes. Modern anatomic prostheses often feature a short stem with predominantly metaphyseal fixation, onto which a humeral head of different diameters—and, when required, eccentric offset—can be mounted. On the glenoid side, several options were available:

- polyethylene components with a keel or peg, fixed into cancellous bone with[24] or without [25,26] bone cement;
- a metal-backed component secured with screws and fitted with a polyethylene liner[27];
- a trabecular tantalum glenoid implanted by press-fit fixation[28].

When only the humeral side was replaced, the procedure was defined as a hemiarthroplasty. From a biomechanical standpoint, satisfactory outcomes could be achieved if three conditions were met: (1) restoration of normal shoulder anatomy; (2) restoration of normal capsular tension; (3) re-establishment of muscular stabilizing and motor function. However, in patients with osteoarthritis associated with rotator cuff insufficiency, results were poor[29]. In these cases,

superior migration of the humeral head subjected the glenoid component to excessive shear forces, ultimately leading to loosening[30,31]. To mitigate this problem, surgeons progressively abandoned TSA in favour of hemiarthroplasty (HA), which provided pain relief but did not significantly improve function[32]. To address these limitations, Grammont introduced a new prosthetic concept: the reverse shoulder prosthesis. The first prototype, the "Trompette" (Medinov®) was developed in 1985 and the first successful clinical cases were published in 1987[33]. Subsequent improvements were made and in 1991 the first generation of modular prostheses – the Delta III (Medinov®) – was introduced[34]. This semiconstrained, modular implant consists of:

- a glenoid component (metaglene) with a central peg fixed to the native glenoid using cortical screws, onto which a glenosphere—approximately two-thirds of a sphere—is mounted;
- a humeral component composed of a proximal cup-shaped portion and a distal stem fixed to the humeral diaphysis with or without cement;
- a polyethylene insert placed on the humeral cup, articulating with the glenosphere[35].

The four fundamental principles of the Grammont reverse prosthesis were: (1) medialization and distalization of the center of rotation compared with the native shoulder, achieved by medializing the glenoid and humerus with a straight stem and a 155° neck–shaft angle to increase the deltoid lever arm during active elevation and abduction; (2) positioning the center of rotation at the bone–implant interface to reduce shearing forces on the glenoid implant; (3) distalization of the humerus to re-tension deltoid fibers; and (4) a semiconstrained configuration to provide a stable fulcrum[23,36,37]. Clinical and functional outcomes improved significantly with this design[38–40]. Nevertheless, the reverse prosthesis also introduced several drawbacks.

One of the main limitations of the original Grammont design arises from the pronounced medialization of the center of rotation. While this configuration enhances deltoid efficiency, it can excessively de-tension the remaining rotator cuff tendons. As a result, patients may experience restricted rotational range of motion or even postoperative instability[36,37]. In addition, the combination of a medialized center of rotation with a 155° humeral neck–shaft angle predisposes the implant to scapular notching, a well-recognized complication of early reverse prosthesis designs. Finally, the altered biomechanics inherent to this construct

significantly modify the shoulder's anatomical load distribution. These changes increase stress on the acromion and scapular spine, raising the risk of fatigue fractures in these regions[36].

2.2 Biomechanics and implant design

The limitations of the original Grammont implant stimulated the development of new prosthetic concepts that progressively incorporated greater degrees of lateralization[36]. On the glenoid side, lateralization can be achieved through several strategies. One approach involves modifying the scapular neck with a structural bone graft, as described in the BIO-RSA (Bony increased offset reverse shoulder arthroplasty) technique, which increases the offset while maintaining stable fixation[41]. Another method relies on metallic augments placed at the baseplate level to shift the center of rotation laterally without altering native bone anatomy[42]. A third option consists of modifying the glenosphere itself, using designs that inherently provide additional lateral offset[43]. Lateralization can also be introduced on the humeral side. This may be accomplished by adopting implants with a more varus neck–shaft angle (typically between 145° and 135°), which reduces the risk of scapular notching; by using curved or short stems that preserve bone stock; or by employing onlay humeral components that facilitate conversion from an anatomic prosthesis when necessary[36].

To better understand the biomechanical implications of different prosthetic designs, a classification system based on the offset of the glenosphere and the humeral implant was developed[44]. The glenoid component was classified as medialized (MG) when the center of rotation (CoR) was located within 5 mm of the native glenoid surface, and as lateralized (LG) when the CoR was positioned at a distance greater than 5 mm from the native glenoid. The humeral component was defined as medialized (MH) when the humeral offset relative to the stem axis was ≤ 15 mm, and as lateralized (LH) when the offset exceeded 15 mm. Based on the combination of glenoid and humeral configurations, four distinct implant constructs were identified: MG/MH, LG/MH, MG/LH, and LG/LH. Overall implant lateralization was quantified as the linear distance between the greater humeral tuberosity and the implant center of rotation, in accordance with the definition proposed by Cogan et al.[37].

2.2.1 MG/MH

Prosthetic designs characterized by medialization of both the glenoid and humeral components maximize the deltoid lever arm but simultaneously diminish the mechanical advantage of the

rotator cuff. This configuration generally preserves abduction and forward elevation, yet rotational movements tend to be compromised. These implants are also associated with a higher incidence of glenoid notching, and subscapularis repair becomes essential to ensure adequate stability. The original Grammont Delta III prosthesis is the archetype of this category, although systems such as the Delta Xtend (DePuy Synthes, Warsaw, IN, USA) and the SMR Reverse (Lima Corporate S.p.A., San Daniele del Friuli, Italy), share similar biomechanical principles[23,36,37].

2.2.2 LG/MH

Among the various configurations, the combination of a lateralized glenoid with a medialized humerus is considered the one that most closely reproduces native shoulder biomechanics[23]. These implants typically feature an inlay humeral component paired with a lateralized glenosphere. Although the center of rotation is shifted laterally compared with MG designs, it remains more medial than in the native shoulder[36,37]. Early generations of this design were associated with higher rates of glenoid loosening, but improvements in fixation methods and implant geometry have significantly reduced this complication. A notable technique that achieves glenoid lateralization without increasing the prosthetic offset is BIO-RSA, which uses a humeral head autograft to lengthen the scapular neck[41]. Despite its biomechanical advantages, it is less commonly used today compared with augmented baseplates or inherently lateralized glenoid components. Examples of implants in this category include the Encore Reverse Shoulder Prosthesis (DJO Surgical, Austin, TX, USA), Inhance (DePuy Synthes, Warsaw, IN, USA), Universe Reverse (Arthrex, Naples, FL, USA), and Tornier Perform (Stryker Corporation, Portage, MI, USA).

2.2.3 MG/LH

Designs that combine a medialized glenoid with a lateralized humeral component aim to merge the advantages of both philosophies. Medialization of the center of rotation enhances the deltoid lever arm, while humeral lateralization improves tensioning of the remaining rotator cuff tendons. Biomechanical studies have shown that MG/LH configurations provide greater deltoid wrapping and reduce cuff shortening compared with MG/MH and LG/MH designs[45]. In these implants, subscapularis repair is often not feasible, yet this does not appear to compromise stability to the same extent as in more medialized systems. MG/LH prostheses typically feature an onlay humeral component combined with a glenosphere offering less than

5 mm of lateral offset. Representative examples include the Equinoxe Reverse Shoulder System (Advita Ortho, Gainesville, FL, USA), Tornier Aequalis Ascend Flex (Stryker Corporation, Portage, MI, USA), and the Medacta Shoulder System (Medacta International SA, Castel San Pietro, Switzerland).

2.2.4 LG/LH

The combination of a lateralized glenoid and a lateralized humerus is used less frequently in clinical practice. Although this configuration can theoretically optimize both deltoid mechanics and cuff tensioning, the cumulative effect of lateralization and distalization increases the mechanical load transmitted to the acromion and scapular spine. As a result, these implants are associated with a higher risk of postoperative acromial stress fractures[37]. Systems such as the Reunion Ascend Flex (Stryker Corporation, Portage, MI, USA) fall into this category, though their use remains limited due to these biomechanical concerns.

2.3 Indications and contraindications

Although cuff tear arthropathy remains the most frequent indication for reverse shoulder arthroplasty, the progressive refinement of implant designs and surgical techniques has significantly broadened its clinical applications. RSA is now used for a wide spectrum of conditions associated with rotator cuff dysfunction or deficiency, including complex proximal humerus fractures, chronic or inveterate glenohumeral dislocations, pseudoparalytic shoulder due to massive irreparable cuff tears without arthritis, glenohumeral osteoarthritis with severe glenoid bone loss, nonunion or malunion of proximal humerus fractures, revision procedures, and even neoplastic disease involving the shoulder girdle[46,47]. Contraindications to RSA include active infection, axillary nerve injury resulting in impaired deltoid innervation, severe glenoid bone loss that compromises secure baseplate fixation, and global deltoid insufficiency[47]. Importantly, partial deltoid dysfunction is not considered an absolute contraindication, as even a partially functional deltoid may still provide meaningful postoperative improvement[48].

2.3.1 Glenohumeral osteoarthritis

Glenohumeral osteoarthritis (GHOA) is a chronic degenerative joint disorder characterized by progressive loss of articular cartilage accompanied by reactive bone formation at the joint margins and within the subchondral bone. Degenerative changes of the glenohumeral joint are

present in up to 17% of patients presenting with shoulder pain, a prevalence that has tripled over the past four decades[49,50]. Although less common than hip or knee osteoarthritis, symptomatic GHOA can be equally disabling because of the essential role of the upper limb in daily activities. Diagnosis is established when radiographic evidence of joint degeneration is accompanied by pain or functional limitation. Cartilage loss and subchondral sclerosis tend to be most pronounced in the superior two-thirds of the humeral head, corresponding to the region that articulates with the glenoid between 60° and 100° of abduction[51]. Osteophyte formation is the most frequent bone alteration, typically located at the anteroinferior humeral head and inferior glenoid, where capsular traction forces are the greatest[52]. These humeral osteophytes are often associated with enthesopathic changes at ligament insertion sites, particularly around the anatomical neck, tuberosities, and bicipital groove[53]. The pathogenesis of GHOA remains incompletely understood. Traditionally, osteoarthritis has been classified into primary (idiopathic) and secondary forms, the latter being more common in patients under 50 years of age but overall up to ten times less frequent than primary disease[54–56]. This dichotomy, however, is now considered overly simplistic, as osteoarthritis is increasingly viewed as a final common pathway shared by a heterogeneous group of disorders that ultimately lead to joint degeneration[57]. Disease progression is influenced by a complex interplay of genetic, behavioural, and environmental factors. Among the non-specific risk factors, advanced age is consistently associated with higher prevalence[55]. Genetic predisposition also plays a significant role, with several studies identifying heritable contributions to osteoarthritis susceptibility[58–60]. Obesity and metabolic syndrome further contribute to disease development, not only through increased mechanical loading but also via systemic inflammatory pathways mediated by adipokines[61,62]. Specific risk factors include occupational or athletic activities that impose high or abnormal mechanical loads on the shoulder, glenohumeral instability, acute traumatic injuries, prior surgical procedures, cuff tear arthropathy, chondrolysis, scapular morphology and glenoid dysplasia, septic arthritis, avascular necrosis of the humeral head, inflammatory arthritides, Charcot (neuropathic) arthropathy, and Milwaukee shoulder syndrome.

2.3.1.1 Mechanical joint overload

Occupational activities that involve heavy manual work, especially in the construction industry, as well as sports requiring repetitive overhead movements—such as baseball, tennis, and weightlifting—expose the glenohumeral joint to substantial mechanical stress. Over time, this repetitive overload accelerates cartilage wear and contributes to the development of

degenerative changes within the joint[51]. The cumulative effect of these forces is especially relevant in individuals who perform overhead tasks for many years, as the repeated cycles of loading and microtrauma gradually exceed the joint's capacity for repair.

2.3.1.2 Glenohumeral instability, prior surgery, and traumatic events

Degenerative changes consistent with glenohumeral osteoarthritis are frequently observed after shoulder dislocations or surgical procedures performed to address instability, with reported prevalence rates ranging from 56% to 68%. Interestingly, despite the high radiographic incidence, clinical symptoms are often mild or even absent[63–65]. These changes may arise from direct chondral injury sustained during the traumatic event, but altered joint biomechanics following instability or its surgical treatment may also play a significant role. The relative contribution of trauma versus surgery remains difficult to determine. Although it is not definitively established whether joint laxity alone predisposes to osteoarthritis, the association between dislocation and subsequent degenerative changes is well documented[63,64,66]. Numerous studies have shown that patients who experience even a single dislocation episode have a markedly increased risk—estimated at 10- to 20-fold—of developing radiographic arthropathy compared with individuals without a history of instability[67]. The risk is further amplified in cases of recurrent dislocations, in patients who sustain their first dislocation at an older age, and in those whose initial injury results from high-energy trauma[63–65] .

Fractures of the proximal humerus or glenoid also accelerate degenerative changes. These injuries can damage cartilage directly, but they may also alter joint biomechanics through malalignment, nonunion, or residual incongruence of the articular surface, all of which contribute to progressive cartilage degeneration[51].

2.3.1.3 Rotator cuff arthropathy

Massive rotator cuff tear arthropathy remains the leading indication for reverse shoulder arthroplasty[23,30,46,47]. This condition is characterized by a combination of glenohumeral joint degeneration and superior migration of the humeral head resulting from a massive, irreparable rotator cuff tear. The loss of cuff integrity disrupts the normal force couples that stabilize the joint, leading to pain, functional impairment, and progressive loss of range of motion. Radiographically, in addition to the classic features of osteoarthritis—joint space narrowing, osteophyte formation, subchondral sclerosis, and altered bony contours—several distinctive

findings may be observed. Superior migration of the humeral head produces erosion of the superior glenoid. As the deltoid becomes unopposed, the humeral head may eventually articulate directly with the undersurface of the acromion, leading to acetabularization of the coracoacromial arch in advanced stages[68]. Another hallmark is the loss of the humeral head's spherical contour, which becomes flattened and assumes a characteristic "mushroom-like" appearance[69]. The condition is more common in women and typically affects the dominant limb[51]. Hamada and colleagues[69–71] proposed a radiographic classification system that describes five progressive stages of arthropathy secondary to massive cuff tears. The grading is based on the degree of subacromial space narrowing—measured as the acromiohumeral interval (AHI)—and on changes in the glenohumeral joint space on standard anteroposterior radiographs. In the earliest stage (grade 1), the AHI is preserved; in grade 2, it is slightly reduced. Grade 3 is characterized by the onset of acromial acetabularization, while grade 4 includes narrowing of the glenohumeral joint space. Grade 5 represents the most advanced stage, marked by collapse of the humeral head. Walch later refined grade 4 by distinguishing two subtypes: grade 4A, in which glenohumeral osteoarthritis occurs without acromial acetabularization, and grade 4B, in which osteoarthritis is accompanied by acetabularization of the acromion. This modification helps better characterize the mechanical environment of the joint and may have implications for treatment planning (figure 2.1).

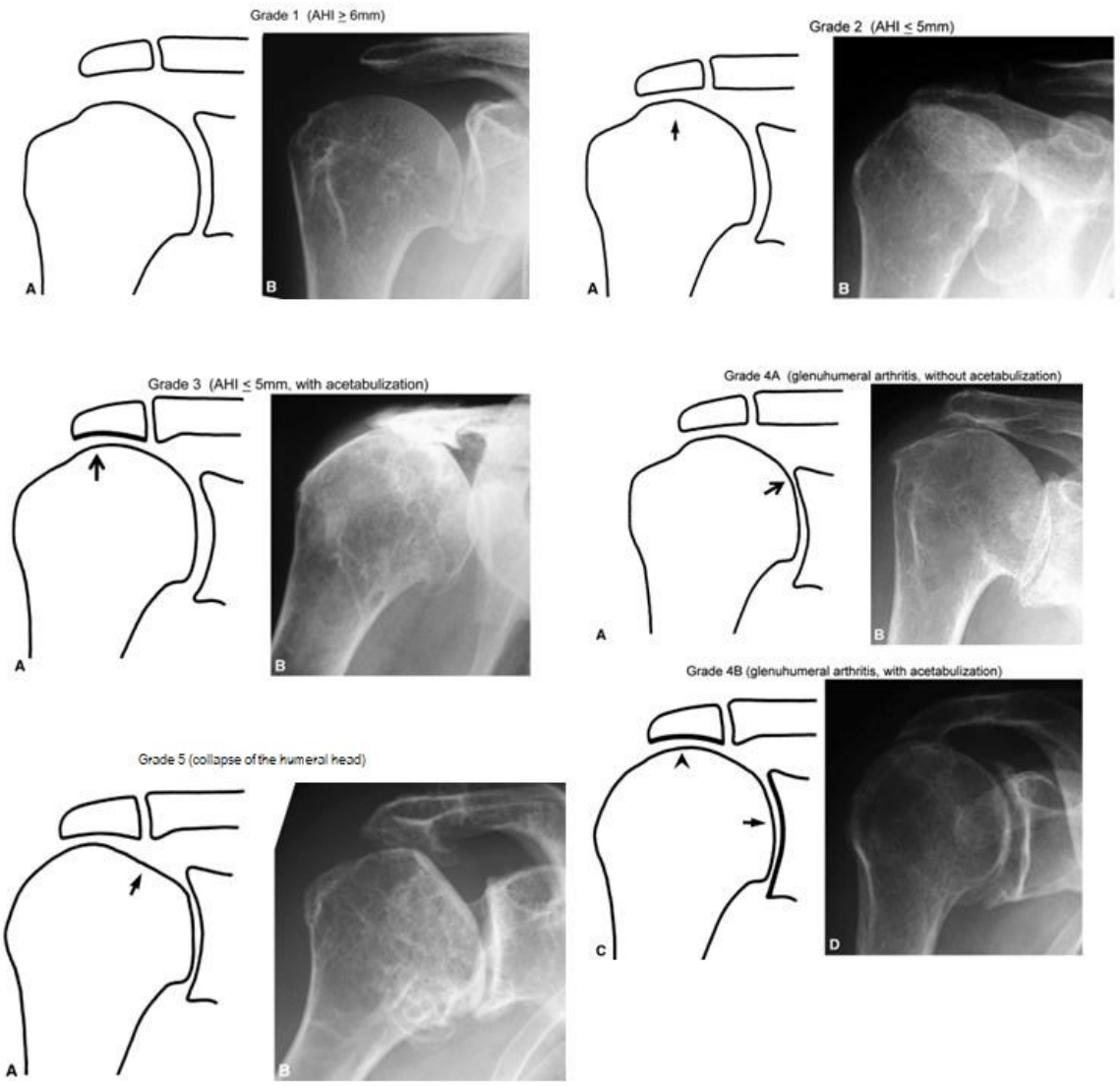

Figure 2.1. *Hamada radiographic classification for arthropathy secondary to massive cuff tears*[69]*.*

In these clinical scenarios, reverse shoulder arthroplasty provides pain relief by replacing the damaged bone structures and restores function by tensioning the deltoid, thereby compensating for the absence of a functional rotator cuff. Long-term follow-up studies have consistently demonstrated implant survivorship exceeding 90%, together with sustained clinical improvement over time[72].

2.3.1.4 Glenohumeral chondrolysis

Glenohumeral chondrolysis represents one of the most severe complications following arthroscopic procedures for shoulder instability. It is characterized by rapid and profound destruction of the articular cartilage, driven by chondrocyte necrosis and breakdown of the

extracellular matrix. This process ultimately culminates in advanced osteoarthritis. A well-documented cause is the postoperative intra-articular infusion of local anesthetics via pain pumps, which has been shown to exert direct chondrotoxic effects[73].

2.3.1.5 Scapular morphology and glenoid dysplasia

Several anatomical features of the scapula have been implicated in the development of glenohumeral osteoarthritis, especially lateral acromial extension and glenoid inclination. These parameters have recently been integrated into a single radiographic measure known as the critical shoulder angle (CSA). A smaller CSA—resulting from a shorter acromion or increased inferior glenoid inclination—augments the compressive forces generated by the deltoid and may predispose the joint to excessive loading and subsequent degenerative changes[74,75].

Glenoid dysplasia, a developmental abnormality of adolescence, is relatively common, with reported prevalence ranging from 14% to 40%[76]. It arises from aberrant development of the glenoid ossification centers, leading to hypoplasia of the inferior glenoid, increased retroversion, flattening of the articular surface, and varying degrees of humeral head subluxation. These structural abnormalities may accelerate degenerative changes and complicate arthroplasty planning[77–80]. Etiology may be idiopathic, familiar, or syndromic, and cases have been described in association with obstetric brachial plexus palsy[81,82].

2.3.1.6 Septic arthritis

Septic arthritis involves the glenohumeral joint in approximately 15% of cases[83] and constitutes an orthopedic emergency. Without prompt diagnosis and treatment, infection can rapidly destroy the joint. Hematogenous spread is the most common mode of infection, although direct inoculation during surgery or trauma, as well as contiguous spread from adjacent sites such as proximal humeral osteomyelitis, may also occur[84].

2.3.1.7 Humeral head avascular necrosis

Avascular necrosis (AVN) of the humeral head results from compromised blood supply, leading to subchondral bone death, collapse, and progressive disruption of joint anatomy and biomechanics. AVN accounts for roughly 5% of all cases of glenohumeral osteoarthritis[85,86] and represents the second most common site of osteonecrosis after the hip[87]. The condition may be idiopathic or secondary to trauma, corticosteroid use, alcoholism, or, more rarely, systemic

disorders such as Gaucher disease, sickle cell anaemia, decompression sickness, or hypercoagulable states[87–89].

2.3.1.8 Inflammatory arthritides

Inflammatory arthritides affecting the shoulder include rheumatoid arthritis, psoriatic arthritis, juvenile idiopathic arthritis, spondyloarthropathies, and systemic lupus erythematosus. Rheumatoid arthritis is the most prevalent and involves the shoulder in 65–90% of patients, with bilateral involvement in nearly half of the cases[90]. Clinical presentation is variable, often delaying diagnosis. In advanced disease, bilateral involvement with central glenoid erosion is typical, and pain is driven more by inflammatory synovitis than by structural degeneration[91]. Crystal arthropathies such as gout and pseudogout may also affect the shoulder, where deposition of urate or pyrophosphate crystals triggers inflammatory destruction of the joint[51].

2.3.1.9 Charcot arthropathy / neuropathic arthropathy

Neuropathic arthropathy, or Charcot shoulder, is a rare but devastating degenerative condition characterized by rapid destruction of bone and soft tissues. It is associated with profound impairment of tactile, proprioceptive, and thermal sensation. Cervical syringomyelia accounts for approximately 75% of cases, although diabetes, chronic alcoholism, and end-stage renal disease have also been implicated[92]. The underlying pathophysiology remains incompletely understood, but both neurovascular and neurotraumatic mechanisms have been proposed, with loss of nociception and proprioception playing a central role[93].

2.3.1.10 Milwaukee shoulder syndrome

Milwaukee shoulder syndrome is a destructive arthropathy that predominantly affects elderly women and is strongly associated with rotator cuff tears and deposition of hydroxyapatite crystals within and around the joint. Identification of these crystals using specific stains such as Alizarin Red is considered diagnostic. Although clinical symptoms may be relatively mild, radiographic progression can be striking, with deep erosions of the humeral head and adjacent soft tissues[94].

2.3.2 Irreparable rotator cuff tears

Massive rotator cuff tears (MRCT) represent extensive lesions of the rotator cuff that are technically challenging to repair and often carry an uncertain prognosis. A universally accepted

definition of MRCT has not yet been established, although the two most widely used classification systems rely either on the degree of tendon retraction or on the number of tendons involved. These tears are typically chronic and are characterized by myotendinous retraction, muscle atrophy, and fatty infiltration—features that significantly compromise the potential for successful repair[95]. When glenohumeral osteoarthritis is absent, but pain is substantial and conservative treatment has failed, surgical intervention may be considered. A variety of procedures are available, and no single technique has emerged as the gold standard. Treatment must therefore be individualized, considering patient age, functional demands, tissue quality, and expectations. Among the surgical options, tenotomy or tenodesis of the long head of the biceps has been shown to provide symptomatic relief in selected patients, particularly when pain is the predominant complaint[71,96]. Subacromial debridement may also improve symptoms by reducing mechanical irritation and inflammation, although it does not restore strength or function[97]. Tendon transfer procedures—most commonly involving the latissimus dorsi—represent another strategy for restoring shoulder function in the setting of irreparable posterosuperior cuff tears. These procedures aim to re-establish a functional force couple and have demonstrated encouraging mid- and long-term outcomes in appropriately selected patients[98–101]. Superior capsular reconstruction has emerged as a more recent alternative, designed to restore superior stability of the glenohumeral joint by reconstructing the superior capsule using autograft or allograft tissue. Both biomechanical and early clinical studies have shown promising results, although long-term data are still evolving[102,103]. Other approaches include functional or partial rotator cuff repair, which aims to restore the balance of force couples even when complete anatomical repair is not feasible[104,105]. Arthroscopic debridement alone may also be considered in low-demand patients, offering pain relief without attempting to restore tendon integrity[106–108]. Reverse shoulder arthroplasty has increasingly been proposed as an alternative for irreparable massive cuff tears, particularly when functional impairment is significant. RSA may provide more predictable improvements in pain and shoulder elevation compared with soft-tissue procedures, even in the absence of glenohumeral arthritis. Its ability to restore function derives from its unique biomechanics, which shift the burden of elevation from the deficient rotator cuff to the deltoid muscle[43,109,110].

2.3.3 Complex proximal humerus fractures

Proximal humerus fractures (PHFs) are the seventh most common fracture type in adults and account for approximately 4–10% of all fractures. Their epidemiology shows a clear bimodal

distribution: in older adults—particularly those with reduced bone quality—they typically occur after low-energy trauma, whereas high-energy mechanisms are more frequently responsible for injuries in patients younger than 55 years[111] . The incidence of PHFs continues to rise in the elderly population, especially among women, and these injuries now represent the third most common fragility fracture. This trend reflects both demographic changes and the increasing prevalence of osteoporosis[112–114]. Choosing the most appropriate treatment requires careful consideration of fracture morphology, patient comorbidities, and functional expectations. The overarching goal is to restore a painless and functional shoulder, regardless of whether management is operative or nonoperative. Treatment decisions must therefore be individualized, balancing the biological potential for healing with the patient's overall health status and activity level[112,115]. Because proximal humerus fractures in older adults are considered fragility fractures, their management—regardless of the chosen treatment—should be embedded within a multidisciplinary pathway aimed at reducing the risk of subsequent fractures. Coordinated care models, such as fracture liaison services, have demonstrated their value in optimizing bone health assessment, initiating appropriate pharmacologic therapy, and improving long-term outcomes in this population[116]. A wide range of surgical strategies is available for the treatment of PHFs. These include closed reduction with percutaneous fixation, as well as closed or open reduction combined with internal fixation using various plate designs[117]. Arthroplasty represents another important option, and its use has increased substantially over the past decade, particularly in older patients with complex fracture patterns[113]. Nonoperative treatment remains a reasonable approach for nondisplaced or minimally displaced fractures, and it is also commonly selected for displaced fractures in elderly individuals with low functional demands or significant comorbidities that preclude surgery. In these cases, conservative management may provide acceptable pain relief and functional recovery without exposing patients to the risks associated with operative intervention[113,114,118]. The optimal surgical strategy for complex proximal humerus fractures in older adults continues to be debated. Osteoporosis, metaphyseal comminution, and compromised bone quality often limit the ability to achieve stable fixation, making osteosynthesis less reliable in this population. For these reasons, many patients may benefit more from arthroplasty than from internal fixation. Both hemiarthroplasty and reverse shoulder arthroplasty have been used in this setting, with RSA increasingly chosen due to its more predictable functional outcomes and reduced dependence on tuberosity healing[112,119,120]. Historically, hemiarthroplasty (HA) was regarded as the preferred surgical option for complex

proximal humerus fractures. This approach was supported by early literature and long-standing clinical practice[121,122]. Over time, however, it became evident that outcomes after HA were highly variable and often difficult to reproduce. Functional recovery depended heavily on anatomic tuberosity healing and on the integrity of the rotator cuff—factors that are frequently compromised in elderly patients with osteoporotic bone. As a result, reverse shoulder arthroplasty has progressively emerged as a more reliable alternative. A growing body of evidence now demonstrates that RSA provides superior functional outcomes, lower reoperation rates, and greater predictability compared with HA in older adults with displaced three- and four-part fractures[122–126]. Case reports and clinical series have further supported its use even in bilateral fracture scenarios[127,128]. These findings have contributed to a paradigm shift in the management of complex fractures in the elderly, with RSA increasingly chosen over HA. The principal theoretical advantage of RSA lies in its biomechanics: unlike HA, it does not rely on tuberosity healing or rotator cuff function to restore elevation. Instead, RSA transfers the primary load of shoulder elevation to the deltoid muscle, allowing satisfactory functional recovery even when the tuberosities fail to heal. This characteristic makes RSA particularly appealing in osteoporotic bone, where tuberosity fixation is often tenuous [113,124,125,127–131]. Nevertheless, numerous studies have shown that when tuberosity repair is feasible and healing occurs, clinical outcomes after RSA are further improved. Patients with healed tuberosities demonstrate better rotation, strength, and overall function compared with those in whom the tuberosities do not unite [131–136]. These findings support the practice of reattaching the tuberosities whenever possible, even in the context of RSA, as doing so may optimize postoperative performance.

The timing of RSA for proximal humerus fractures has also been investigated. Comparative studies evaluating acute versus delayed RSA have not identified significant differences in long-term outcomes between the two groups. However, patients treated acutely tend to experience faster functional recovery in the early postoperative period, suggesting a potential advantage in proceeding with surgery without unnecessary delay[137,138].

2.3.4 Revision surgery

Since its introduction into clinical practice, reverse shoulder arthroplasty has progressively established itself as a versatile and reliable option in the revision setting. It is now widely used to address failures of previous shoulder implants—whether anatomic or reverse—as well as

failed rotator cuff repairs and unsuccessful open reduction and internal fixation (ORIF) of proximal humerus fractures[139]. Its ability to restore function in the presence of compromised soft tissues makes RSA particularly valuable in these complex scenarios.

2.3.4.1 Failure of previous prosthetic implant

The number of shoulder arthroplasties performed worldwide has increased steadily in recent years, a trend that is expected to continue. As a consequence, the burden of revision procedures is also expected to increase accordingly[140,141]. The underlying causes of implant failure vary depending on the type of primary prosthesis. In anatomic total shoulder arthroplasty, the most common reasons for failure are rotator cuff insufficiency and loosening of the glenoid component[142]. Hemiarthroplasty, on the other hand, typically fails due to progressive rotator cuff degeneration or erosion of the native glenoid surface[143]. Primary reverse implants may fail because of instability, infection, or component loosening[144,145]. Across all these scenarios, RSA has emerged as an effective salvage procedure. Numerous studies have demonstrated that conversion to RSA improves pain, functional outcomes, and range of motion regardless of the type of failed primary implant[142,146,147]. This versatility reflects the biomechanical advantages of RSA, which relies on the deltoid rather than the rotator cuff to restore elevation. Early reports suggested that revision RSA yielded inferior functional outcomes compared with primary RSA[142,148–150]. However, more recent studies have questioned this assumption, showing that modern implants and refined surgical techniques can achieve results comparable to those of primary procedures, even in younger patients[151,152]. Despite these encouraging findings, revision RSA remains a demanding procedure and is consistently associated with higher complication rates than primary arthroplasty[150,152]. Factors such as bone loss, soft-tissue deficiency, and altered anatomy contribute to the increased technical complexity and risk profile. Nevertheless, when carefully planned and executed, revision RSA offers a reliable solution for restoring function and alleviating pain in patients with failed shoulder arthroplasty.

2.3.4.2 Failure of rotator cuff repair

A wide range of therapeutic options is available for the management of failed rotator cuff repair, and the choice among them depends on both surgeon-related factors—such as technical expertise and preferred surgical philosophy—and patient-related variables, including age, functional demands, tissue quality, and comorbidities. Revision rotator cuff repair may be attempted in selected cases, with or without the use of allograft augmentation. Other strategies

include tendon transfers, superior capsular reconstruction, subacromial balloon spacers, and tuberosity reshaping. Reverse shoulder arthroplasty represents an additional option, particularly when soft-tissue quality is poor or when previous attempts at repair have failed to restore function[139]. Each of these approaches carries distinct indications and limitations, and treatment must be tailored to the individual patient.

2.3.4.3 Failure of internal fixation for proximal humerus fractures

Reverse shoulder arthroplasty can also serve as an effective salvage procedure following failed open reduction and internal fixation (ORIF) of proximal humerus fractures[139,153,154]. Several studies have demonstrated that RSA performed after unsuccessful ORIF can lead to meaningful improvements in pain, range of motion, and overall shoulder function[155]. Despite these advantages, outcomes after revision RSA are generally inferior to those achieved with primary RSA. Patients undergoing revision procedures tend to experience lower functional scores and higher complication rates, reflecting the technical challenges associated with altered anatomy, bone loss, and compromised soft tissues[156]. For this reason, careful patient selection and accurate preoperative counselling are essential to ensure that expectations align with achievable results.

2.3.5 Tumours

In patients requiring extensive resection of the proximal humerus and rotator cuff due to malignant tumours, several reconstructive strategies have been described, including massive allografts, arthrodesis, and various types of prosthetic reconstruction. Reverse shoulder arthroplasty has become an important option in this context, offering the potential for functional restoration even in the absence of a functional rotator cuff. However, a fundamental prerequisite for RSA implantation in oncologic reconstruction is the integrity of the axillary nerve and the deltoid muscle, without which the prosthesis cannot function properly[47].

2.4 Complications

Reported complication rates after reverse shoulder arthroplasty vary widely, ranging from 19% to 68%. This variability reflects differences in surgeon experience, implant design, and patient populations across studies. Notably, complication rates are consistently higher in the revision setting than in primary procedures[157,158]. The spectrum of complications associated with RSA is

broad and includes acromial and scapular spine fractures, hematoma formation, infection, instability, mechanical failure of the baseplate, neurologic injury, periprosthetic fractures, and scapular notching[157,159]. Importantly, the relative frequency of these complications has evolved over time. Whereas instability was historically the most common complication, periprosthetic infection has become increasingly prevalent over the last decade—a trend likely attributable to improvements in implant design and surgical technique[160,161].

2.4.1 Instability

Postoperative instability remains one of the most challenging complications of RSA, with reported rates ranging from 2% to 31%[160,162]. Instability tends to occur early, most frequently within the first six months after surgery, and approximately half of all dislocations present within the first three months[163]. A number of patient-related risk factors have been identified, including obesity, male sex, prior shoulder surgery, and subscapularis insufficiency[164,165]. Intraoperative factors also play a critical role. Inadequate tensioning of the deltoid and surrounding soft tissues is a well-recognized contributor to postoperative instability [32,162,166].

Implant malpositioning—particularly errors in humeral version—can predispose to mechanical impingement and subsequent dislocation[167]. Subscapularis insufficiency further increases the risk of instability, especially in designs that rely on its contribution to anterior stability[168]. Surgical approach also influences stability. Several studies have reported a higher risk of dislocation when RSA is performed through a deltopectoral approach compared with an anterosuperior approach, likely due to differences in soft-tissue handling and deltoid tensioning[32,150,160,169]. Prosthetic design is another key determinant. Implants with a 155° neck–shaft angle exhibit greater intrinsic instability than those with a more varus configuration, reflecting differences in deltoid wrapping and joint constraint[170]. When instability occurs within the first three months after surgery, it is most often attributable to technical error during the surgical procedure—typically inadequate soft-tissue tensioning or suboptimal implant positioning[171]. Early recognition and appropriate management are therefore essential to prevent recurrent dislocation and preserve implant function.

2.4.2 Infection

Postoperative infection is a well-recognized complication of reverse shoulder arthroplasty, with reported rates ranging from 1% to 15%. These values are consistently higher than those

observed after anatomic shoulder arthroplasty, reflecting both the greater soft-tissue dissection required for RSA and the more complex patient populations in which it is often performed[171,172]. Infection rates are even higher in the revision setting, where compromised soft tissues, prior implants, and altered anatomy further increase susceptibility[160]. Although advances in perioperative protocols have improved prevention and early detection, infection remains one of the most challenging complications to manage following RSA.

2.4.3 Scapular notching

Scapular notching is a complication unique to reverse shoulder arthroplasty and is reported with an incidence ranging from 50% to 96%. It typically develops within the first six months after surgery and, in many cases, remains radiographically stable thereafter[38,173]. Nonetheless, some long-term studies have documented progressive notching over time, suggesting that its natural history may vary depending on implant design and patient-specific factors[171]. Mechanically, scapular notching results from repetitive impingement between the polyethylene humeral insert and the inferior scapular neck during adduction[38]. Several factors may contribute to its development, including loosening of the glenoid baseplate, suboptimal component positioning, and intrinsic characteristics of the prosthetic design[174,175]. It is clinically relevant because it may compromise glenoid fixation, reduce range of motion, and negatively affect long-term outcomes. Radiographically, scapular notching is classified according to the Nerot–Sirveaux system, which distinguishes four grades based on the extent of bone loss on a true anteroposterior shoulder radiograph[176]: grade 1 indicates erosion limited to the inferior pillar of the scapular neck; grade 2 extends to the level of the inferior screw; grade 3 progresses beyond the screw; and grade 4 reaches beneath the baseplate (figure 2.2).

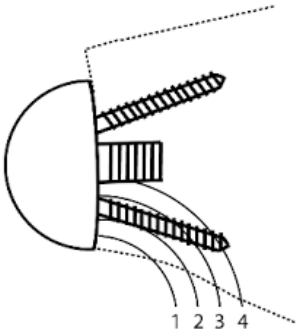

Figure 2.2. *Nerot-Sirveaux classification for scapular notching*[177]*.*

The first two grades are generally attributed to mechanical erosion, whereas grades 3 and 4 reflect a biological response to polyethylene wear debris. Multiple strategies have been

proposed to reduce the risk of notching. These include the use of eccentric glenospheres with inferior offset, inferior placement of the baseplate to maximize clearance, and the adoption of glenoid components with increased lateral offset—achieved through bone grafting or metal augmentation. Humeral components with a more varus neck–shaft angle may also reduce impingement by improving deltoid wrapping and joint mechanics[46,72,178]. Collectively, these design and technical refinements have contributed to a gradual reduction in the incidence and severity of scapular notching in modern RSA.

2.4.4 Neurologic injury

Neurologic injury is a recognized complication of shoulder arthroplasty—both anatomic and reverse—with a reported incidence between 1% and 4 %[179,180]. These injuries most commonly involve traction to the brachial plexus during surgical manipulation, particularly during exposure and reduction maneuvers[180]. Evidence suggests that neurologic complications occur more frequently after reverse shoulder arthroplasty than after anatomic total shoulder arthroplasty. This increased risk is likely related to the greater degree of humeral distalization required in RSA and the more demanding glenoid exposure, both of which may place additional tension on neural structures[181]. Although many nerve injuries are transient, they can significantly affect early postoperative recovery and functional outcomes.

2.4.5 Scapular fractures

Scapular fractures represent another complication specific to reverse shoulder arthroplasty, with an incidence ranging from 0.8% to 7.2%[164]. Several mechanisms have been implicated. Excessive deltoid tensioning can increase stress on the acromion and scapular spine[172], while improper placement of the superior baseplate screw—particularly when directed toward the base of the scapular spine—may predispose to fracture[182]. Additionally, osteoporotic bone may be unable to tolerate the altered load distribution imposed by the prosthetic components, further increasing susceptibility[183]. Clinically, acromial insufficiency fractures or displacement of an *os acromiale* typically present with pain and reduced shoulder motion [171,172,184]. Scapular spine fractures, in particular, may lead to significant functional impairment and often require open reduction and internal fixation to restore stability[169]. Postoperative scapular fractures are associated with poorer clinical outcomes and a higher likelihood of revision surgery, underscoring the importance of careful surgical technique, appropriate implant positioning, and attention to bone quality in minimizing this complication[164].

CHAPTER 3 – Emerging technologies in shoulder arthroplasty

Reverse shoulder arthroplasty has transformed the management of shoulder pathology over the past decades, enabling the treatment of conditions that were once considered irreparable—such as cuff tear arthropathy, severe glenoid deformities, and complex revision cases. Despite these advances, the long-term success of RSA remains closely tied to the management of the glenoid side, which continues to represent the principal limiting factor for implant stability, survivorship, and functional outcomes[32,185,186]. The substantial anatomical variability of the glenoid, combined with the frequent presence of bone loss and abnormalities in three-dimensional orientation, has exposed the limitations of traditional approaches based on two-dimensional imaging, intraoperative anatomical landmarks, and surgeon experience alone. These conventional methods may be insufficient in complex cases, where even small deviations in implant positioning can significantly affect biomechanics and fixation quality[6,187,188].

In response to these challenges, recent years have seen the emergence and rapid dissemination of new technologies designed to enhance understanding of patient-specific anatomy, improve the accuracy of implant placement, and increase the predictability of clinical outcomes[30,189].

These innovations can be broadly grouped into two categories:

- **Computer-assisted technologies**, which rely on deterministic models and structured decision-support systems for surgical planning and execution. This group includes CT-based 3D planning, patient-specific instrumentation (PSI), and intraoperative navigation.
- **Artificial intelligence (AI)–based systems**, which introduce a data-driven paradigm capable of identifying patterns, predicting outcomes, and supporting clinical decision-making through the analysis of large datasets.

This chapter provides a systematic overview of these emerging technologies, examining their rationale, potential advantages, limitations, and future perspectives in the context of shoulder arthroplasty.

3.1 Computer-assisted technologies in reverse shoulder arthroplasty

Over the past two decades, computer-assisted orthopaedic surgery (CAOS) has progressively reshaped preoperative planning and intraoperative execution in arthroplasty. These technologies offer improved accuracy, reproducibility, and customization compared with conventional techniques. Initially developed for neurosurgery and spine surgery, CAOS gained widespread adoption in hip and knee arthroplasty[190] before expanding into shoulder surgery, where the complex anatomy and biomechanics make digital support particularly valuable[191,192]. In its broadest sense, CAOS encompasses a heterogeneous group of systems that differ in their degree of autonomy and in the way they interact with the patient during surgery. Passive systems do not perform surgical actions themselves; instead, they assist the surgeon by enhancing preoperative planning, enabling virtual simulation, and providing intraoperative guidance. Semi-active systems introduce a limited degree of mechanical assistance, although the surgeon remains in full control of the operative steps. Active systems represent the most advanced category, as they are capable of autonomously executing preprogrammed surgical actions, thereby reducing—or even eliminating—the need for manual intervention during specific phases of the procedure. Despite these differences, all CAOS platforms share several fundamental principles. Each system relies on the definition of a "therapeutic object," which corresponds to the patient's anatomy; a "virtual object," which represents the surgical plan; and a "navigator," the hardware–software interface that links the real and virtual environments. This connection is established through a sequence of phases—set-up, registration, planning, and execution—that allow the surgeon to translate a virtual plan into a precise intraoperative action[191,192].

It is important to distinguish these technologies from artificial intelligence. Computer-assisted surgery relies on static, rule-based models that generate outputs directly from predefined geometric relationships. In contrast, AI and machine learning systems incorporate automated learning processes, enabling them to infer patterns from data and generate predictions based on prior examples. Without such learning capabilities, CAOS cannot be considered a form of artificial intelligence in the strict sense[190,191].

In shoulder arthroplasty, CAOS should therefore be viewed as a decision-support and execution-support tool. Its primary goals are to enhance understanding of patient-specific anatomy, improve the precision of implant placement, and optimize glenoid fixation—while

preserving the surgeon's central role in clinical decision-making. Within this domain fall CT-based 3D preoperative planning, patient-specific instrumentation, intraoperative navigation, and, in selected applications, augmented reality.

3.1.1 Preoperative planning

A thorough assessment of glenoid morphology—particularly glenoid version and inclination—is fundamental for selecting an appropriate therapeutic strategy. Osseous remodelling is present in approximately 40% of patients with cuff tear arthropathy[193,194], and in these cases posterosuperior glenoid erosion is frequently observed as a consequence of progressive superior migration of the humeral head[193,195]. Favard proposed a classification system describing glenoid erosion patterns based on the location and extent of bone loss on the superior and inferior aspects of the glenoid[38]. Historically, glenoid morphology was evaluated using plain radiographs and two-dimensional computed tomography (CT) scans. One of the earliest standardized methods was described by Friedman, who assessed glenoid version on an axial CT slice just inferior to the coracoid process. The technique involves drawing a line through the centre of the glenoid and the medial border of the scapula (the Friedman line), a perpendicular neutral version line, and a line connecting the anterior and posterior glenoid rims. The angle between the Friedman line and the glenoid rim line represents the glenoid version. Retroversion or anteversion is determined by the position of the glenoid rims relative to the neutral version line: a posterior rim located medially indicates retroversion (negative angle), whereas a medially positioned anterior rim indicates anteversion (positive angle). Normal retroversion typically ranges from 0° to 8°[196]. Although widely adopted, the Friedman method has proven insufficient for a comprehensive evaluation of scapular morphology. Over time, three-dimensional reconstructions of tomographic images have been introduced, enabling a more accurate assessment of scapular and glenoid morphology, thereby overcoming the inherent limitations of two-dimensional imaging. The introduction of three-dimensional CT reconstructions has significantly improved the accuracy of glenoid and scapular assessment, overcoming many limitations of two-dimensional imaging. Three-dimensional CT has become a key tool in the evaluation of glenohumeral osteoarthritis[189,197–199], allowing detailed characterization of glenoid deformities and improving the reliability of morphologic classifications such as the Walch system[200]. This enhanced precision aids in identifying complex variants, including B3 and D types[201]. Three-dimensional reconstructions also correct distortions caused by patient positioning within the scanner, enabling more reliable

measurements of retroversion and humeral head subluxation[201]. By providing a detailed understanding of glenoid geometry—including version, inclination, and the degree of wear—3D CT plays a central role in anticipating technical challenges and optimizing surgical planning.

The overarching goal of preoperative planning is to correct posterior glenoid bone loss and pathological retroversion to restore the native joint line. Modern CT-based 3D planning software allows surgeons to evaluate multiplanar deformities and to select the most appropriate implant type, baseplate design, and optimal positioning on the native glenoid. These platforms also support planning of deformity correction through reaming, bone grafting, or the use of augmented baseplates, while minimizing the risk of excessive medialization of the glenoid component[189,202–205]. Augmented baseplates were specifically developed to address glenoid bone loss without relying solely on eccentric reaming or bone grafting, thereby preserving bone stock and improving the biomechanical environment for fixation[198].

3.1.2 Patient-specific instrumentation (PSI)

Patient-specific instrumentation was originally developed for total knee arthroplasty and has subsequently been successfully adapted to shoulder arthroplasty. PSI relies on CT-based preoperative planning to design customized surgical guides that match the patient's anatomy, thereby assisting the surgeon in achieving accurate glenoid component placement. By translating the virtual plan into a physical guide, PSI has the potential to improve the precision of implant positioning during surgery. Recent advances in 3D planning platforms and additive manufacturing have enabled the production of sterile PSI guides and three-dimensional glenoid models for intraoperative use. These developments have facilitated the integration of PSI into routine clinical practice, improving the accuracy of measurements and execution compared with conventional instrumentation[206]. Emerging evidence suggests that PSI may also reduce variability between experienced and less-experienced surgeons, potentially contributing to more standardized outcomes in reverse shoulder arthroplasty[207].

3.1.3 Intraoperative navigation

Although RSA provides excellent clinical outcomes, complication rates remain substantial, ranging from 19% to 68%[208]. Among these complications, failure of the glenoid component is particularly significant. Inaccurate baseplate positioning is strongly associated with postoperative instability, increased mechanical stress at the bone–implant interface, early

loosening, and inferior functional outcomes[209]. The stability of the glenoid baseplate depends primarily on fixation of the central post or peg, with the number and configuration of screws varying according to implant design. The introduction of locking screws has markedly reduced component failure rates, but optimal screw placement remains essential to maximize screw length, achieve cortical purchase, and secure fixation in regions of optimal bone density[23]. Consequently, precise positioning and stable fixation of the baseplate are critical determinants of implant longevity and postoperative function[198,210]. Achieving accurate alignment and fixation can be technically demanding due to limited exposure, anatomical variability, and deformities caused by chronic pathology. Intraoperative navigation addresses these challenges by enabling real-time reproduction of the preoperative plan. Navigation systems guide the surgeon during glenoid preparation and implant placement, allowing adjustments in baseplate inclination, version, medialization, and screw trajectories. This technology enhances the precision of glenoid component positioning and helps maximize screw length while preserving bone stock[198,199,211,212]. Real-time guidance is particularly valuable for the inferior screw, because it lies close to the load-transfer region of the humeral component that contributes to baseplate stability[175,198].

3.1.4 Augmented reality

The concept of the metaverse encompasses a virtual environment that merges physical and digital realities, enabling interaction through technologies such as augmented reality, virtual reality, and artificial intelligence. In augmented reality, digital information is superimposed onto the physical world, enhancing the user's perception and interaction with the environment[213]. Augmented reality has been applied across multiple surgical specialties with the goal of improving intraoperative performance. In shoulder arthroplasty, AR—often integrated with navigation systems—has been proposed as a tool to enhance the accuracy of glenoid component placement and potentially improve functional outcomes. By generating a three-dimensional virtual model of the patient's glenoid that can be visualized preoperatively and intraoperatively through smart glasses, AR allows surgeons to access relevant anatomical and planning information directly within their field of view. Additional data can be incorporated into the model as needed, provided it has been uploaded to the device beforehand[214]. Early studies indicate that AR may improve the accuracy of glenoid positioning, particularly with respect to inclination[215].

In its basic form, augmented reality functions as an extension of computer-assisted surgery. However, more advanced systems incorporate computer-vision algorithms and automated segmentation, which may rely on artificial intelligence techniques. These hybrid platforms represent a promising evolution toward increasingly intelligent and adaptive surgical guidance systems[214].

3.2 Artificial intelligence and machine learning

Artificial intelligence (AI) is broadly defined as the branch of computer science dedicated to developing systems capable of performing tasks that typically require human intelligence, including reasoning, complex pattern recognition, and decision-making[216,217]. Within this broader ecosystem, machine learning (ML) represents the most clinically relevant subset. ML focuses on algorithms that learn autonomously from data, progressively improving their performance without being explicitly programmed for a specific target variable[218–221]. Whereas traditional computing relies on deterministic "if–then" logic, ML adopts an inductive, data-driven paradigm. By processing large datasets (Big Data)—which in shoulder arthroplasty may include demographic information, three-dimensional radiographic measurements, and longitudinal clinical outcomes—ML systems can identify nonlinear relationships that conventional statistical approaches may fail to detect[222,223]. In orthopaedics, this shift is redefining technological support by moving from purely technical assistance toward true personalization of treatment. One of the earliest and most consolidated applications concerns the optimization of preoperative imaging. Deep learning algorithms—an advanced ML approach based on neural networks—can perform automated segmentation of CT scans, producing accurate 3D reconstructions and rapidly identifying anatomical landmarks while reducing human error and planning time[224,225]. However, the most transformative contribution of AI lies in its ability to support predictive and precision surgery. ML models trained on large clinical datasets can estimate patient-specific postoperative outcomes, including expected improvements in range of motion or functional scores such as ASES and Constant [217,226–229].

3.2.1 Systems for predicting clinical outcomes

One of the most prominent ML-based decision-support tools in shoulder arthroplasty is Predict+ (Advita Ortho, Gainesville, Florida, USA). According to published descriptions, Predict+ is a machine-learning predictive analytics platform trained on a dataset of more than 6,500

patients. Using a streamlined set of 19 preoperative variables, it generates personalized forecasts of postoperative outcomes at multiple time points, ranging from 3 months to 7 years. Its primary purpose is to support shared decision-making and to help align patient expectations by providing individualized predictions for pain and functional recovery after anatomic or reverse total shoulder arthroplasty. The system requires input of 19 variables, including demographic characteristics, diagnosis and comorbidities, patient-reported pain and function, and range-of-motion measurements across multiple planes (e.g., forward elevation, abduction, external rotation, internal rotation). Optionally, widely used clinical scores such as the ASES[230] and Constant–Murley scores may also be incorporated[231]. Despite their potential, predictive models are highly dependent on the quality, completeness, and representativeness of the datasets on which they are trained. Unbalanced datasets or under-representation of specific patient groups can introduce systematic bias and limit the generalizability of predictions across different clinical settings[222]. Even when trained on large real-world cohorts, the geographic origin of the data and the healthcare practices from which they derive may introduce biases that limit applicability to populations with different demographic, socioeconomic, or clinical characteristics. Another important limitation is the “black box” phenomenon, characteristic of many advanced ML algorithms—particularly deep neural networks—in which the internal decision-making process is not interpretable by humans. When the contribution of individual variables to a prediction cannot be clearly understood, surgeons may find it difficult to critically evaluate the output and integrate it appropriately into clinical decision-making—an especially relevant concern in arthroplasty, where decisions have long-term biomechanical consequences[190,232]. When models do not provide clear explanations of how individual variables contribute to predictions, surgeons may find it difficult to critically appraise outputs and integrate them appropriately into decision-making—an especially relevant issue in arthroplasty, where decisions have long-term functional and biomechanical implications. Moreover, current outcome-prediction systems do not yet fully incorporate difficult-to-quantify variables such as soft-tissue quality, patient adherence to rehabilitation, individual expectations, and psychosocial factors, all of which can meaningfully influence postoperative outcomes. Accordingly, AI-generated predictions should be interpreted as probabilistic estimates: AI should not be considered a substitute for clinical judgment, but rather a complementary tool supporting the surgeon’s decision-making process.

CHAPTER 4 – Rationale and aims

The present thesis adopts a modular structure in which each chapter addresses a specific component of the decision-making and surgical pathway in reverse shoulder arthroplasty. To avoid redundancy, the shared theoretical background is presented here as a general rationale, while the subsequent chapters separately describe the materials and methods, results, and discussion pertaining to each research objective.

4.1 General rationale

Glenohumeral osteoarthritis associated with a massive rotator cuff tear, in patients considered for reverse shoulder arthroplasty, represents a particularly complex scenario in orthopaedic surgery. This complexity arises from the coexistence of glenoid deformities, reduced bone stock, and alterations in the three-dimensional orientation of the scapula. The long-term survivorship and functional performance of the prosthesis depend largely on optimal management of the glenoid side, especially regarding baseplate positioning and the quality of fixation. Errors in version and inclination, excessive medialization, and insufficient screw fixation have been consistently associated with instability, early loosening, and inferior clinical outcomes[32,185,233]. Traditional techniques based on two-dimensional imaging and intraoperative anatomical landmarks present intrinsic limitations. They do not allow accurate representation of multiplanar glenoid deformities, are strongly operator-dependent, and exhibit substantial interobserver variability, particularly in complex cases[188,234–236]. In response to these challenges, computer-assisted technologies—particularly three-dimensional CT-based preoperative planning and intraoperative navigation—have been introduced to reduce variability, improve the accuracy of glenoid component positioning, and optimize implant fixation[187,191,237]. Three-dimensional CT planning allows a detailed evaluation of glenoid morphology, including version, inclination, the extent and location of bone loss, and the humeral head–glenoid relationship. This enables simulation of different strategies for managing bone loss—such as reaming, bony or metallic augments, or structural grafting—and facilitates selection of the most appropriate implant for each case[196,238]. This should lead to a more accurate understanding of bony defects and a more rational use of augmented baseplates, a more precise definition of glenoid coverage, offset, and component orientation, and a better prediction of intraoperative technical challenges.

CT-based intraoperative navigation completes this process by transferring the preoperative plan into the operating room in real time. Through a spatial tracking system, the surgeon receives immediate feedback on changes in baseplate position—such as version, inclination, and medialization—as well as on screw trajectories. This facilitates a more faithful replication of the preoperative plan, maximizes screw length while preserving bone stock, and reduces the risk of suboptimal positioning, particularly in deformed glenoids[207,214,215].

Parallel to these developments, the introduction of machine learning–based outcome prediction systems has opened the way to a more predictive and personalized surgical approach. These tools aim to improve preoperative decision-making and patient expectation management[219,221,222,239].

Among these systems, Predict+ (Advita Ortho, Gainesville, Florida, USA) represents a notable example of an ML-based tool applied to shoulder arthroplasty. Despite encouraging preliminary evidences[198,211,212], several important questions remain unresolved. These include the reliability of preoperative planning, the true accuracy of outcome prediction systems, the real-world impact of computer-assisted technologies in daily clinical practice, and their actual translation into improved clinical outcomes. In light of these considerations, the present thesis aims to provide a systematic and integrated assessment of emerging technologies in reverse shoulder arthroplasty through a series of complementary studies that investigate the entire surgical pathway—from preoperative planning to outcome prediction, surgical execution, and postoperative clinical evaluation.

4.2 Specific aims

The present work aims to evaluate the role and clinical impact of new technologies—preoperative planning, intraoperative navigation, and outcome prediction systems—in reverse shoulder arthroplasty. Specifically, the objectives are:

- **To evaluate interobserver agreement** in preoperative planning for glenohumeral osteoarthritis cases considered for reverse shoulder arthroplasty, with analysis of implant selection and defect-correction strategies.

- **To analyse the accuracy and consistency of outcome-prediction systems** by comparing preoperative predictions with observed clinical and functional results at follow-up.
- **To assess the impact of combining preoperative planning with intraoperative navigation** on surgical execution—particularly baseplate selection, orientation, and screw length—in a consecutive series of procedures performed by a single surgeon.
- **To evaluate short-term clinical and functional outcomes** in patients undergoing reverse shoulder arthroplasty using either the conventional technique or intraoperative technological support.

CHAPTER 5 – Technological platform and workflow

5.1 Imaging acquisition protocol

5.1.1 Acquisition timing

The preoperative CT scan should be obtained within 6 months prior to surgery to minimise the risk of anatomical changes occurring between image acquisition and the surgical procedure. CT imaging provides superior visualisation of glenoid morphology and potential bony defects compared with conventional radiographs.

5.1.2 Patient preparation

For image acquisition, the patient is positioned supine on the CT table with the head directed towards the gantry. The limb to be examined is placed adducted alongside the body, with the arm maintained in neutral humeral rotation. Intravenous contrast must not be used, as it may hamper visualization of the bony anatomy. The patient must remain completely still throughout the examination to avoid motion artefacts.

5.1.3 CT scanner settings

Images must be acquired as axial slices without gantry tilt (i.e., no rotation), using standard "CT" mode with Hounsfield Unit encoding. A peak kilovoltage of at least 120 kVp is recommended, together with a tube current of 240 mA or higher, and a pitch value ≤ 1. A "bone" reconstruction kernel should be selected, ideally with high-definition acquisition settings when available; specific recommended parameters may vary depending on the manufacturer. Slice thickness (collimation/detector width) and slice spacing (slice increment or reconstruction interval) must be ≤ 1.25 mm. Both parameters must remain equal and constant throughout the entire examination, with no overlap between slices. The minimum allowable spacing is 0.3 mm, the maximum is 1.25 mm, and the recommended value is 0.625 mm. With 1.25 mm spacing, the cumulative error—arising from the model, camera, acquisition device, and intraoperative tools—can be maintained below 2% / 2 mm (manufacturer data). A spacing of 0.625 mm may further improve accuracy by reducing model-related error, although this comes at the cost of increased radiation exposure. Square pixels must be used consistently across all images. Regarding spatial resolution, the display field of view (DFOV) must encompass the entire scapula of the examined shoulder, including the medial border and the inferior tip. Bilateral

acquisition should be performed separately to avoid unnecessarily enlarging the DFOV and increasing radiation dose. The DFOV should typically measure 25–30 cm (10–12 inches for a 512×512 matrix). The minimum acceptable image resolution is 0.3×0.3 mm/pixel (512 pixels representing at least 15 cm/6”), whereas the maximum is 1.0×1.0 mm/pixel (512 pixels representing no more than 50 cm/20”). If metallic components are present within the DFOV, all available measures should be applied to minimise metal artefacts while maintaining a low radiation dose. Recommended metal artefact reduction (MAR) settings include single-energy CT acquisition at 140 kVp and 330 mA, supplemented by any manufacturer-specific MAR algorithms. All parameters are summarised in Table 5.1.

Axial format	No rotation	Gantry tilt 0°	Image orientation 1 0 0 0 1 0
Modality	CT		Hounsfield encoding
Recommended setting	Peak kilovoltage Milliamperage Pitch		120kVp or higher 240 mA or higher <1
Reconstruction kernel	Bone HD Acquisition if available		Built-in filter General Electrics: BONE Toshiba: FC30 Siemens: B41 Philips: L
Slice thickness (collimator/detector width)	< 1.25 mm	Equal and constant No overlap	Min distance 0.3 mm Max distance 1.25 mm
Slice spacing (slice increment or reconstruction interval)			Recommended distance 0.625 mm
Pixels square	Constant for all images		
DFOV	Tde entire indicated scapula (including medial border and distal tip) Bilateral acquisition to be acquired independently 25-30 cm (10-12 in) Matrix size 512 x 512 pixel Min resolution 0.3 x 0.3 mm/pixel		512 pixels >15 cm/6 in Max resolution 1.0 x 1.0 mm/pixel 512 pixels <50 cm/20 in
MAR (only if metal hardware is present in the DFOV)	single energy CT		
	Peak kilovoltage Milliamperage	140 kVp 330 mA	Do not use auto-mA nor dose reduction protocol
	Available built-in algorithms are to be applied		General Electrics: SmartMAR Siemens: iMAR Toshiba: SEMAR Philips: O-MAR

Table 5.1*. Settings for CT-Scan acquisition protocol to be used with Shoulder Planning App for pre-operative planning and intraoperative navigation[198]. CT: computed tomography; HD: high*

definition; DFOV: display field over view; MAR: Metal Artifact Reduction; iMAR: iterative MAR; SEMAR: single-energy MAR; O-MAR: MAR for orthopedic implants.

5.1.4 Image format

Images must be exported as uncompressed, non-encrypted DICOM files. The exported raw dataset must contain only the axial series, with files named in strict sequential numerical order, without gaps or duplicate filenames. No additional series—such as sagittal or coronal reconstructions—or scout images should be included. In most cases, the exported series comprises approximately 200 to 450 images. The tags and values listed in Table 5.2 must be present in the exported files to ensure compatibility with planning and navigation applications (Advita Guided Personalized Surgery software; AdvitaGPS™, BlueOrtho, Gières, France). The examination may be rejected if image quality is compromised, for example due to patient motion during acquisition, metal artefacts, poor overall image quality, or missing data or tags.

DICOM Tag	Name	Accepted values
(0002,0010)	Transfer syntax	1.2.840.10008.1.2 (Implicit VR Endian) 1.2.840.10008.1.2.1 (Explicit VR Little Endian) 1.2.840.10008.1.2.2 (Explicit VR Big Endian)
(0020,0037)	Image orientation patient	1/0/0/0/1/0

VR: value representation

***Table 5.2**. Tags and Included values to be present in the exported files[198].*

5.2 Preoperative planning software

5.2.1 Case creation

Once acquired, the CT study is uploaded to the online planning platform. The user must then select the DICOM image series to be used for reconstruction. The software automatically scans all subfolders and proposes suitable series—specifically axial series—while excluding others. After the series is selected, a scan preview is displayed. The operator must confirm that the entire scapula is included within the field of view and specify the operative side (right or left). The full study may also be reviewed in axial, sagittal, and coronal planes.

At this stage, the system requires entry of case information (patient ID and scheduled surgery date) and automatically anonymises the images. For intraoperative navigation, the CT study must undergo manual segmentation by an engineering team, followed by surgeon validation, after which the processed dataset is transferred to a USB device for intraoperative use. This step requires 24–48 hours. However, once the case has been created, the reconstruction and planning process can begin immediately.

The first step involves identifying the scapular centre and the trigonum on axial slices (Figure 5.1). The Friedman axis can then be adjusted on two-dimensional axial and coronal views, with a three-dimensional view available for verification (Figure 5.2). The user is subsequently asked to identify peripheral glenoid landmarks, including the superior and inferior poles and the anterior and posterior margins (Figure 5.3). The 3D reconstruction can then be refined by removing bone segments erroneously included in the model but not belonging to the scapula (for example, portions of the clavicle).

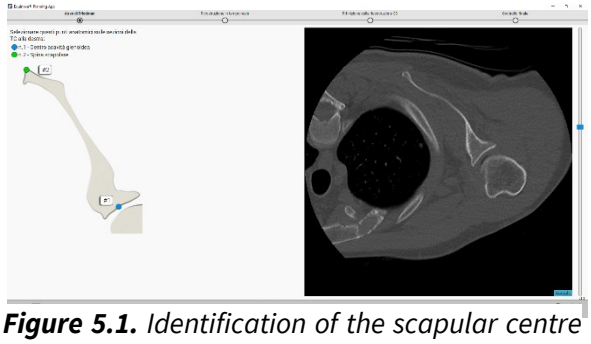

Figure 5.1. *Identification of the scapular centre and the trigonum on TC axial slices.*

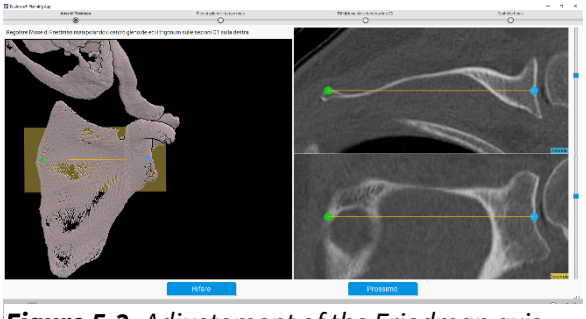

Figure 5.2. *Adjustement of the Friedman axis.*

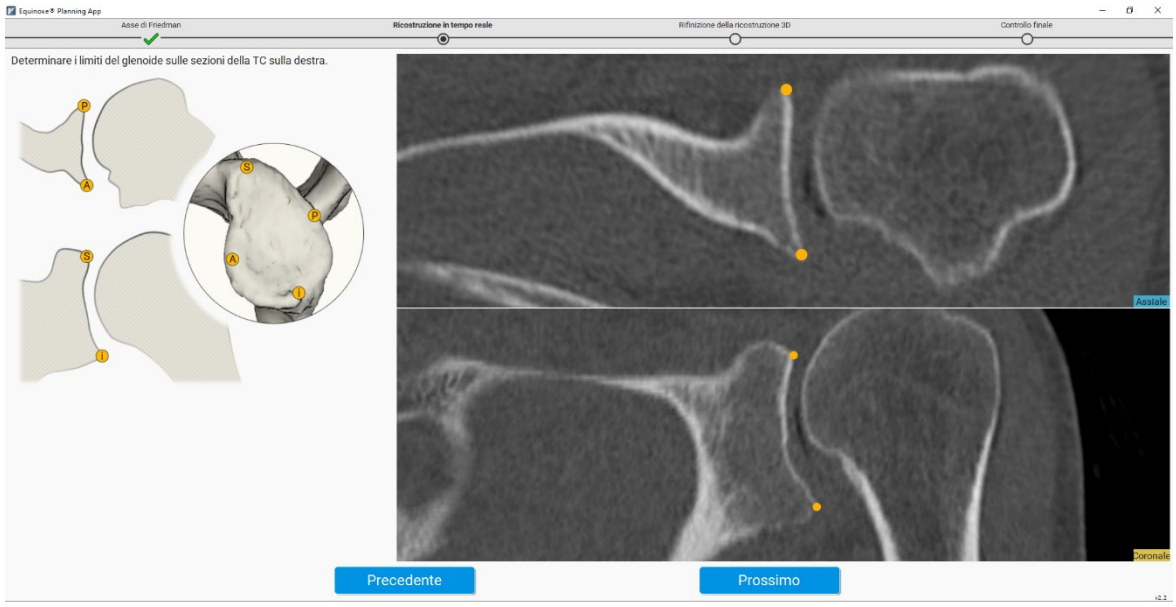

Figure 5.3. *Location of glenoid landmarks: superior and inferior poles, anterior and posterior margins.*

At this point, the system generates a three-dimensional scapular model and allows the user to validate reconstruction accuracy. Areas of uncertain accuracy are highlighted in orange or red on the 3D model. These may arise from low bone density, cysts, or humeral head impaction, which can make it difficult to distinguish the humeral articular surface from the glenoid. Markedly altered or complex anatomy may also lead to reconstruction errors at this stage.

5.2.2 Planning

Implant planning can be performed at this stage even before the manual segmentation carried out by the engineering team is completed. Planning may be undertaken separately for the glenoid component and the humeral component, and the joint can subsequently be assessed globally by combining the two plans. Throughout the planning process, the software allows measurement of both linear distances and angular parameters.

5.2.2.1 Scapula

The Shoulder Planning App displays the native scapular anatomy, including version, inclination, and overall dimensions (height and width). This enables the surgeon to appreciate the patient-specific morphology and the complexity of pathological alterations relative to a normal glenoid. The surgeon first selects the implant type (anatomic or reverse) and then chooses among the available components. In reverse shoulder arthroplasty, different baseplate options—standard, augmented, or long-peg—may be selected, and their position on the glenoid articular surface can be adjusted. It should be noted that the implant is automatically centred on the Friedman axis. The software provides both colour-coded and numerical feedback on the percentage of contact between the bony glenoid and the baseplate (grey indicating no contact; green indicating contact <0.5 mm; dark green indicating reaming >2 mm). The desired bone–implant contact is >75–80% to maximise long-term osteointegration, although biomechanical studies suggest that 50% coverage may maintain micromotion levels comparable to those observed with 75–100% contact[240]. The software also reports baseplate position (version, height, anteroposterior translation) and the medialisation or lateralisation of the centre of rotation relative to the native centre of rotation and to bony landmarks relevant in RSA. It is essential to rotate the virtual 3D scapular model in all planes and axes to verify baseplate positioning, particularly with respect to the central peg. Primary stability is enhanced, and the risk of intraoperative fracture reduced, when the peg is fully contained within bone without perforation or cortical contact at the scapular neck. A 2D verification is also recommended

(Figure 5.4). During baseplate placement, the surgeon can assess the amount of bone that must be removed from the articular surface and determine the inclination and version that best maximise baseplate-to-bone contact. Finally, the glenosphere can be selected according to size and degree of lateralisation (standard or expanded).

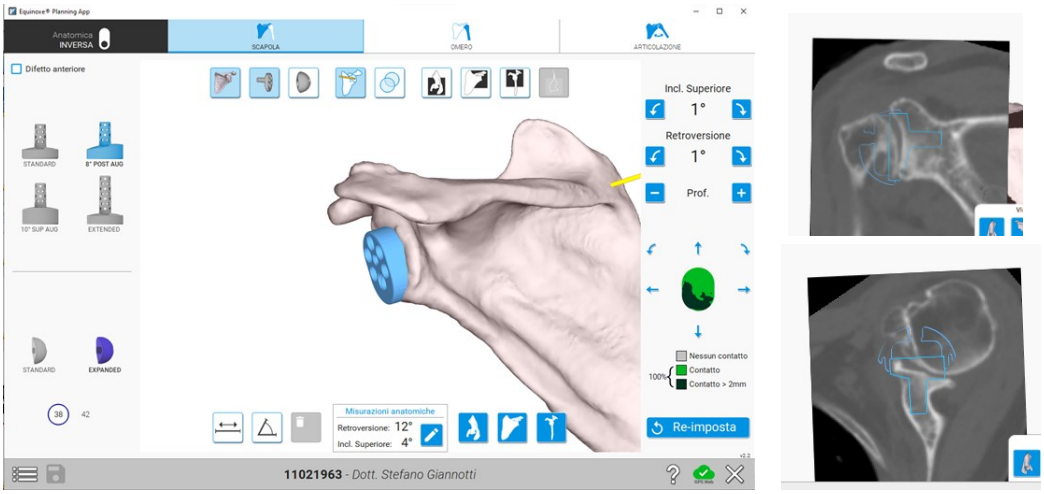

***Figure 5.4**. Surgeon can choose dimension and type of baseplate, and where to position it. The software gives coloured and numeric feedback of the percentage of contact between bone and metal. A 2D check is recommended.*

5.2.2.2 Humerus

Planning of the humeral component offers several options. The humeral cut may be defined in terms of resection level, retroversion, and cut inclination. The surgeon must then select the stem type (standard or long in the case of reverse shoulder arthroplasty) and the remaining components, including the adapter tray and polyethylene insert (standard or constrained). As in the scapular planning stage, the resection level and its parameters, as well as the implant components, may be adjusted as required.

5.2.2.3 Joint

Before globally assessing the joint with the selected implant and determining the degrees at which impingement occurs, the patient's neutral abduction must be set. Because neutral abduction is influenced by patient BMI, this parameter must be considered at this stage. The subsequent screen displays impingement ranges, which may be affected by the presence of osteophytes, and allows dynamic evaluation of the construct. Prosthetic components may be modified to assess their effect on range of motion. The system also provides measurements of

lateralisation and lengthening relative to the initial anatomical position, which vary according to implant selection.

5.3 Intraoperative navigation system

The preoperative plan is uploaded into the intraoperative application and patient data are verified. The navigation system hardware consists of a platform with a touchscreen monitor positioned in a sterile field at the patient's feet, together with surgical instruments equipped with optical trackers. The optical trackers are first registered and calibrated on the computer, after which the surgical incision is performed.

A deltopectoral approach is mandatory because a tracker must be placed on the coracoid, requiring exposure of the coracoid process. To ensure adequate exposure and minimise soft-tissue tension throughout the procedure, the incision should begin approximately 1–1.5 cm proximal to the coracoid tip. Following skin incision and subscapularis tenotomy, the humeral side is prepared using conventional instrumentation. Once the coracoid tip has been adequately prepared, the fixed scapular tracker is secured with two threaded screws to the inferolateral surface at the base of the coracoid process, ensuring that the tracker post is oriented towards the camera. Care must be taken not to loosen or displace the tracker during the procedure, as it serves as the reference for the entire operation. The glenoid is then exposed, with careful soft-tissue removal as required. Using tracked handheld instruments, guided acquisition of the main anatomical landmarks is performed: the anterior and posterior surfaces and base of the coracoid process; the superior, inferior, anterior, and posterior margins of the glenoid surface; lines along the anterior, inferior, and posterior glenoid rim; and lines along the anterior and inferior glenoid neck. This process enables verification and superimposition of the 3D model onto the patient's actual anatomy. Correspondence between the registered points and the CT-based anatomy is displayed through colour feedback: green indicates perfect correspondence, yellow indicates acceptable matching, and red indicates unacceptable registration (Figure 5.5). If necessary, acquisitions may be repeated fully or partially.

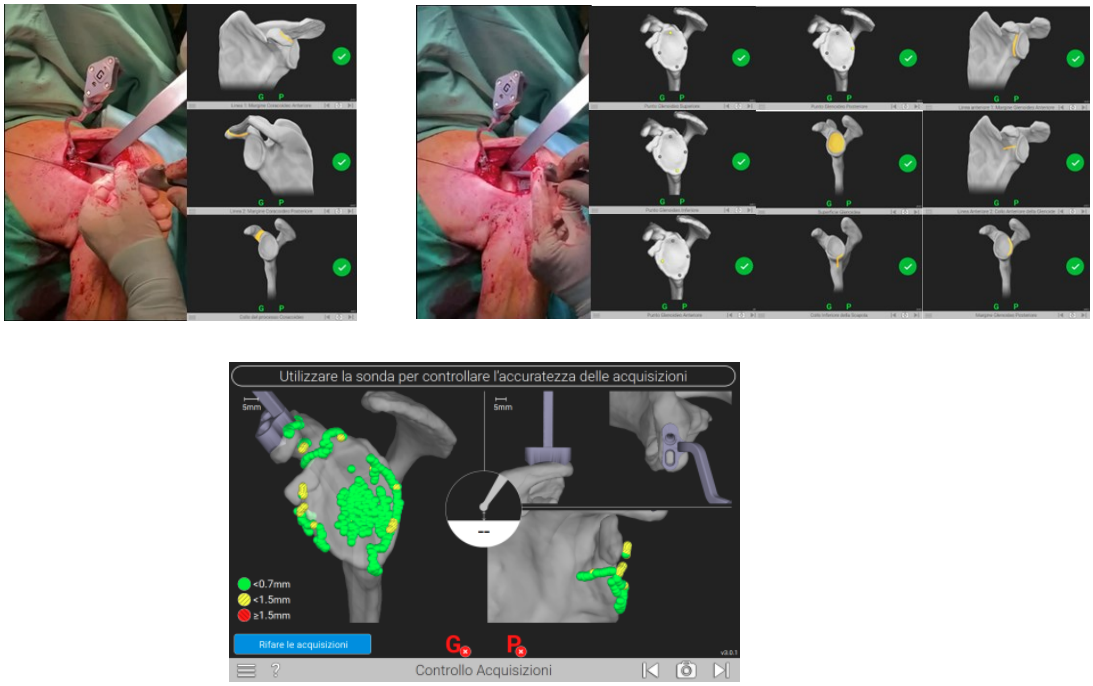

Figure 5.5. *The acquisition process. After positioning the tracker on the coracoid process, (A) the surgeon identifies the main anatomical landmarks on both the coracoid process (anterior and posterior surfaces and base) and (B) the glenoid surface (superior, inferior, anterior, and posterior margins of the glenoid surface; lines along the anterior, inferior, and posterior glenoid rim; and lines along the anterior and inferior glenoid neck). (C) At the end of the procedure correspondence between the registered points and the CT-based anatomy is displayed through colour feedback.*

Once the matching procedure is completed, the preoperative plan is displayed on the platform screen. Each subsequent step—centring, reaming, creation of the central peg hole, and preparation for screw placement—is performed under navigated guidance using tracked instruments, with real-time feedback on the touchscreen monitor (Figure 5.6 and 5.7).

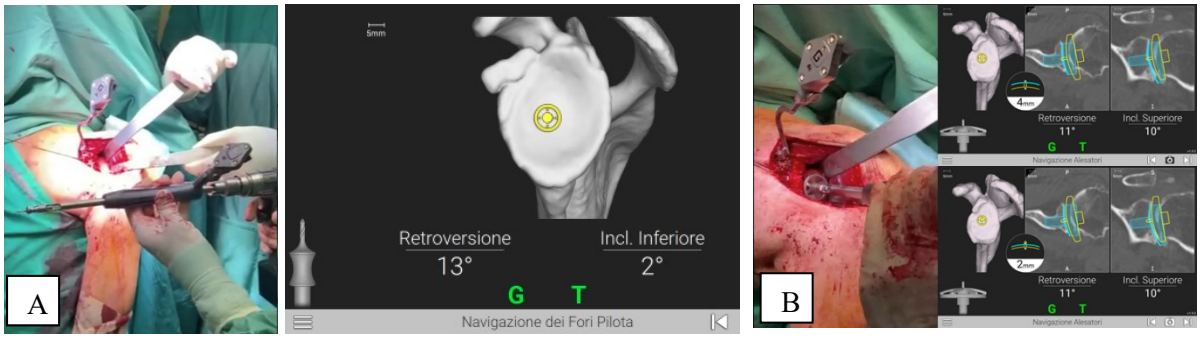

Figure 5.6. *Intraoperative navigation. (A) Pilot hole and (B) Glenoid reaming.*

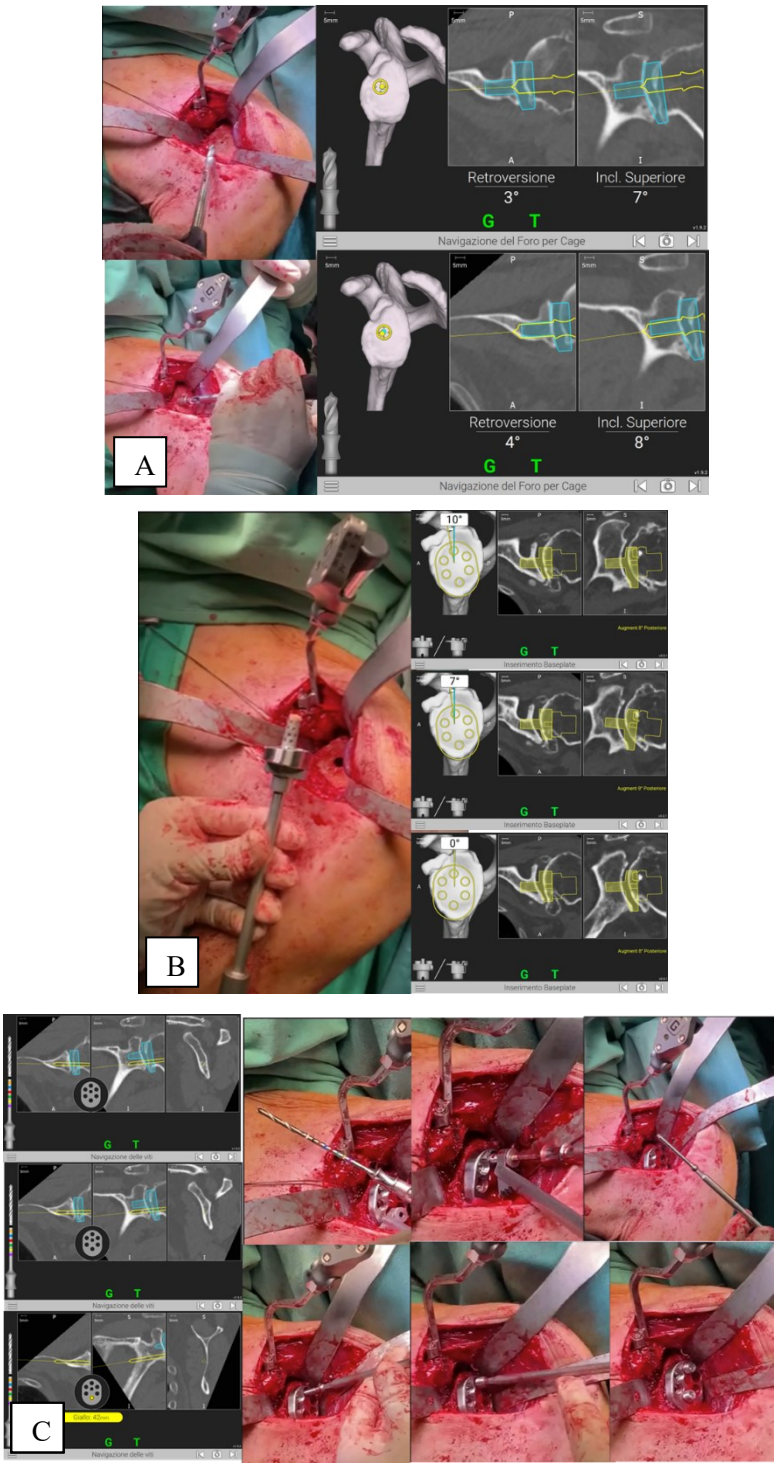

Figure 5.7. *Intraoperative navigation. (A) Creation of central peg hole, (B) baseplate positioning and (C) preparation for screws placement.*

After the central peg hole is created and the baseplate is positioned, its placement is checked against the plan. Screw length is determined using a colour code displayed both on the drill tip and on the touchscreen monitor. Once screw placement is completed, intraoperative navigation concludes with removal of the coracoid tracker. The procedure then continues conventionally with placement of the glenosphere (impacted and secured onto the baseplate), definitive humeral implantation, and subscapularis repair. Fixation of the humeral stem may be

achieved either with bone cement or by press-fit fixation; the choice depends on bone quality and morphology and is independent of whether intraoperative navigation is used.

5.4 Predict +

The Predict+ system employs machine-learning methods to identify relationships that would otherwise be difficult to detect between input variables—such as patient demographic characteristics and comorbidities—and output variables, including postoperative pain or range of motion. It is defined as a data-driven outcome-prediction system that uses preoperative information to estimate postoperative results in patients undergoing anatomic or reverse total shoulder arthroplasty. This predictive analytics platform was introduced into clinical practice in 2020.

Predict+ was trained on a database of more than 6,500 patients; two thirds of the dataset were used to construct the predictive model, and the remaining third was used for model validation[226,241]. 19 inputs with the strongest influence on postoperative outcomes were selected for model optimisation from the 291 variables recorded for each patient. The system provides predictions—ranging from 3 months to 7 years after surgery—for the visual analogue scale (VAS) for pain, range of motion, global shoulder function, and the Shoulder Arthroplasty Smart Score (SAS). The SAS is a multidomain assessment of shoulder function incorporating three objective range-of-motion measurements (active forward elevation, active internal rotation, active external rotation) and three subjective daily measures of pain and functional capacity.

CHAPTER 6 – Interobserver reliability of preoperative planning

Despite the growing adoption of reverse shoulder arthroplasty and the introduction of advanced three-dimensional planning systems, no universal consensus or shared gold standard currently exists regarding optimal criteria for preoperative planning. Homogeneous guidelines defining indications for baseplate selection, its inclination and version, and strategies for correcting glenoid defects are lacking. Planning therefore remains strongly dependent on the surgeon's experience and individual preferences. On this basis, the present multicentre study was designed to assess interobserver variability in RSA preoperative planning, specifically analysing the consistency of implant selection and defect-correction strategies among expert surgeons, with the aim of identifying common decision-making patterns that could also support less experienced clinicians.

6.1 Materials and methods

6.1.1 Study design and population

A multicentre cross-sectional observational study was conducted involving nine Italian orthopaedic surgeons from different specialist centres, each with documented experience in shoulder arthroplasty (>50 RSA procedures per year). Each surgeon independently performed preoperative planning for 81 RSA cases using a dedicated software version, starting from identical three-dimensional reconstructions generated by the AdvitaGPS™ software (BlueOrtho, Gières, France) and validated by the biomedical engineering team as described in Chapter 5.2. These reconstructions served as the "gold standard planning", ensuring identical initial anatomical inputs for all participants.

The 81 cases represented a spectrum of glenoid deformities, subdivided as follows:

- 15 with a predominantly inclination defect.
- 17 with a predominantly retroversion defect.
- 15 with a significant combined defect (inclination and retroversion).
- 15 with a dimensionally small glenoid.
- 19 with a central defect (Walch E1-type glenoid).

All data were derived from anonymised preoperative digital archives of real clinical cases, and the data could not be used to re-identify any patient.

6.1.2 Planning protocol

Starting from the "gold standard" reconstructions, each surgeon could either accept or freely modify the software-proposed plan, adjusting anatomical parameters (including the Friedman axis) according to their own surgical strategy. Each participant was required to complete full preoperative planning for all 81 cases, working independently and without access to the plans generated by other surgeons. The variables analysed included: whether the anatomical parameters provided were modified; planned prosthetic parameters (baseplate version, inclination, and rotation expressed in degrees; contact depth expressed in millimetres); degree of defect correction (i.e., the difference between native inclination/version and the planned baseplate values); type of baseplate selected (standard, superior augment, posterior augment, long peg); type of glenosphere (standard or expanded); and glenosphere diameter (36, 38, 42, or 46 mm). Final plans were exported and stored in a centralised anonymised database for statistical analysis, while still allowing identification of the surgeon who performed each plan.

6.1.3 Statistical analysis

Data processing was performed using IBM SPSS Statistics for Windows, version 30 (IBM Corp., Armonk, NY, USA). For continuous variables (inclination, version, contact depth, rotation), interobserver reproducibility was assessed using the Intraclass Correlation Coefficient (ICC 2,1), interpreted as follows: <0.50 poor agreement; 0.50–0.75 moderate agreement; 0.75–0.90 good agreement; >0.90 excellent agreement. Differences among surgeons were analysed using repeated-measures ANOVA after verifying normality with the Shapiro–Wilk test or using the Friedman test when normality assumptions were not met. Categorical variables (baseplate type; glenosphere type and diameter) were analysed using frequencies and percentage agreement, and Fleiss' kappa (κ) to measure agreement among multiple observers. Interpretation followed the Landis and Koch scale (<0.00 poor agreement; 0.00–0.20 slight agreement; 0.21–0.40 fair agreement; 0.41–0.60 moderate agreement; 0.61–0.80 substantial agreement; 0.81–1.00 almost perfect agreement). Correlations between defect pattern and selected baseplate type were assessed using the Chi-square test or Fisher's exact test when appropriate. All analyses accounted for the cluster effect (81 cases × 9 surgeons = 729 total

observations). Statistical significance was set at $\alpha = 0.05$, with 95% confidence intervals reported for ICC and Fleiss' kappa.

6.2 Results

Nine Italian orthopaedic surgeons, all with extensive experience in shoulder arthroplasty (>50 RSA procedures per year), independently completed preoperative planning for 81 consecutive cases of glenohumeral arthropathy, yielding a total of 729 analysed plans. Each plan was generated from the same "gold standard" three-dimensional reconstructions produced by the Advita Shoulder Planning App software and validated by the engineering team, thereby eliminating variability related to anatomical segmentation and isolating differences attributable solely to clinical decision-making.

6.2.1 Changes to the software plan and behavioural variability

Most surgeons modified the original software-proposed plan, with a mean modification rate of 51% ± 27% (individual range 0–91%). This behavioural heterogeneity manifested in three distinct patterns. A group of "conservative" surgeons accepted the software plan in most cases (<30% modifications). A "selective" group intervened only in a minority of cases (35–50% modifications, predominantly in combined defects). A third "interventionist" group systematically modified more than 80% of plans.

Decision heterogeneity was quantified using Fleiss' κ for the yes/no modification of the Friedman axis, revealing systematic disagreement among the nine surgeons ($\kappa = -0.093$, $z = -4.67$, $p < 0.001$). A negative kappa value indicates not only a lack of agreement, but a tendency for surgeons to disagree more than would be expected by chance alone.

6.2.2 Interobserver reliability for quantitative variables: single vs mean measures

Interobserver reliability for continuous variables (baseplate version, inclination, rotation, and contact depth) was assessed using the Intraclass Correlation Coefficient (ICC 2,1; two-way random-effects model with absolute agreement), distinguishing between single-measure reliability and reliability of aggregated mean measures to estimate, respectively, the reliability of a single measurement performed by an individual surgeon and the reliability of the averages of the measurements obtained from all the surgeons. In addition, Cronbach's α was reported as a measure of internal consistency and as a complementary assessment of the overall coherence

of the measurements. The F test associated with the ICC model, along with the corresponding degrees of freedom, was used to determine whether the variability between cases was significantly higher that the variability related to interobserver disagreement or measurement errors. Results are summarised in Table 6.1.

Parameter	ICC single-measure (95% CI)	ICC mean measures (95% CI)	α Cronbach	Test F (df 69,552)	p-value
Baseplate version (°)	0.334 (0.216–0.464)	0.819 (0.713–0.886)	0.704	3.382	**<0.001**
Baseplate rotation (°)	0.131 (0.067–0.217)	0.576 (0.394–0.714)	0.704	3.382	**<0.001**
Glenosphere diameter (mm)	0.233 (0.141–0.345)	0.732 (0.597–0.826)	0.816	5.446	**<0.001**

Table 6.1. *Interobserver reproducibility for continuous planning variables among the nine surgeons (ICC 2,1 with absolute agreement). Values are shown for single-measure and mean-measures ICC with 95% confidence intervals; and Cronbach's α, F statistics (with associated degrees of freedom, df) and p-values are reported. In* ***bold*** *statistically significant differences.*

Single measures, reflecting the reliability of a single surgical assessment, showed poor agreement (ICC range 0.12–0.41):

- Baseplate version: ICC = 0.334 (95% CI 0.216–0.464)
- Baseplate rotation: ICC = 0.131 (95% CI 0.067–0.217)
- Glenosphere diameter: ICC = 0.233 (95% CI 0.141–0.345)

Conversely, mean measures, obtained by aggregating the assessments of the nine surgeons, reached moderate-to-good values:

- Baseplate version: ICC = 0.819 (95% CI 0.713–0.886), Cronbach's α = 0.704
- Baseplate rotation: ICC = 0.576 (95% CI 0.394–0.714), Cronbach's α = 0.704
- Glenosphere diameter: ICC = 0.732 (95% CI 0.597–0.826), Cronbach's α = 0.816

All F tests were highly significant ($p < 0.001$), confirming statistical robustness. These data show that individual surgeon judgment is intrinsically unstable (single ICC <0.40), whereas collective consensus produces reliable estimates (mean ICC >0.70) for aggregate applications, such as developing evidence-based guidelines or decision-support algorithms.

6.2.3 Multiobserver agreement for categorical variables: Fleiss' κ analysis

Agreement for categorical prosthetic choices was assessed using Fleiss' κ, which extends Cohen's κ overall agreement on baseplate type (standard, superior augment, posterior augment, long peg, anterior augment) was weak-to-moderate ($\kappa = 0.325$, $z = 24.6$, $p < 0.001$), with variable category-specific values: posterior augment ($\kappa = 0.393$) and anterior augment ($\kappa = 0.335$) showed the greatest consistency, whereas extended cage reached only $\kappa = 0.198$. For glenosphere diameter (36, 38, 42, 46 mm), agreement was weak ($\kappa = 0.214$, $z = 12.9$, $p < 0.001$), with 42 mm as the category with the highest concordance ($\kappa = 0.267$) and 46 mm showing systematic disagreement ($\kappa = -0.048$, $p = 0.015$). Finally, selection of glenosphere type (standard vs expanded) showed very poor agreement ($\kappa = 0.090$, $z = 4.51$, $p < 0.001$), confirming high clinical subjectivity for this parameter.

6.2.4 Influence of defect pattern on decisions and descriptive parameters

Non-parametric analyses demonstrated the presence of rational and systematic decision patterns strongly correlated with glenoid morphotype.

The Kruskal–Wallis test on baseplate version across the five defect types revealed highly significant differences ($H = 48.079$, $df = 4$, $p < 0.001$), with mean ranks reflecting coherent corrective strategies: isolated retroversion (mean rank = 279.66, n = 151) required the greatest version correction, differing significantly from the other categories (all $p < 0.001$ with Bonferroni correction); combined defects (mean rank = 320.99, n = 134) differed from inclination ($p = 0.014$) and central erosion ($p = 0.001$); whereas inclination (mean rank = 398.62, n = 133), small glenoid (384.40, n = 129), and central erosion (410.98, n = 171) showed overlapping ranks, indicating similar corrective approaches.

This association was further supported by the frequency analysis of baseplate type selection ($\chi^2 = 187.4$, $p < 0.001$), which highlighted rational preferences: inclination defects favoured superior augment (68% of choices), retroversion favoured posterior augment (55%) and long peg (29%),

while small glenoids and central defects favoured a standard baseplate (45% and 52%, respectively). Results are summarized in Table 6.2.

Glenoid defect	N° cases	Mean rank version (Kruskal-Wallis)	% Superior augment	% Posterior augment	% Standard
Retroversion	151	279.66	8%	55%	31%
Combined	134	320.99	35%	22%	28%
Small	129	384.40	12%	18%	45%
Inclination	133	398.62	68%	5%	22%
Central (E1)	171	410.98	15%	12%	52%

Table 6.2. *Distribution of mean ranks of baseplate version correction and baseplate type preferences according to glenoid defect patterns. Data include case volume for each morphotype, statistical mean ranks for version adjustments (derived from Kruskal-Wallis test), and the percentage frequency of use for different baseplate designs. Results are consistent with the observation that the surgical approach adopted across the surgeons is dependent on the preoperative anatomical defect.*

From a descriptive perspective, the mean degree of defect correction was 12° ± 7° for version and 9° ± 5° for inclination, with a mean contact depth of 2.1 ± 1.3 mm. For the glenosphere, 78% of choices were standard designs, with preferred diameters of 38 mm (52%) and 42 mm (28%), confirming an overall conservative tendency in implant choices, tempered by clear anatomy-specific adaptations in the patterns described above.

6.3 Discussion

Despite the increasing adoption of three-dimensional preoperative planning in RSA, the present multicentre study is one of the few investigations in the international literature to systematically quantify interobserver variability among expert surgeons under conditions of complete anatomical standardisation—that is, with all participants starting from the same preoperative plan.

A previous study[242] analysed 49 anatomic shoulder arthroplasty cases planned by nine U.S. surgeons, reporting mean ICC values of 0.45–0.62 for glenoid version and inclination, and Cohen's κ = 0.28 for prosthetic choices, with intra-surgeon variability ranging from 12° to 18°. More recently, other authors[243] evaluated RSA planning in a Brazilian multicentre context,

finding ICC = 0.51–0.67 for angular parameters and Fleiss' κ = 0.32 for augmented baseplates, with patterns similar to those observed in the present study (posterior augment in 52% of retroversion defects). Compared with these contributions, the present work is characterized by a larger sample and an exclusive focus on RSA.

The systematic disagreement regarding whether to modify the Friedman axis likely reflects the absence of a shared and standardized criterion for measuring and reporting glenoid version and for defining the reference axis. In this context, this variability may potentially be related to different levels of trust bestowed upon the software-derived 3D reconstructions[244]. Consistent with this interpretation, it has been reported that[245] different measurements strategies (manual 2D vs 3D measurements) can yield significantly different glenoid version values, with 3D derived measurements being more retroverted than 2D measurements in most of the cases (73%), despite excellent intra and inter observer reproducibility for 2D measurements. Overall, these data suggest that at least part of the observed disagreement during planning may be attributable not only to operator-dependent choices, but also to intrinsic methodological variability related to measurement[244,245].

The present findings delineate a scenario characterised by high individual decision variability (single ICC <0.40; Fleiss' κ <0.40), counterbalanced by reliable collective consensus (mean ICC 0.58–0.82) and by rational decision patterns strongly correlated with glenoid defect type (Kruskal–Wallis $p < 0.001$; χ^2 $p < 0.001$). These results highlight the presence of shared, implicit clinical criteria among experts despite the absence of formal standardisation and underscore the potential value of evidence-based guidelines derived from aggregated expert consensus.

This study has limitations. The most relevant include a moderate sample size—although considerably larger than comparable studies in the literature—and the exclusive involvement of Italian surgeons, which may limit the generalisability of the findings to an international context.

6.4 Conclusions

This multicentre study demonstrates that in RSA preoperative planning, substantial individual decision variability among expert surgeons (single ICC <0.40; Fleiss' κ −0.093 to 0.325) is counterbalanced by reliable collective consensus (mean ICC 0.58–0.82). Decision patterns appear rational and strongly correlated with glenoid defect type (Kruskal–Wallis $p < 0.001$):

retroversion defects favour posterior augments (55%), inclination defects favour superior augments (68%), and small or central glenoids favour standard baseplates (45–52%). These findings support the development of standardised protocols based on collective expert consensus, with the aim of improving the reproducibility of RSA planning and providing structured guidance for less experienced surgeons.

CHAPTER 7 – Outcome prediction systems

The integration of artificial intelligence and machine learning algorithms into orthopaedic surgery has opened new perspectives in personalized patient management. This chapter aims to critically analyse the reliability of outcome prediction systems, tools designed to anticipate postoperative clinical and functional results based on global databases and individual parameters. By comparing the preoperative predictions provided by the software with the real outcomes observed during follow-up, the investigation seeks to define the accuracy and consistency of these predictive models, assessing their clinical usefulness both as guidance for the surgeon and as a communication tool for managing patient expectations.

7.1 Materials and Methods

7.1.1 Study design and population

This retrospective study included two distinct cohorts of consecutive patients. All patients underwent reverse shoulder arthroplasty with intraoperative navigation using AdvitaGPS™ (BlueOrtho, Gières, France). The two-cohort design addressed two independent objectives.

Primary objective. The predictive accuracy of Predict+ (Advita Ortho, Gainesville, FL, USA) for range of motion (forward elevation, abduction, internal rotation, external rotation) and pain (VAS) was evaluated. Preoperative predictions were compared with observed clinical outcomes at a minimum follow-up of 6 months. We also compared postoperative ROM with the impingement-free ROM estimated by the planning system (Chapter 5.2). Inclusion criteria were as follows: complete Predict+ preoperative data, at least one postoperative Grashey-view radiograph (true AP shoulder view), clinical follow-up ≥6 months, and no major complications (revision arthroplasty, periprosthetic infection, implant dislocation). Patients with incomplete follow-up, major complications, or missing data were excluded.

Secondary objective. The secondary objective assessed agreement among DSA (distalization shoulder angle) and LSA (lateralization shoulder angle) measurements performed on postoperative radiographs, on the planning system using 3D reconstructions, and on 3D reconstructions but using a bidimensional measurement approach. Inclusion criteria for this analysis were broader and mainly required postoperative imaging (true AP shoulder radiograph) and availability of preoperative planning.

This two-cohort structure allowed precise analysis of both the clinical predictive reliability of the system and the geometric/instrumental consistency of distalization and lateralization parameters, maximizing the use of available data.

7.1.2 Measurement protocol

All 2D measurements were performed using a digital goniometer (APP Angle Meter 360°, precision 0.1°). ROM assessment included active abduction (aAB), active forward elevation (aFE), active internal rotation, and active external rotation (aRE) (Figure 7.1).

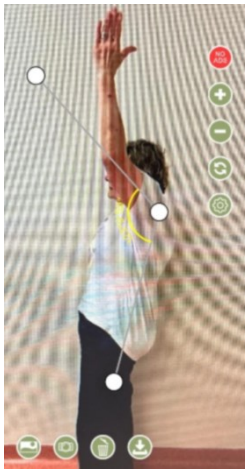

Figure 7.1. *Active ROM was measured using a dedicated smartphone goniometer application (angle meter 360°). When considering active forward elevation, as in this case, measurement technique and patient positioning were adjusted to account for the patient's increased thoracic kyphosis, thereby minimizing systematic error related to trunk posture.*

The same tool was used for DSA and LSA measurements (Figure 7.2).

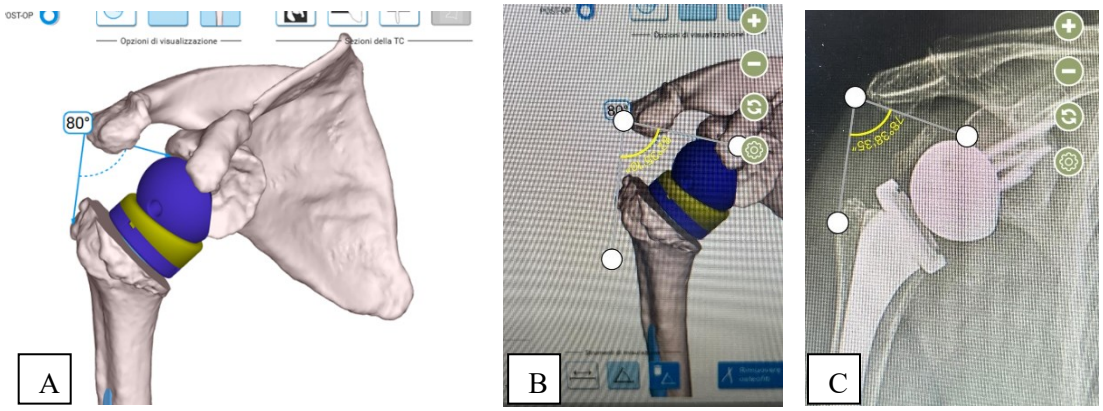

Figure 7.2. *Angles measurement workflow (three methods compared). The LSA was measured using three different approaches: (A) direct measurement on the 3D model within the Advita Shoulder Planning App; (B) measurement on a standardized 2D rendering of the same 3D reconstruction using the smartphone Angle Meter 360° application, and (C) measurement on conventional 2D radiographs. The same measurement workflow was applied to the DSA.*

Before angular measurements, the implant configuration was reconstructed using intraoperative data to reproduce the patient's postoperative geometry as closely as possible. To reduce random error, each researcher performed repeated measurements (five per variable) independently. Inter-measurement agreement was assessed using the Intraclass Correlation Coefficient (ICC). Given the high internal reliability (ICC 0.97), the mean value was used for subsequent comparisons. Pain was assessed using the VAS scale. The impingement-free ROM reported by the software was also recorded.

7.1.3 Statistical analysis

Statistical analysis was performed using IBM SPSS Statistics for Windows, version 30 (IBM Corp., Armonk, NY, USA). Statistical significance was set at $\alpha = 0.05$. Data distribution was assessed using the Shapiro–Wilk test. Given the small sample size and the frequent lack of normality, non-parametric tests were applied when appropriate. Predictive accuracy of the software versus observed postoperative outcomes (ROM, VAS) was assessed using Spearman's correlation coefficient (ρ). Correlations were interpreted as weak ($\rho < 0.30$), moderate ($\rho = 0.30$–0.59), or strong ($\rho \geq 0.60$). Differences among DSA and LSA measurements obtained with different methods were analysed using repeated-measures ANOVA. When normality assumptions were violated, the Friedman test was used. Agreement among measurement techniques was assessed using the Intraclass Correlation Coefficient (ICC) with a two-way random effects model, single measurement (ICC 2,1). ICC values were interpreted as poor (<0.50), moderate (0.50–0.75), good (0.75–0.90), or excellent (>0.90). The 95% confidence interval was reported for each ICC. Mean Absolute Error (MAE) was calculated as a summary accuracy metric for each parameter (ROM in degrees; VAS in points). For pairwise comparisons between methods, systematic bias and limits of agreement were further explored using Bland–Altman plots, reporting the mean difference and 95% limits of agreement.

7.2 Results

7.2.1 Primary objective – Predict+ accuracy and 3D kinematic planning reliability

A consecutive series of 10 patients was identified (9 F, 1 M). Mean age was 74.6 ± 7 years (range 62–86). Mean follow-up was 21.9 ± 7 months (range 9–29). Results are summarized in Tables 7.1 and 7.2.

Parameter (mean ± standard deviation, SD)	Predict+	Real	Difference	ρ	p	MAE
VAS	1.7 ± 0.9	1.0 ±1.8	+0.7	-0.18	0.575	1.4
aAB (°)	114.6 ± 21.0°	83.9 ± 11.5°	+30.7°	0.15	**0.002**	32.1°
aFE (°)	131.6 ±20.1°	129.1 ± 17.0°	+2.5°	0.33	0.770	18.4°
aER (°)	31.5 ± 8.5°	36.7 ± 13.7°	-5.2°	0.19	0.575	12.6°

aAB, active abduction; aFE, active forward elevation; aRE, active external rotation.

Table 7.1. *Comparative analysis of predictive accuracy of Predict+ with respect to observed clinical outcomes in terms of patient-reported pain (VAS) and active range of motion (aROM). Data are reported as mean ± standard deviation (SD). Mean difference between measurements, Spearman's rank correlation coefficient (ρ), p-values and Mean Absolute Error (MAE) are also detailed. In* ***bold,*** *statistically significant differences.*

Parameter (mean ± standard deviation, SD)	Simulated 3D	Real	Diff	ρ	p	MAE
aAB (°)	65.0 ± 12.9°	83.9 ± 11.5°	-18.9°	0.09	**0.010**	21.4°
aFE (°)	70.6 ± 10.5°	129.1 ± 17.0°	-58.5°	0.45	**<0.001**	58.1°
aRE (°)	63.0 ± 22.9°	36.7 ± 13.7°	+26.3°	-0.09	0.134	27.7°

aAB, active abduction; aFE, active forward elevation; aRE, active external rotation.

Table 7.2. *Comparative analysis of predictive accuracy of 3D kinematic planning simulations in estimating postoperative active impingement-free range of motion (aROM) with respect to observed clinical outcomes. Data are reported as mean ± standard deviation (SD). The mean difference between measurements, Spearman's rank correlation coefficient (ρ), p-values and Mean Absolute Error (MAE) are also provided. In* ***bold,*** *statistically significant differences.*

Minimum clinically important difference (MCID) values derived from established RSA studies were used as a clinical benchmark to interpret discrepancies between predictions and observed results[246–249]. MCID values were: 1.4–1.6 points for VAS[246,247], 7–13° for active abduction[247], 12–16° for active forward elevation[247], and 3–5° for active external rotation[247]. No references were identified for active internal rotation.

Overall, Predict+ showed different performance patterns across outcomes. For VAS pain, the model overestimated pain by +0.7 points (MAE 1.4) and the difference was not significant ($p = 0.58$). This error remained below the reported VAS MCID (1.4–1.6 points). However, subject-level correlation was weak and negative ($\rho = -0.18$). For active abduction, Predict+ systematically overestimated ROM by +30.7° (MAE 32.1°; $p = 0.002$). This difference exceeded the MCID by approximately 2–4 times. Correlation at the individual level was negligible ($\rho = 0.15$; $p = 0.68$). This supports limited patient-specific reliability despite acceptable mean-level agreement. For active forward elevation, Predict+ produced similar mean values to the observed outcomes (+2.5°; $p = 0.77$). The mean difference was below the MCID. Nevertheless, individual-level correlation remained limited ($\rho = 0.33$; $p = 0.36$), suggesting that apparent accuracy may reflect error compensation at the group level rather than stable individual prediction. For active external rotation, Predict+ slightly underestimated outcomes (−5.2°; $p = 0.58$). The magnitude was close to the reported MCID range (3–5°). Individual correlation was weak ($\rho = 0.19$).

The 3D kinematic planning simulation showed clinically relevant errors and poor agreement with clinical ROM. For active abduction, simulated ROM was lower than observed (−18.9°; MAE 21.4°; $p = 0.01$), exceeding the MCID despite opposite direction compared with Predict+. Correlation was minimal ($\rho = 0.09$). For forward elevation, the simulated ROM markedly underestimated observed outcomes (−58.5°; MAE 58.1°; $p < 0.001$), indicating substantial limitations of the simulation. For external rotation, the simulation overestimated outcomes (+26.3°; MAE 27.7°) with negligible correlation($\rho = -0.09$; $p= 0.134$).

7.2.2 Secondary objective – agreement among DSA and LSA measurements across methods

A consecutive series of 28 patients was identified (19 F, 9 M). Mean age was 74.6 ± 7 years (range 60–87). Results are summarized in Table 7.3.

Parameter (°)	2D X-ray (mean ± standard deviation, SD)	CT 3D planning (mean ± standard deviation, SD)	CT 2D axial in planning (mean ± standard deviation, SD)	p ANOVA	ICC (95% CI)	Bland–Altman bias
DSA	142.3 ± 7.2°	140.5 ± 6.8°	141.1 ± 7.0°	**0.04**	0.72 (0.54-0.84)	-1.8° (-6.2/+2.6°)
LSA	88.4 ± 5.9°	89.5 ± 6.1°	89.2 ± 6.0°	0.21	0.74 (0.57-0.86)	-1.1° (-4.8/+2.6°)

DSA: Distalization Shoulder Angle; LSA: Lateralization Shoulder Angle; CT: Computed Tomography; ICC: Intraclass Correlation Coefficient; CI: Confidence Interval.

Table 7.3. *Inter-method agreement analysis for distalization shoulder angle (DSA) and lateralization shoulder angle (LSA) measurements. Data are presented as mean ± standard deviation (SD) comparing three modalities: 2D X-Rays, 3D CT planning software calculations, and manual 2D measurements performed on 3D CT reconstructions using a digital protactor. Statistical evaluation includes one way ANOVA, ICC with 95% CI, and Bland-Altamn bias. In* ***bold****, statistically significant differences.*

Agreement among methods was moderate for both angles. For DSA, the mean difference across techniques was statistically significant (p = 0.04). Mean values were 142.3 ± 7.2° (2D X-ray), 140.5 ± 6.8° (CT 3D), and 141.1 ± 7.0° (CT 2D). This suggests a small but systematic measurement bias. ICC for DSA was 0.72 (95% CI 0.54–0.84), consistent with moderate agreement.

For LSA, no significant differences were found (p = 0.21). Mean values were 88.4 ± 5.9° (2D X-ray), 89.5 ± 6.1° (CT 3D), and 89.2 ± 6.0° (CT 2D). ICC for LSA was 0.74 (95% CI 0.57–0.86), again indicating moderate agreement.

Bland–Altman analysis showed wider limits of agreement for DSA than for LSA. For DSA, the bias was −1.8° with limits of agreement −6.2° to +2.6°. For LSA, the bias was −1.1° with limits of agreement −4.8° to +2.6°. Although mean biases were small, the limits of agreement remained relatively wide, suggesting that the techniques may not be fully interchangeable at the individual level. Overall, DSA and LSA appear clinically useful as static postoperative descriptors. CT-based planning may reduce perspective distortion compared with 2D radiographs.

7.3 Discussion

Machine learning (ML) algorithms and artificial intelligence technologies are increasingly being adopted across multiple fields, including medicine. In the specific context of ML models applied to shoulder arthroplasty, literature[223] has shown that these tools have the potential to improve clinical outcomes by influencing decision-making and enabling more patient-tailored treatment strategies. However, systemic issues related to transparency, reproducibility, and external validation must be addressed before these technologies can be implemented widely in routine clinical practice.

Within this framework, the primary aim of the present study was to evaluate, in a consecutive cohort of patients undergoing reverse shoulder arthroplasty, the accuracy of an ML-based predictive system (Predict+) and the reliability of 3D kinematic simulation (impingement-free ROM) in representing real clinical outcomes. In this context, although metrics such as the mean difference and mean absolute error (MAE) are commonly used to describe the overall performance of a model, their validity as decision-support tools in clinical practice also requires patient-specific reliability—namely, the ability to preserve a stable relationship between predicted and observed values at the individual level. Despite evidence supporting the reliability of predictive models for clinical outcomes[223,226,227,250], in the present cohort Predict+ demonstrated heterogeneous performance across different functional endpoints.

Regarding pain, the model showed a limited mean overestimation, with an MAE of 1.4, which is nevertheless nearly twice that reported in other studies[239]. Given a mean reference MCID of 1.5[246,247], the average error falls within a clinically acceptable range, suggesting that the software may provide a plausible estimate of pain. However, the lack of a statistically significant positive correlation ($\rho = -0.18$) indicates that the tool may have limited utility for personalized patient counselling. With respect to range of motion (ROM), active abduction represented the most critical endpoint, with Predict+ overestimating clinical values by approximately 31° (MAE 32.1°); this difference was statistically significant ($p = 0.002$) and substantially greater than the reported MCID (7–13°)[246,247]. A similar pattern was observed for external rotation. Conversely, for forward flexion, a moderate positive correlation was observed ($\rho = 0.33$), with minimal discrepancy between predicted and observed values and an MAE only slightly above the MCID. Overall, these findings were consistent, although not fully comparable, with other cohorts. For example, Caprili et al.[239] reported lower MAE for active abduction (18–25°), whereas Kumar et

al.[226] reported weighted MAEs of approximately 1.4 for VAS pain, 21.8° for abduction, and 19.2° for forward flexion, suggesting that predictive performance may vary across cohorts and clinical settings.

The 3D kinematic simulation showed large and systematic discrepancies compared with clinically measured active mobility across all planes, in line with a previous study in the literature[229]. This systematic failure of 3D kinematic planning to identify impingement-free ROM—particularly evident for forward elevation—can be directly explained by the biomechanical limitations of the static scapular model used in the 3D planning system[251]. In RSA patients, shoulder kinematics differs substantially from native anatomy: scapulothoracic rhythm is significantly reduced, meaning that these patients elevate the arm relying much more on scapulothoracic motion than on glenohumeral motion. This increased scapular contribution after RSA is not represented in the static models of the 3D planning system, which essentially depict glenohumeral motion with a fixed scapula; conversely, it is well established that post-RSA patients exhibit dynamic compensatory mechanisms.

The secondary objective of this study was to assess agreement among angular measurements (DSA and LSA) obtained using three different approaches (2D radiographic measurements, measurements from 3D planning, and “2D” measurements on 3D reconstructions). In sharp contrast with dynamic parameters, inter-method agreement for the static angles DSA and LSA showed moderate reliability (ICC 0.72–0.84), with negligible systematic biases (−1.1°/−1.8°), despite statistically significant differences for DSA ($p = 0.04$). Bland–Altman analysis confirmed a small mean bias (approximately 1°–2°) but relatively wide limits of agreement, suggesting that these approaches cannot be considered fully interchangeable when high individual-level precision is required.

In summary, Predict+ performs well on aggregated means (aFE within MCID) but fails individual prediction ($\rho < 0.33$), whereas 3D planning is systematically inaccurate (MAE 21–58°). Both tools exceed MCID thresholds for most parameters and are therefore clinically unreliable for patient-specific applications, although they may still be useful for epidemiological counselling. The absence of statistically significant differences between methods in ROM measurements ($p > 0.05$) should not be interpreted as equivalence of techniques. Low or negative ICC values indicate marked subject-specific variability, suggesting that the software does not provide

reliable estimates of real ROM despite overlapping mean values. Moreover, kinematic planning is not reliable in providing information on real shoulder kinematics.

A major methodological strength of the present study is the adoption of an evaluation approach focused on patient-specific performance, which has not yet been extensively explored in the literature and overcomes the limitation of relying solely on group-mean analyses. Exclusive reliance on mean values may mask clinically relevant discrepancies, because overestimations and underestimations can statistically compensate for each other, yielding only an apparent accuracy that does not reflect true precision at the individual level. Integrating metrics such as MAE and association coefficients enabled the identification of clinically meaningful discrepancies, providing a more rigorous assessment of the actual reliability of the predictive tools under investigation. Nevertheless, the present study also has limitations. First, it includes a relatively small, single-centre sample, which may limit generalizability to larger populations or cohorts with different demographic characteristics. In addition, the mean follow-up was shorter than 2 years, which may not fully capture long-term functional evolution.

7.4 Conclusions

This study critically analysed the predictive accuracy of the Predict+ software and the consistency of 3D kinematic planning in predicting functional outcomes after reverse shoulder arthroplasty and also assessed agreement in the measurement of angular metrics (DSA and LSA) using different systems. Results show that, although both systems demonstrate good, aggregated consistency of mean values, their reliability at the patient-specific level remains limited. Prospectively, multicentre studies with larger samples and algorithms trained on European datasets may improve the robustness and generalizability of predictive models. In conclusion, this work shows that AI-based outcome prediction in orthopaedic surgery is a useful tool but still in a maturation phase, and at present it cannot replace the surgeon’s clinical decisions.

CHAPTER 8 – Impact of 3D CT planning and intraoperative navigation on clinical practice: a single-surgeon experience

The aim of this chapter is to document the transition from an empirical preoperative planning approach to a data-guided strategy. It evaluates how the combined use of 3D CT-based preoperative planning and intraoperative navigation affects the technical execution of reverse shoulder arthroplasty, with particular focus on glenoid baseplate selection and fixation. Through a retrospective review of a consecutive case series, this study investigates whether these technologies act not only as technical aids, but as determinants of surgical personalization and optimization of bony anchorage.

8.1 Materials and Methods

8.1.1 Study design

A retrospective study was conducted using exclusively anonymised patient data extracted from our institutional database. After surgery, paper records are routinely archived and include patient initials, date of birth, diagnosis, operative time, implanted components, and the postoperative radiograph.

Inclusion criteria comprised a diagnosis of cuff tear arthropathy or eccentric glenohumeral osteoarthritis requiring reverse shoulder arthroplasty, procedures performed by the same senior shoulder surgeon, and availability of a postoperative true anteroposterior (AP) shoulder radiograph (Grashey view). To minimise selection bias towards either severely deformed glenoids or near-physiological anatomy, patients undergoing RSA for post-traumatic osteoarthritis, complex proximal humerus fractures, revision procedures, custom implants, oncological indications, or failures after previous ORIF of proximal humerus fractures were excluded.

Eligible patients were stratified into three groups according to the technology used during the index procedure: conventional surgery (CON), planning-only surgery (PLAN), and navigated surgery (NAV). Because intraoperative navigation requires preoperative 3D CT-based planning, planning was mandatory for all NAV cases. Computer-assisted technologies were introduced into clinical practice in October 2018; therefore, all procedures performed before this date were

allocated to the CON group. Procedures performed thereafter were assigned to PLAN when only preoperative 3D CT planning was used (Advita Shoulder Planning App, BlueOrtho, Gières, France), or to NAV when intraoperative navigation was additionally employed (Guided Personalized Surgery Shoulder system; AdvitaGPS™, BlueOrtho, Gières, France).

This design enabled independent assessment of the impact of preoperative planning versus intraoperative navigation and allowed exploration of a potential learning-curve effect associated with progressive adoption of computer-assisted technologies.

8.1.2 Outcomes and measurements

For each included patient, the following intraoperative variables were collected: baseplate type (standard versus augmented), number of glenoid fixation screws, screw length, the proportion of cases in which only two screws were used, and operative time. Screw trajectory was also assessed by measuring the inclination of the superior and inferior screws relative to the central peg.

Angular measurements were performed manually using Cabri Géomètre II Plus, Version 1.4 (Cabrilog, Grenoble, France). Because only digitised postoperative radiographs were available (rather than DICOM files), all measurements were performed directly on these digitised images. To minimise measurement error, two investigators independently performed repeated measurements (five per variable) for both superior and inferior screw inclinations. Inter-rater agreement was assessed using the Intraclass Correlation Coefficient (ICC), both overall and within each subgroup. Given the high internal reliability, the mean value of the repeated measurements was used for subsequent group comparisons (Table 8.1).

Group	**ICC Sup (95% CI)***	**ICC Inf (95% CI)#**
Global	0.983 (0.979-0.987)	0.984 (0.980-0.988)
CONV	0.984 (0.975-0.991)	0.988 (0.988-0.995)
PLAN	0.973 (0.957-0.985)	0.943 (0.909-0.967)
NAV	0.971 (0.96-0.98)	0.965 (0.952-0.976)

*ICC for the inclination of the superior screws are reported. CI: Confidence Interval.
ICC for the inclination of the inferior screws are reported. CI: Confidence Interval.

Table 8.1*. Intraclass Correlation Coefficient (ICC) for screws' inclination.*

8.1.3 Statistical analysis

Statistical analyses were performed using IBM SPSS Statistics for Windows, version 30 (IBM Corp., Armonk, NY, USA). Statistical significance was set at $p < 0.05$; non-significant results are reported as n.s. in the text, with exact p-values provided in the tables.

Continuous variables were analysed using the Kruskal–Wallis test after confirming non-normal distribution (Shapiro–Wilk test) and non-homogeneity of variances (Levene's test). When significant differences were identified, post-hoc Dunn testing with Bonferroni correction was applied.

Categorical variables were compared using the Chi-square test with Yates correction or the Fisher–Freeman–Halton test when at least one expected cell count was <5. Significant findings were further explored using Fisher's exact tests on relevant subgroups, applying Bonferroni correction (corrected $\alpha = 0.0167$).

8.2 Results

A consecutive series of 158 patients meeting all inclusion criteria was identified, comprising 111 females and 47 males, with a mean age (± standard deviation, SD) of 74.2 ± 6.6 years (range 34–87). Demographic characteristics and surgical data for the CON, PLAN, and NAV groups are summarised in Table 8.2.

A power analysis was performed using IBM SPSS Statistics for Windows, version 30 (IBM Corp., Armonk, NY, USA), with $\alpha = 0.05$ and a desired statistical power of 80%. For the primary endpoint "number of screws" (expected mean difference $\Delta = 0.3$ screws; SD = 0.7), the achieved power was 92.3%, with a minimum required sample size of 32 patients per group. For mean screw length ($\Delta = 7.4$ mm; SD = 4.5 mm), statistical power reached 100%, with a minimum of 12 patients per group. For the "frequency of two-screw fixation", power was 87.6%, with a minimum total sample size of 58 patients. The actual sample sizes in the present study (CON: 42 patients; PLAN: 35 patients; NAV: 81 patients) were therefore adequate—and in some cases larger than required—to detect clinically meaningful differences in the primary outcomes, ensuring high statistical robustness.

	CON	**PLAN**	**NAV**	***p****
Overall surgical volume	42	35	81	
Gender male / female	11 / 31	11 / 24	25 / 56	0.84
Age (mean ± SD, range)	73.9 ± 5.6 (64-87)	74.3 ± 5.8 (61-86)	74.3 ± 7.3 (34-87)	0.55
Screws' number (mean ± SD, range)	2.4 ± 0.7 (2-4)	2.3 ± 0.6 (2-4)	2.1 ± 0.5 (2-5)	**0.02** CON-PLAN: 0.29 **CON-NAV: 0.008** PLAN-NAV: 0.19
Frequency of 2 screws used in total	71.4%	80%	90%	**0.028** CON-PLAN: 0.435 **CON-NAV: 0.0106** PLAN-NAV:0.145
Screws' length (mean ± SD, range)	29.1 ± 3.2 (25-40)	34.1 ± 5 (18-46)	36.5 ± 4.8 (22-46)	**0** **CON-PLAN: <0.00001** **CON-NAV: 0** **PLAN-NAV: 0.0019**
Baseplate type Standard/augmented	1 / 4	19 / 16	44 / 37	**< 0.00001** **CON-PLAN: <0.00001** **CON-NAV: <0.00001** PLAN-NAV: 1
Surgical time (mean ± SD, range)	101.3 ± 34.7 (60-255)	90.2 ± 24.5 (50-145)	101 ± 23.2 (50-160)	**0.05** CON-PLAN: 0.13 CON-NAV: 0.44 **PLAN-NAV: 0.0148**
Superior screw' inclination (mean ± SD, range)	12.4 ± 6.8 (0.8 – 3.4)	5.5 ± 5.1 (0.4 – 21.9)	5.3 ± 5.1 (0.1 – 24.1)	**< 0.00001** **CON-PLAN: < 0.00001** **CON-NAV: < 0.00001** PLAN-NAV: 0.488
Inferior screw' inclination (mean ± SD, range)	10.5 ± 8.6 (0.5 – 33.1)	4.1 ± 3.1 (0.7 – 13.6)	5 ± 4.6 (0.4 – 18.7)	**< 0.00001** **CON-PLAN: 0.00014** **CON-NAV: 0.0001** PLAN-NAV: 0.51

*When a statistically significant difference was highlighted, multiple comparisons have been made to understand which populations differ more. In **bold**, statistically significant differences.
CON: conventional surgery group; PLAN: planned surgery group; NAV: navigated surgery group.

Table 8.2. *Characteristics of the three groups.*

The three groups were comparable in terms of demographic characteristics, including sex distribution and mean age. In contrast, statistically significant differences emerged across all intraoperative parameters. Regarding the number of implanted screws, a significant difference was observed between the CON and NAV groups ($p = 0.008$), whereas no significant differences were found between the remaining group comparisons. A similar pattern was noted for the frequency of two-screw fixation, with a significant difference between CON and NAV ($p = 0.0106$).

Mean screw length differed significantly among all groups, with the shortest screws used in the CON group (29.1 ± 3.2 mm; range 25–40) and the longest in the NAV group (36.5 ± 4.8 mm; range 22–46). With respect to the use of augmented baseplates, statistically significant differences were observed for CON vs PLAN ($p < 0.00001$) and CON vs NAV ($p < 0.00001$), whereas no difference was detected between PLAN and NAV (p = n.s.).

A similar trend was identified when analysing superior and inferior screw inclination. In both the NAV and PLAN groups, screw trajectories were more parallel to the central peg compared with the CON group, indicating a more controlled and reproducible fixation strategy. Regarding operative time, the only statistically significant difference was found between the PLAN and NAV groups ($p = 0.01$), corresponding to an increase of approximately 11 minutes when intraoperative navigation was used. However, this difference was not considered clinically meaningful.

8.3 Discussion

Baseplate positioning in RSA is fundamental to preventing implant failure, loosening, and biomechanical alterations that may compromise function and clinical outcomes. Baseplate seating, version, inclination, and offset are all essential determinants of implant survival[252,253]. However, native glenoid anatomy is highly variable, even before considering the additional challenges posed by poor bone quality and bone defects in arthritic joints. Accurate positioning and stable fixation are further complicated by the difficulty of achieving adequate exposure, identifying anatomical landmarks, and the inherently small size of the glenoid. Incorrect screw placement may also endanger surrounding soft tissues, including the axillary nerve (inferior screw), the suprascapular nerve (superior screw), and adjacent vascular structures. Although the central fixation element is considered the primary contributor to baseplate stability, screw

number and screw positioning appear to play a secondary role in achieving primary fixation[23,254–258]. Nevertheless, the use of at least two peripheral screws remains recommended—one superior screw directed towards the base of the coracoid process and one inferior screw directed towards the scapular pillar[259]— while additional screws are typically reserved for cases in which adequate fixation cannot otherwise be achieved. Based on currently available evidence, the present study appears to be the only report in the literature analysing the independent contribution of preoperative planning and intraoperative navigation in real-world clinical practice. More specifically, it is the only study to evaluate the practical impact of a surgeon's experience with navigation systems even when navigation is not used during the procedure.

The results of this retrospective analysis demonstrate that the introduction of 3D CT-based preoperative planning and intraoperative navigation leads to a significant modification of glenoid surgical strategy, even when comparing patient groups matched for sex and age. These findings are consistent with previous literature and can be summarised as follows: increased use of augmented baseplates (91% NAV vs 8% CON)[198,260,261], reduced mean screw number (2.1 ± 0.5 NAV vs 2.4 ± 0.7 CON; $p = 0.008$), and increased mean screw length (36.5 ± 4.8 mm NAV vs 29.1 ± 3.2 mm CON; $p < 0.001$)[198,262–265]. Screw trajectory orientation also differed significantly, with screws placed more parallel to the central peg in the NAV group (superior: 5.3°; inferior: 5.0°) compared with the CON group (superior: 12.4°; inferior: 10.5°; $p < 0.001$).

The near-systematic use of augmented baseplates in PLAN (86%) and NAV (91%) underscores the central role of 3D planning in quantifying glenoid bone loss[196,266]. Moreover, the absence of a difference between PLAN and NAV supports the interpretation that the principal effect occurs during the preoperative planning phase, irrespective of whether navigation is subsequently used intraoperatively. Discrepancies reported in some case series[263] may reflect selection bias, as "conventional" procedures may still have been preceded by 3D CT planning, thereby diminishing the apparent contrast between groups.

Regarding screw number, a statistically significant difference in achieving fixation with fewer screws—specifically two screws—was observed only between CON and NAV (2.4 vs 2.1 screws; 71.4% vs 90% two-screw fixation), with no significant differences between PLAN and NAV. This pattern may indicate a learning-curve effect shared by both 3D CT planning and navigation, rather than an effect attributable exclusively to navigation.

In contrast, screw length differed significantly across all groups: NAV had the longest screws, whereas CON had the shortest. This finding suggests two closely related implications. First, real-time feedback provided by intraoperative navigation enables the surgeon to verify drill position continuously and objectively, thereby maximising screw length while maintaining adequate purchase and avoiding cortical perforation—an advantage that cannot be replicated by preoperative planning alone or by conventional techniques. Second, navigation may induce a learning effect capable of modifying surgical technique even in subsequent non-navigated procedures. This hypothesis is supported by the observation that screw trajectory orientation did not differ significantly between NAV and PLAN, suggesting that experience gained through navigation enhances spatial awareness of glenoid anatomy and improves the surgeon's ability to select optimal screw trajectories to engage maximal bone stock.

With respect to operative time, the 11-minute increase observed in NAV compared with PLAN (101 ± 23.2 vs 90.2 ± 24.5 minutes; $p = 0.015$) is attributable to the matching and tracking workflow and is consistent with previous reports[198]. The shorter operative time in PLAN may reflect two interacting factors: accurate preoperative planning facilitates anticipation of intraoperative challenges, and PLAN cases were performed more recently, potentially benefiting from cumulative surgical experience.

This study has limitations, including its retrospective, non-randomised design, which may restrict generalisability. Furthermore, correlations with short- to mid-term clinical outcomes were not assessed. Nevertheless, the single-centre, single-surgeon design and the exclusion of complex cases reduce confounding related to learning curves and to the inclusion of highly complex cases that could bias intraoperative measurements.

Conclusions

To conclude, the findings of this study suggest that systematic implementation of computer-assisted technologies in shoulder arthroplasty results in a substantial shift in surgical paradigm. The transition from a predominantly empirical approach to one grounded in objective, measurable data enables a more rational and personalised surgical strategy. First, 3D CT-based planning—by providing accurate quantification of glenoid bone loss—was associated with a proactive and rational use of augmented baseplates, preserving bone stock and avoiding excessive reaming, with potential long-term biomechanical benefits.

Second, intraoperative navigation appears to be an effective tool for optimising primary mechanical stability: real-time feedback facilitates maximisation of screw length and alignment of screw trajectories more parallel to the central peg, thereby improving bony fixation and reducing the risk of complications associated with suboptimal positioning.

Finally, the adoption of these technologies may contribute to progressive standardisation of surgical performance. The data suggest that experience gained with intraoperative navigation may exert a lasting training effect, positively influencing procedures performed without navigation.

Further short-, mid-, and long-term studies are required to determine whether this technical and radiographic optimisation translates into improved implant survivorship and non-inferior clinical and functional outcomes, as anticipated.

CHAPTER 9 – Short-term clinical outcomes

This chapter analyses short-term clinical and functional outcomes in a consecutive series of patients undergoing reverse shoulder arthroplasty. The comparison focuses on conventional surgery versus procedures performed with intraoperative navigation, evaluating parameters such as joint mobility and VAS pain score, with the aim of determining the true clinical impact of these technological innovations. Parts of this chapter are adapted from our open-access article published in Medicina (https://www.mdpi.com/journal/medicina), distributed under the Creative Commons Attribution (CC BY) license.

9.1 Materials and Methods

9.1.2 Study design

A retrospective observational study was conducted, including all reverse shoulder arthroplasties performed at our Institution up to December 2022. Patients were included according to the following criteria: (1) diagnosis of eccentric glenohumeral osteoarthritis or cuff tear arthropathy, with a healthy contralateral shoulder; (2) RSA performed with preoperative three-dimensional computed tomography (3D CT)-based planning (Advita Shoulder Planning App; BlueOrtho, Gières, France); (3) surgery performed by the same experienced surgeon; (4) use of a single implant model (Equinoxe® Reverse System; Advita Ortho, Gainesville, FL, USA); and (5) completion of a minimum follow-up of 24 months.

Patients with previous scapular or humeral fractures were excluded, as were those undergoing RSA for proximal humeral fractures, revision procedures (for failed proximal humerus osteosynthesis or previous arthroplasty), or cases requiring a custom implant. Patients with a history of surgery on the contralateral shoulder were also excluded.

Patients were divided into two groups according to the surgical technique: the NAV group, comprising procedures performed with intraoperative navigation, and the CONV group, comprising procedures performed with the conventional technique. No allocation criteria based on glenoid defect severity were applied in either group, in order to avoid selection bias. Until 2018, when intraoperative navigation technology was introduced at our centre, all procedures were performed conventionally. Thereafter, conventional surgery was reserved for patients in whom coracoid process damage prevented secure fixation of the scapular tracker

without additional risk, or when validation of the preoperative plan was not available on the day of surgery

9.1.3 Preoperative phase

All patients underwent a preoperative shoulder CT scan and surgical planning using the Advita Shoulder Planning App (BlueOrtho, Gières, France), as described in Chapters 5.1 and 5.2.

9.1.4 Surgical procedure

All procedures were performed by the same senior surgeon, with extensive experience in RSA for both traumatic and chronic degenerative indications. The same implant model was used in all cases. Patients were classified according to whether a conventional or navigated technique was used (as described in Chapter 5.3). To reduce blood loss, tranexamic acid was administered intravenously and intra-articularly when not contraindicated, as previously described[267], and a drain was left in situ for 24 hours.

9.1.5 Postoperative management

All patients followed the same postoperative protocol to minimise variability in functional outcomes attributable to differences in rehabilitation. The arm was immobilised in a 45° abduction brace for 3 weeks, allowing passive shoulder mobilisation while avoiding end-range rotation. This approach reduced tension on the subscapularis and improved prosthetic stability. During this period, active and passive mobilisation of the elbow and wrist was permitted.

After brace removal at 3 weeks, physiotherapy was initiated. Active exercises for forward elevation and abduction were encouraged from the third postoperative week. Rotational movements and strengthening exercises were introduced from the fifth postoperative week. Lifting heavy loads was prohibited for at least 9 weeks and return to unrestricted activities was permitted after 3 months.

9.1.6 Clinical and radiographic assessment

All patients underwent clinical and radiographic follow-up at 1, 3, 6, and 12 months postoperatively, and annually thereafter. Shoulder function was assessed using the Constant Score[231], analysing both absolute values and differences relative to the healthy contralateral

limb. Because the Constant Score (range 0–100) is not particularly accurate for strength assessment and may not fully reflect functional outcomes, some authors recommend comparison with a sex- and age-matched control group[268] or the use of contralateral limb as an individualised reference[269]. Patient-reported outcomes were further assessed using the DASH (Disability of the Arm, Shoulder and Hand) score[270], where 0 represents the best outcome and 100 the worst. True anteroposterior (Grashey) radiographs[271] were obtained at each follow-up visit. Glenoid notching was graded according to the Nerot–Sirveaux classification[177].

9.1.7 Statistical analysis

Normality of quantitative variables was assessed using the Shapiro–Wilk test. Because the data were not normally distributed, non-parametric tests were used for both continuous and categorical variables. Specifically, the Mann–Whitney test was applied for continuous variables, and the Chi-square test for categorical variables, with Yates' correction when the total number of observations ranged between 40 and 200. Fisher's exact test was used for samples smaller than 40 observations.

Statistical significance was set at $p < 0.05$. Non-significant results were reported as "n.s." in the text, while exact p-values were provided in the tables. All analyses were performed using IBM SPSS Statistics for Windows, version 30 (IBM Corp., Armonk, NY, USA).

9.2 Results

A consecutive series of 80 patients met the inclusion criteria, comprising 22 men and 58 women, with a mean age of 74 ± 5.7 years (range 58–84) and a mean follow-up of 41.9 ± 23.6 months (range 24–72). Results were reported at the latest available follow-up. The mean Constant Score was 67 ± 16 points (range 25–91), with a mean difference of 10 ± 10 points (range 0–50) between the operated and contralateral shoulders. The mean DASH score was 20 ± 19 points (range 0.8–84.1).

Differences between the NAV and CONV groups in demographic characteristics, functional outcomes, and complications are presented in Table 9.1.

	NAV	CONV	p
Demographics			
Gender (Male/Female)	16 / 37	6 / 21	0.24
Age (years); mean ± SD (range)	74.6 ± 6 (58-84)	73.8 ± 5 (62-82)	0.41
FU (months); mean ± SD (range)	30 ± 19 (24-71)	54.5 ± 32 (24-108)	**0.002***
Intraoperative characteristics			
Surgical time (min); mean ± SD (range)	98 ± 22 (55-150)	91 ± 22 (55-145)	0.19
Augmented baseplates	36%	25%	0.9
Screws' number; mean ± SD (range)	2 ± 0.5 (2-5)	2.6 ± 0.8 (2-4)	**0.0047***
Screws length (mm); mean ± SD (range)	36 ± 5 (22-46)	31 ± 4 (18-42)	**< 0.00005***
Functional outcomes (points); mean ± SD (range)			
Constant Score	66 ± 16 (25-88)	68 ± 16 (32-91)	0.56
Δ Constant Score	10 ± 10 (0-50)	10 ± 9.6 (0-30)	0.96
DASH Score	18 ± 18 (0.8-84.1)	26.4 ± 23 (0.8-71.7)	0.28
Complications			
Blood transfusion	7.5%	7.4%	0.18
Others	9.4%	11%	1
Revision	5.6%	11%	0.66

Table 9.1. *Characteristics of the NAV and CONV group regarding demographics, implant features, functional outcomes and complication rate. The two groups are homogeneous according to male-female ratio and mean age. In* ***bold*** *statistically significant differences.*

The two groups were comparable in terms of age and sex distribution (p = n.s.); however, the CONV group had a significantly longer mean follow-up (p = 0.002). No statistically significant differences were observed in perioperative blood transfusion requirements, revision rates, functional outcomes (Constant Score and DASH), or overall complication rates.

In the NAV group, five complications were recorded: grade 1 glenoid notching (1 case), an intraoperative humeral fracture not requiring stem modification (1 case), an acromial fracture (1 case), a mesoacromial fracture (1 case), and a late infection (1 case). Three of these complications (the infection and the two acromial/mesoacromial fractures) required revision surgery. In the CONV group, three complications occurred, all requiring revision: late infection (1 case), implant dislocation (1 case), and fracture of the humeral adapter tray component (1 case). No neurovascular injuries were observed in either group. Similarly, the use of augmented baseplates did not differ significantly between groups (p = n.s.).

The NAV group used significantly fewer screws (p = 0.0047) but screws of significantly greater length (p < 0.00005) compared with the CONV group. NAV procedures also required, on average, 7 minutes longer than conventional procedures, although this difference was not statistically significant (p = n.s.).

9.3 Discussion

Reverse shoulder arthroplasty is a well-established surgical procedure for the treatment of advanced cuff tear arthropathy. Over time, its indications have expanded to include eccentric glenohumeral osteoarthritis with severe glenoid deformity[272–274], complex proximal humerus fractures[112,132,275–277], oncological conditions[278] and revision arthroplasty in the presence of substantial bone loss[265]. Despite its clinical success, RSA is associated with a relatively high complication rate—reported between 19% and 68%[208], including haematoma, neurological injury, periprosthetic fractures, infection, instability, dislocation, scapular notching, impingement, acromial fractures, and mechanical failure of the baseplate[265,279].

Among these complications, failure of the glenoid component is one of the most frequent postoperative issues. Inaccurate glenoid positioning has been associated with humeral instability, increased stresses at the bone–implant interface, early implant failure, and suboptimal clinical outcomes[209]. Consequently, accurate positioning and stable fixation of the

baseplate are essential to ensure implant stability, satisfactory postoperative function, and long-term prosthesis survival[80,198,199,210,280,281]. However, achieving these goals is technically demanding due to limited intraoperative visibility, poor definition of bony landmarks, and the complex morphology of the glenoid, particularly in pathological conditions.

For these reasons, appropriate preoperative planning and the use of intraoperative tools capable of supporting the surgeon in reducing technical error play a key role, particularly in shoulder surgery. Three-dimensional CT-based preoperative planning, combined with intraoperative navigation systems, has been progressively adopted to address these challenges. These technologies improve the accuracy of component placement—similarly to what is already established in hip and knee arthroplasty—and promote greater implant stability and preservation of bone stock by enabling the use of fewer but longer screws. These advantages are supported by the existing literature[198,263,279,281]. It has also been demonstrated that using a higher number of screws may reduce the bone stock available for baseplate fixation[258]. This concept, together with the physiological anatomical constraints of the glenoid, is particularly relevant when considering potential revision procedures. Native glenoid bone stock is extremely limited, and its preservation may allow revision arthroplasty using less complex systems, thereby reducing the risk of complications for the patient.

The present study confirms that patients treated with 3D CT-based preoperative planning and intraoperative navigation (NAV group) required fewer screws—but of greater length—compared with the CONV group. These findings are consistent with the literature[198,260,263,279,281,282], particularly with a recent systematic review and meta-analysis[262] reporting comparable results across six clinical studies. Differences emerge, however, regarding baseplate selection. The use of these tools allows the surgeon to better understand patient-specific anatomy and to select the most appropriate baseplate to compensate for bony defects[282]. According to the results of the present study, no differences were found between groups in the use of augmented baseplates, as already described by some authors[263]. In other studies, however, opposite results have been reported[198,260,279,282–284]. This discrepancy may be explained by the fact that all procedures included in the present study were planned using 3D CT, meaning that no true control group existed for the “planning” variable.

With respect to surgical time, the NAV group showed a mean increase of 7 minutes per procedure. This difference is attributable to the time required for image acquisition and

alignment between the 3D CT model and the patient's anatomy. However, this increase was neither statistically nor clinically significant[263,284], unlike what has been reported in some studies[281,283].

Given the relative novelty of intraoperative navigation technology, the currently available literature remains limited and mainly reports short-term results in small patient samples. The present study contributes to this field by confirming the absence of significant differences in objective and subjective outcomes between the NAV and CONV groups. Both the Constant Score and the DASH score were comparable between groups, in agreement with previous studies[260,263,279]. However, interpretation of these findings is not straightforward. Different considerations regarding outcome quality emerge when analysing the absolute Constant Score versus the score difference between the operated and contralateral shoulders. A mean Constant Score of 67 points suggests a moderate result; however, it is well known that this score has limitations in strength assessment and is influenced by factors such as patient age and sex. A more accurate evaluation may involve comparison with a healthy population matched for demographic characteristics[268] or the use of the contralateral shoulder as an individualised reference[269]. In our study, the mean Constant Score difference between the operated and contralateral shoulders was approximately 10 points in both groups, a value indicative of an excellent outcome. Moreover, in 59% of patients, clinical outcomes were comparable to those of the contralateral shoulder, and in 40% of these cases they were even better than those of the non-operated shoulder. This finding highlights the limitations of relying solely on the absolute Constant Score to evaluate real clinical outcomes.

In the present study, complication and revision rates were comparable between the two groups, despite conflicting evidence in the literature[279]. In the NAV group, the complication rate was 9% and included grade 1 scapular notching (1.8%), infection (1.8%), intraoperative humeral fractures (1.8%), acromial fractures (1.8%), and mesoacromial fractures (1.8%). The revision rate in this group was 5.6%.

In the CONV group, the complication rate was slightly higher (11%), with a similar revision rate because all complications required reoperation. Specifically, cases of infection (3.7%), implant dislocation (3.7%), and humeral tray component fracture (3.7%) were observed. These results are consistent with previous studies[260,279,285]. No neurovascular injuries were detected in either group. This finding is particularly relevant, as it supports the safety of these new technologies—

especially intraoperative navigation—which allows insertion of longer screws while reducing the risk of injury to neurovascular structures.

No significant differences in transfusion rates were found between the two groups (7.5% vs 7.4%), likely due to the adoption of a standardised intraoperative blood-loss management protocol applied uniformly to all patients in the absence of contraindications.

This study has several strengths as well as limitations. All procedures were performed by a single experienced surgeon, reducing operator-related variability and the influence of the learning curve typically associated with navigation systems on operative time. Although this may be considered a limitation, in studies with relatively small sample sizes—such as the present one—it can also represent a strength by reducing potential operator-related bias. In addition, patients were not preselected based on the complexity of the glenoid defect, limiting the risk of bias in postoperative outcomes related to defect severity.

The sample size of 80 patients is reasonably representative; however, the unequal distribution between the NAV and CONV groups may limit generalisability. Moreover, follow-up duration was significantly longer in the CONV group, which may have contributed to the higher complication rate observed in this group, although the difference was not statistically significant. Similarly, follow-up in the NAV group can still be considered short term; therefore, some complications—such as glenoid component loosening—may not yet have occurred. Considering that longer screws provide more stable baseplate fixation, the hypothesis is that, in the long term, the revision rate may remain stable and potentially lower than that associated with conventional procedures; however, this hypothesis must be confirmed by long-term studies.

Finally, the retrospective design represents an additional limitation. Although the results are consistent with the existing literature, prospective studies with longer follow-up are needed to clarify definitively the potential benefits of intraoperative navigation technology.

9.4 Conclusions

The combination of 3D CT-based preoperative planning and intraoperative navigation proved to be a safe and reliable strategy, yielding clinical outcomes comparable to those achieved with standard instrumentation and without increasing the risk of complications. The principal advantages include enhanced implant stability through the accurate placement of fewer but

longer screws, thereby optimising fixation while preserving native bone stock—an aspect of particular importance in the context of potential future revision procedures.

Given the relatively recent introduction of these technologies, long-term data regarding complication rates and implant survivorship are not yet available. Further prospective studies with extended follow-up are therefore required to fully elucidate the potential long-term benefits of intraoperative navigation.

CHAPTER 10 – General conclusions

Management of glenoid bone loss remains one of the principal challenges in reverse shoulder arthroplasty, as it critically affects implant stability, optimal baseplate positioning, and ultimately clinical and functional outcomes. In recent years, the introduction of advanced technologies—such as three-dimensional CT-based planning, intraoperative navigation, and artificial intelligence systems—has profoundly reshaped both surgical decision-making and operative execution. These developments have raised new questions regarding the influence of surgeon experience, the degree to which decisions can be standardised, and the true added value of these tools in everyday clinical practice.

This doctoral work approached the topic from an integrated perspective, systematically analysing the contribution of new technologies across the entire RSA pathway: from preoperative planning, through intraoperative decision-making to postoperative clinical outcomes. The overall findings allow several scientifically and clinically relevant considerations to be drawn.

The first original contribution of this thesis is the demonstration that, even among experienced surgeons, RSA planning in the presence of glenoid bone loss is characterised by substantial individual variability. Low interobserver agreement at the level of the single planner indicates that the selection of baseplate type, augment configuration, and angular correction is strongly influenced by personal preferences, prior experience, and individual interpretation of pathological anatomy. However, the aggregated analysis revealed that this variability is not random. When decisions are examined at the group level, they converge towards rational and reproducible patterns. The high reliability of mean measurements and the significant association between glenoid defect type and corrective strategy suggest the presence of shared biomechanical principles that implicitly guide surgical decision-making. This finding supports the notion that 3D planning does not eliminate variability, but rather renders its structure explicit, thereby providing a foundation for the development of evidence-based protocols.

The second axis of this thesis involved a critical appraisal of artificial intelligence systems applied to RSA. Predict+—described in the literature as a machine-learning–based prediction tool for shoulder arthroplasty—serves as an illustrative example of this class of systems. The analysis demonstrated that aggregated outcome predictions are generally accurate and

clinically meaningful, indicating a potential role for AI as a population-level decision-support instrument. Nevertheless, the weak correlation observed at the individual level highlights the current limitations of these systems in achieving true patient-specific personalisation. These results indicate that, at present, artificial intelligence cannot replace the surgeon's clinical judgement but may complement it by providing probabilistic information that can support counselling and strategic planning. Looking ahead, the incorporation of larger and more diverse datasets, more detailed anatomical variables, and longitudinal follow-up data may enhance the individual predictive performance of such systems.

The third contribution of this thesis demonstrates that advanced planning and intraoperative navigation significantly influence surgical execution, even in expert hands. The increased use of augmented baseplates, the selection of longer screws, and the reduction in the number of screws collectively suggest heightened awareness of residual bone quality and a more targeted fixation strategy. These findings imply that navigation does not merely enhance geometric precision but may also promote standardisation of intraoperative decisions by reducing technical variability and increasing reproducibility of the surgical act. This aspect is particularly relevant for surgical training, skill transferability, and overall operative safety.

Comparison of clinical outcomes between navigated and conventional RSA revealed comparable mid-term results, confirming the non-inferiority of navigation-assisted surgery relative to the traditional technique. This observation aligns with current literature and underscores that the value of new technologies should not be sought solely in immediate improvements in clinical outcomes. Rather, their contribution lies in enhancing the quality of decision-making, improving execution precision, and reducing technical errors. From this perspective, the technologies examined in this thesis can be regarded as enabling tools that support surgeons in managing complex cases.

Overall, this thesis indicates that 3D planning and intraoperative navigation are safe and effective tools that can render glenoid management in RSA more standardisable and traceable. In contrast, AI-based predictive models currently exhibit only partial clinical maturity, requiring more representative datasets, more detailed anatomical variables, and more robust external validation. Prospective, multicentre studies with longer follow-up will be essential to clarify the impact of these technologies on implant survivorship, healthcare costs, and the long-term reduction of complications.

REFERENCES

1. Howell S, Galinat B. The glenoid-labral socket. A constrained articular surface. *Clin Orthop Relat Res*. 243:122-125.
2. Cole BJ, Provencher MT. Safety Profile of Bioabsorbable Shoulder Anchors. *Arthrosc - J Arthrosc Relat Surg*. 2007;23(8):912-913. doi:10.1016/j.arthro.2007.06.003
3. Cuéllar R, Ruiz-Ibán MA, Cuéllar A. Anatomy and Biomechanics of the Unstable Shoulder. *Open Orthop J*. 2017;11(1):919-933. doi:10.2174/1874325001711010919
4. Gil JA, DeFroda S, Owens BD. Current Concepts in the Diagnosis and Management of Traumatic, Anterior Glenohumeral Subluxations. *Orthop J Sport Med*. 2017;5(3). doi:10.1177/2325967117694338
5. Neer CS 2nd. Displaced proximal humeral fractures. I. Classification and evaluation. *J Bone Jt Surg Am*. 52((6)):1077-1089.
6. Walch G, Badet R, Boulahia A, Khoury A. Morphologic study of the glenoid in primary glenohumeral osteoarthritis. *J Arthroplasty*. 1999;14(6):756-760. doi:10.1016/S0883-5403(99)90232-2
7. Ide J, Maeda S, Takagi K. Normal Variations of the Glenohumeral Ligament Complex: An Anatomic Study for Arthroscopic Bankart Repair. *Arthrosc - J Arthrosc Relat Surg*. 2004;20(2):164-168. doi:10.1016/j.arthro.2003.11.005
8. Fox AJS, Fox OJK, Schär MO, Chaudhury S, Warren RF, Rodeo SA. The glenohumeral ligaments: Superior, middle, and inferior: Anatomy, biomechanics, injury, and diagnosis. *Clin Anat*. 2021;34(2):283-296. doi:10.1002/CA.23717
9. Boardman ND, Debski RE, Warner JJ, et al. Tensile properties of the superior glenohumeral and coracohumeral ligaments. *J Shoulder Elbow Surg*. 1996;5(4):249-254. doi:10.1016/S1058-2746(96)80050-4
10. Ticker JB, Bigliani LU, Soslowsky LJ, Pawluk RJ, Flatow EL, Mow VC. Inferior glenohumeral ligament: geometric and strain-rate dependent properties. *J Shoulder Elbow Surg*. 1996;5(4):269-279. doi:10.1016/S1058-2746(96)80053-X
11. Ticker JB, Flatow EL, Pawluk RJ, et al. The inferior glenohumeral ligament: A correlative investigation. *J Shoulder Elb Surg*. 2006;15(6):665-674. doi:10.1016/j.jse.2005.11.006
12. Anastasi G, Capitani S, Carnazza M, et al. *Trattato Di Anatomia Umana, Vol. 1*.
13. Iannotti J, Richard DP. *Netter. Atlante Di Anatomia. Fisiopatologia e Clinica. Apparato Locomotore. Vol. 1: Arto Superiore*.; 2013.
14. McCausland C, Sawyer E, Eovaldi B, Varacallo M. *Anatomy, Shoulder and Upper Limb, Shoulder Muscles*.; 2022.
15. DeFranco MJ, Cole BJ. Current perspectives on rotator cuff anatomy. *Arthroscopy*. 2009;25(3):305-320. doi:10.1016/J.ARTHRO.2008.07.023
16. Gupta H, Robinson P. Normal shoulder ultrasound: anatomy and technique. *Semin Musculoskelet Radiol*. 2015;19(3):203-211. doi:10.1055/S-0035-1549315
17. Maruvada S, Madrazo-Ibarra, A Varacallo M. *Anatomy, Rotator Cuff*.; 2022.
18. Burkhead WZ, Scheinberg RR, Box G. Surgical anatomy of the axillary nerve. *J shoulder Elb Surg*. 1992;1(1):31-36. doi:10.1016/S1058-2746(09)80014-1
19. Flatow EL, Bigliani LU, April EW. An anatomic study of the musculocutaneous nerve and its relationship to the coracoid process. *Clin Orthop Relat Res*. 1989;244:166-171.
20. Yang HJ, Gil YC, Jin JD, Ahn SV, Lee HY. Topographical anatomy of the suprascapular nerve and vessels at the suprascapular notch. *Clin Anat*. 2012;25(3):359-365. doi:10.1002/CA.21248
21. Bakhsh W, Nicandri G. Anatomy and Physical Examination of the Shoulder. *Sports Med*

Arthrosc. 2018;26(3):e10-e22. doi:10.1097/JSA.0000000000000202
22. Cooper D, O'Brien S, Warren R. Supporting layers of the glenohumeral joint. An anatomic study. *Clin Orthop Relat Re*. 1993;Apr(289):144-145.
23. Franceschi F, Giovannetti E, Sanctis D, Gupta A, Athwal GS, Di G. Reverse Shoulder Arthroplasty -State of the Art Reverse shoulder arthroplasty : State-of-the-art. *J ISAKOS*. 2023;(June). doi:10.1016/j.jisako.2023.05.007
24. Merolla G, Paladini P, Campi F, Porcellini G. Efficacy of anatomical prostheses in primary glenohumeral osteoarthritis. *Chir Organi Mov*. 2008;91(2):109-115. doi:10.1007/S12306-007-0019-Y
25. Merolla G, Ciaramella G, Fabbri E, Walch G, Paladini P, Porcellini G. Total shoulder replacement using a bone ingrowth central peg polyethylene glenoid component: a prospective clinical and computed tomography study with short- to mid-term follow-up. *Int Orthop*. 2016;40(11):2355-2363. doi:10.1007/S00264-016-3255-7
26. Matsen FA, Iannotti JP, Churchill RS, et al. One and two-year clinical outcomes for a polyethylene glenoid with a fluted peg: one thousand two hundred seventy individual patients from eleven centers. *Int Orthop*. 2019;43(2):367-378. doi:10.1007/S00264-018-4213-3
27. Merolla G, Cerciello S, Marenco S, Fabbri E, Paladini P, Porcellini G. Comparison of shoulder replacement to treat osteoarthritis secondary to instability surgery and primary osteoarthritis: a retrospective controlled study of patient outcomes. *Int Orthop*. 2018;42(9):2147-2157. doi:10.1007/S00264-018-3969-9
28. Merolla G, Chin P, Sasyniuk TM, Paladini P, Porcellini G. Total shoulder arthroplasty with a second-generation tantalum trabecular metal-backed glenoid component: Clinical and radiographic outcomes at a mean follow-up of 38 months. *Bone Joint J*. 2016;98-B(1):75-80. doi:10.1302/0301-620X.98B1.36620
29. Neer CS, Craig E V., Fukuda H. Cuff-tear arthropathy. *J Bone Joint Surg Am*. 1983;65(9):1232-1244. doi:10.2106/00004623-198365090-00003
30. Stratton JA, Bayer SH, Arner JW. Reverse Shoulder Arthroplasty: History, Indications, Design, Outcomes, and Complications. *Oper Tech Orthop*. 2024;34(4):101149. doi:10.1016/j.oto.2024.101149
31. Franklin JL, Barrett WP, Jackins SE, Matsen 3rd FA. Glenoid loosening in total shoulder arthroplasty. Association with rotator cuff deficiency. *J Arthroplast*. Published online 1988.
32. Boileau P, Watkinson DJ, Hatzidakis AM, Balg F. Grammont reverse prosthesis : Design , rationale , and biomechanics. *J Shoulder Elb Surg*. Published online 2005:147-161. doi:10.1016/j.jse.2004.10.006
33. Grammont P, Trouillod P, Laffay J, Deries X. Study and development of a new shoulder prosthesis [Article in French]. *Rhumatologie*. 1987;(39):407-418.
34. Grammont PM, Baulot E. Delta shoulder prosthesis for rotator cuff rupture. *Orthopedics*. 1993;16(1):65-68. doi:10.3928/0147-7447-19930101-11
35. Roche CP. Reverse Shoulder Arthroplasty Biomechanics. *J Funct Morphol Kinesiol*. 2022;7(1). doi:10.3390/JFMK7010013
36. Werthel J, Walch G, Vegehan E, et al. Lateralization in reverse shoulder arthroplasty : a descriptive analysis of different implants in current practice. Published online 2019.
37. Cogan CJ, Ho JC, Entezari V, Iannotti JP, Ricchetti ET. The Influence of Reverse Total Shoulder Arthroplasty Implant Design on Biomechanics. *Curr Rev Musculoskelet Med*. Published online 2023:95-102. doi:10.1007/s12178-023-09820-8
38. Sirveaux F, Favard L, Oudet D, et al. Grammont inverted total shoulder arthroplasty in the treatment of glenohumeral osteoarthritis with massive rupture of the cuff RESULTS

OF A MULTICENTRE STUDY OF 80 SHOULDERS. *J Bone Jt Surg [Br]*. 2004;86:388-395. doi:10.1302/0301-620X.86B3

39. Werner C, Steinmann P, Gilbart M, Gerber C. Treatment of painful pseudoparesis due to irreparable rotator cuff dysfunction with the Delta III reverse-ball-and-socket total shoulder prosthesis. *J Bone Joint Surg Am*. 2005;87(7):1476-1486. doi:10.2106/JBJS.D.02342
40. Naveed MA, Kitson J, Bunker TD. The Delta III reverse shoulder replacement for cuff tear arthropathy: a single-centre study of 50 consecutive procedures. *J Bone Joint Surg Br*. 2011;93(1):57-61. doi:10.1302/0301-620X.93B1.24218
41. Boileau P, Moineau G, Roussanne Y, O'Shea K. Bony Increased Offset-Reversed Shoulder Arthroplasty (BIO-RSA). *JBJS Essent Surg Tech*. 2017;7(4):e37. doi:10.2106/JBJS.ST.17.00006
42. Katz D, Valenti P, Kany J, Elkholti K, Werthel JD. Does lateralisation of the centre of rotation in reverse shoulder arthroplasty avoid scapular notching? Clinical and radiological review of one hundred and forty cases with forty five months of follow-up. *Int Orthop*. 2016;40(1):99-108. doi:10.1007/S00264-015-2976-3
43. Mulieri P, Dunning P, Klein S, Pupello D, Frankle M. Reverse shoulder arthroplasty for the treatment of irreparable rotator cuff tear without glenohumeral arthritis. *J Bone Joint Surg Am*. 2010;92(15):2544-2556. doi:10.2106/JBJS.I.00912
44. Routman H, Flurin P, Wright T, Zuckerman J, Hamilton M, Roche C. Reverse Shoulder Arthroplasty Prosthesis Design Classification System. *Bull Hosp Jt Dis*. 2013;Dec(73 Suppl 1):S5-14.
45. Roche C, Diep P, Hamilton M, et al. Impact of inferior glenoid tilt, humeral retroversion, bone grafting, and design parameters on muscle length and deltoid wrapping in reverse shoulder arthroplasty. *Bull Hosp Jt Dis*. 2013;71(4):284-293.
46. Ackland DC, Patel M, Knox D. Prosthesis design and placement in reverse total shoulder arthroplasty. *J Orthop Surg Res*. Published online 2015:1-9. doi:10.1186/s13018-015-0244-2
47. Familiari F, Rojas J, Doral MN, Mcfarland EG. Shoulder & Elbow Reverse total shoulder arthroplasty. 2018;3(February). doi:10.1302/2058-5241.3.170044
48. Lädermann A, Walch G, Denard PJ, et al. Reverse shoulder arthroplasty in patients with pre-operative impairment of the deltoid muscle. *Bone Joint J*. 2013;95-B(8):1106-1113. doi:10.1302/0301-620X.95B8.31173
49. Harkness EF, Macfarlane GJ, Silman AJ, McBeth J. Is musculoskeletal pain more common now than 40 years ago?: Two population-based cross-sectional studies. *Rheumatology (Oxford)*. 2005;44(7):890-895. doi:10.1093/RHEUMATOLOGY/KEH599
50. Cadogan A, Laslett M, Hing WA, McNair PJ, Coates MH. A prospective study of shoulder pain in primary care: prevalence of imaged pathology and response to guided diagnostic blocks. *BMC Musculoskelet Disord*. 2011;12. doi:10.1186/1471-2474-12-119
51. Ibounig T, Simons T, Launonen A, Paavola M. Glenohumeral osteoarthritis: an overview of etiology and diagnostics. *Scand J Surg*. 2021;110(3):441-451. doi:10.1177/1457496920935018
52. Kerr R, Resnick D, Pineda C, Haghighi P. Osteoarthritis of the glenohumeral joint: a radiologic-pathologic study. *AJR Am J Roentgenol*. 1985;144(5):967-972. doi:10.2214/AJR.144.5.967
53. Neer 2nd C. Replacement arthroplasty for glenohumeral osteoarthritis. *J Bone Jt Surg Am*. 1974;Jan(56(1)):1-13.
54. Saltzman MD, Mercer DM, Warme WJ, Bertelsen AL, Matsen FA. Comparison of patients undergoing primary shoulder arthroplasty before and after the age of fifty. *J Bone Joint*

Surg Am. 2010;92(1):42-47. doi:10.2106/JBJS.I.00071
55. Kobayashi T, Takagishi K, Shitara H, et al. Prevalence of and risk factors for shoulder osteoarthritis in Japanese middle-aged and elderly populations. *J Shoulder Elb Surg*. 2014;23(5):613-619. doi:10.1016/j.jse.2013.11.031
56. Oh JH, Chung SW, Oh CH, et al. The prevalence of shoulder osteoarthritis in the elderly Korean population: Association with risk factors and function. *J Shoulder Elb Surg*. 2011;20(5):756-763. doi:10.1016/j.jse.2011.01.021
57. Dieppe PA, Lohmander LS. Pathogenesis and management of pain in osteoarthritis. *Lancet*. 2005;365(9463):965-973. doi:10.1016/S0140-6736(05)71086-2
58. Fernandez-Moreno M, Rego I, Carreira-Garcia V, Blanco F. Genetics in osteoarthritis. *Curr Genomics*. 2008;9(8):542-547. doi:10.2174/138920208786847953
59. Loughlin J. Genetic contribution to osteoarthritis development: current state of evidence. *Curr Opin Rheumatol*. 2015;27(3):284-288. doi:10.1097/BOR.0000000000000171
60. Chapman K, Valdes AM. Genetic factors in OA pathogenesis. *Bone*. 2012;51(2):258-264. doi:10.1016/j.bone.2011.11.026
61. Thijssen E, Van Caam A, Van Der Kraan PM. Obesity and osteoarthritis, more than just wear and tear: pivotal roles for inflamed adipose tissue and dyslipidaemia in obesity-induced osteoarthritis. *Rheumatology (Oxford)*. 2015;54(4):588-600. doi:10.1093/RHEUMATOLOGY/KEU464
62. Tu C, He J, Wu B, Wang W, Li Z. An extensive review regarding the adipokines in the pathogenesis and progression of osteoarthritis. *Cytokine*. 2019;113:1-12. doi:10.1016/j.cyto.2018.06.019
63. Kavaja L, Pajarinen J, Sinisaari I, et al. Arthrosis of glenohumeral joint after arthroscopic Bankart repair: A long-term follow-up of 13 years. *J Shoulder Elb Surg*. 2012;21(3):350-355. doi:10.1016/j.jse.2011.04.023
64. Hovelius L, Saeboe M. Neer Award 2008: Arthropathy after primary anterior shoulder dislocation-223 shoulders prospectively followed up for twenty-five years. *J Shoulder Elb Surg*. 2009;18(3):339-347. doi:10.1016/j.jse.2008.11.004
65. Van Der Zwaag HM, Brand R, Obermann WR, Rozing PM. Glenohumeral osteoarthrosis after Putti-Platt repair. *J Shoulder Elb Surg*. 1999;8(3):252-258. doi:10.1016/S1058-2746(99)90138-6
66. Plath JE, Aboalata M, Seppel G, et al. Prevalence of and Risk Factors for Dislocation Arthropathy: Radiological Long-term Outcome of Arthroscopic Bankart Repair in 100 Shoulders at an Average 13-Year Follow-up. *Am J Sports Med*. 2015;43(5):1084-1090. doi:10.1177/0363546515570621
67. Marx RG, McCarty EC, Montemurno TD, Altchek DW, Craig E V., Warren RF. Development of arthrosis following dislocation of the shoulder: A case-control study. *J Shoulder Elb Surg*. 2002;11(1):1-5. doi:10.1067/mse.2002.119388
68. Ruosi L, Dubini L, Faoro M, Castagna A. Artropatia di cuffia : iter diagnostico e terapeutico. Published online 2022:63-67.
69. Hamada K, Yamanaka K, Uchiyama Y, Mikasa T, Mikasa M. A radiographic classification of massive rotator cuff tear arthritis. *Clin Orthop Relat Res*. 2011;469(9):2452-2460. doi:10.1007/S11999-011-1896-9
70. Hamada K, Fukud H, Mikasa M, Kobayashi Y. Roentgenographic findings in massive rotator cuff tears. A long-term observation. *Clin Orthop Relat Res*. 1990;254:92-96.
71. Walch G, Edwards TB, Boulahia A, Nové-Josserand L, Neyton L, Szabo I. Arthroscopic tenotomy of the long head of the biceps in the treatment of rotator cuff tears: Clinical and radiographic results of 307 cases. *J Shoulder Elb Surg*. 2005;14(3):238-246. doi:10.1016/j.jse.2004.07.008

72. Cuff D, Pupello D, Virani N, Levy J, Frankle M. Reverse shoulder arthroplasty for the treatment of rotator cuff deficiency. *J Bone Joint Surg Am*. 2008;90(6):1244-1251. doi:10.2106/JBJS.G.00775
73. Matsen FA, Papadonikolakis A. Published evidence demonstrating the causation of glenohumeral chondrolysis by postoperative infusion of local anesthetic via a pain pump. *J Bone Joint Surg Am*. 2013;95(12):1126-1134. doi:10.2106/JBJS.L.01104
74. Zaid MB, Young NM, Pedoia V, Feeley BT, Ma CB, Lansdown DA. Anatomic shoulder parameters and their relationship to the presence of degenerative rotator cuff tears and glenohumeral osteoarthritis: a systematic review and meta-analysis. *J Shoulder Elb Surg*. 2019;28(12):2457-2466. doi:10.1016/j.jse.2019.05.008
75. Moor BK, Bouaicha S, Rothenfluh DA, Sukthankar A, Gerber C. Is there an association between the individual anatomy of the scapula and the development of rotator cuff tears or osteoarthritis of the glenohumeral joint?: A radiological study of the critical shoulder angle. *Bone Joint J*. 2013;95-B(7):935-941. doi:10.1302/0301-620X.95B7.31028
76. Harper KW, Helms CA, Haystead CM, Higgins LD. Glenoid dysplasia: incidence and association with posterior labral tears as evaluated on MRI. *AJR Am J Roentgenol*. 2005;184(3):984-988. doi:10.2214/AJR.184.3.01840984
77. Allen B, Schoch B, Sperling JW, Cofield RH. Shoulder arthroplasty for osteoarthritis secondary toglenoid dysplasia: An update. *J Shoulder Elb Surg*. 2014;23(2):214-220. doi:10.1016/j.jse.2013.05.012
78. Johnson MH, Paxton ES, Green A. Shoulder arthroplasty options in young (<50 years old) patients: Review of current concepts. *J Shoulder Elb Surg*. 2015;24(2):317-325. doi:10.1016/j.jse.2014.09.029
79. Bonnevialle N, Mansat P, Mansat M, Bonnevialle P. Hemiarthroplasty for osteoarthritis in shoulder with dysplastic morphology. *J Shoulder Elb Surg*. 2011;20(3):378-384. doi:10.1016/j.jse.2010.07.006
80. Colasanti GB, Troiano E, De Sensi AG, et al. A Reverse Shoulder Arthroplasty Implantation With Custom-Made Humerus and Intraoperative GPS Navigation in a Rare Case of Unilateral Hip and Shoulder Dysplasia Associated With a Bone Marrow Mosaic PTEN Truncating Variant: Case Report. *J shoulder Elb Arthroplast*. 2023;7. doi:10.1177/24715492231211123
81. Kambhampati SBS, Birch R, Cobiella C, Chen L. Posterior subluxation and dislocation of the shoulder in obstetric brachial plexus palsy. *J Bone Joint Surg Br*. 2006;88(2):213-219. doi:10.1302/0301-620X.88B2.17185
82. Pearl ML, Edgerton BW, Kon DS, et al. Comparison of arthroscopic findings with magnetic resonance imaging and arthrography in children with glenohumeral deformities secondary to brachial plexus birth palsy. *J Bone Joint Surg Am*. 2003;85(5):890-898. doi:10.2106/00004623-200305000-00018
83. Randelli P, Della Valle A. *Ortopedia e Traumatologia. Piccin*.; 2023.
84. Wu KA, Kugelman DN, Seidelman JL, Seyler TM. Native Joint Septic Arthritis. *Antibiot (Basel, Switzerland)*. 2024;13(7). doi:10.3390/ANTIBIOTICS13070596
85. Parsons IV IM, Weldon EJ, Titelman RM, Smith KL. Glenohumeral arthritis and its management. *Phys Med Rehabil Clin N Am*. 2004;15(2):447-474. doi:10.1016/j.pmr.2003.12.001
86. Matsen 3rd FA, Wirth M. Glenohumeral arthritis and its management. In: *The Shoulder (Rockwood & Matsen, Saunders)*. ; 1998:840-964.
87. Hasan SS, Romeo AA. Nontraumatic osteonecrosis of the humeral head. *J Shoulder Elb Surg*. 2002;11(3):281-298. doi:10.1067/mse.2002.124347
88. Hernigou P, Hernigou J, Scarlat M. Shoulder Osteonecrosis: Pathogenesis, Causes,

Clinical Evaluation, Imaging, and Classification. *Orthop Surg*. 2020;12(5):1340-1349. doi:10.1111/OS.12788
89. Zuo J, Sano H, Yamamoto N, et al. Humeral head osteonecrosis in an adolescent amateur swimming athlete: a case report. *Sports Med Arthrosc Rehabil Ther Technol*. 2012;4(1). doi:10.1186/1758-2555-4-39
90. Lehtinen J, Kaarela K, Belt E, Jautiainen H, MJ K, Lehto M. Incidence of glenohumeral joint involvement in seropositive rheumatoid arthritis. A 15 year endpoint study. *J Rheumatol*. 2000;Feb(27(2)):347-350.
91. Thomas T, Noël E, Goupille P, Duquesnoy B, Combe B. The rheumatoid shoulder: Current consensus on diagnosis and treatment. *Jt Bone Spine*. 2006;73(2):139-143. doi:10.1016/j.jbspin.2005.03.013
92. Snoddy MC, Lee DH, Kuhn JE. Charcot shoulder and elbow: a review of the literature and update on treatment. *J Shoulder Elb Surg*. 2017;26(3):544-552. doi:10.1016/j.jse.2016.10.015
93. Wang X, Li Y, Gao J, Wang T, Li Z. Charcot arthropathy of the shoulder joint as a presenting feature of basilar impression with syringomyelia: A case report and literature review. *Medicine (Baltimore)*. 2018;97(28). doi:10.1097/MD.0000000000011391
94. Dieppe PA, Doherty M, Macfarlane DG, Hutton CW, Bradfield JW, Watt I. Apatite associated destructive arthritis. *Br J Rheumatol*. 1984;23(2):84-91. doi:10.1093/RHEUMATOLOGY/23.2.84
95. Sevivas N, Ferreira N, Andrade R, et al. Reverse shoulder arthroplasty for irreparable massive rotator cuff tears: a systematic review with meta-analysis and meta-regression. *J Shoulder Elb Surg*. 2017;26(9):e265-e277. doi:10.1016/j.jse.2017.03.039
96. Boileau P, Baqué F, Valerio L, Ahrens P, Chuinard C, Trojani C. Isolated arthroscopic biceps tenotomy or tenodesis improves symptoms in patients with massive irreparable rotator cuff tears. *J Bone Joint Surg Am*. 2007;89(4):747-757. doi:10.2106/JBJS.E.01097
97. Gartsman GM. Massive, irreparable tears of the rotator cuff. Results of operative debridement and subacromial decompression. *J Bone Joint Surg Am*. 1997;79(5):715-721. doi:10.2106/00004623-199705000-00011
98. Gerber C. Latissimus dorsi transfer for the treatment of irreparable tears of the rotator cuff. *Clin Orthop Relat Res*. 1992;Feb(275):152-160.
99. Gerber C, Maquieira G, Espinosa N. Latissimus dorsi transfer for the treatment of irreparable rotator cuff tears. *J Bone Jt Surg*. 2006;88(1):113-120. doi:10.2106/JBJS.E.00282
100. Miniaci A, MacLeod M. Transfer of the latissimus dorsi muscle after failed repair of a massive tear of the rotator cuff. A two to five-year review. *J Bone Joint Surg Am*. 1999;81(8):1120-1127. doi:10.2106/00004623-199908000-00007
101. Nové-Josserand L, Costa P, Liotard JP, Safar JF, Walch G, Zilber S. Results of latissimus dorsi tendon transfer for irreparable cuff tears. *Orthop Traumatol Surg Res*. 2009;95(2):108-113. doi:10.1016/j.otsr.2008.10.002
102. Mihata T, Lee TQ, Watanabe C, et al. Clinical results of arthroscopic superior capsule reconstruction for irreparable rotator cuff tears. *Arthroscopy*. 2013;29(3):459-470. doi:10.1016/J.ARTHRO.2012.10.022
103. Mihata T, McGarry MH, Pirolo JM, Kinoshita M, Lee TQ. Superior capsule reconstruction to restore superior stability in irreparable rotator cuff tears: a biomechanical cadaveric study. *Am J Sports Med*. 2012;40(10):2248-2255. doi:10.1177/0363546512456195
104. Cuff DJ, Pupello DR, Santoni BG. Partial rotator cuff repair and biceps tenotomy for the treatment of patients with massive cuff tears and retained overhead elevation: midterm outcomes with a minimum 5 years of follow-up. *J Shoulder Elb Surg*. 2016;25(11):1803-

1809. doi:10.1016/j.jse.2016.04.001
105. Berth A, Neumann W, Awiszus F, Pap G. Massive rotator cuff tears: functional outcome after debridement or arthroscopic partial repair. *J Orthop Traumatol*. 2010;11(1):13-20. doi:10.1007/S10195-010-0084-0
106. Esch JC, Ozerkis LR, Helgager JA, Kane N, Lilliott N. Arthroscopic subacromial decompression: Results according to the degree of rotator cuff tear. *Arthroscopy*. 1988;4(4):241-249. doi:10.1016/S0749-8063(88)80038-0
107. Gartsman GM. Massive, irreparable tears of the rotator cuff. Results of operative debridement and subacromial decompression. *J Bone Joint Surg Am*. 1997;79(5):715-721. doi:10.2106/00004623-199705000-00011
108. Ogilvie-Harris DJ, Demaziere A. Arthroscopic debridement versus open repair for rotator cuff tears. A prospective cohort study. *J Bone Joint Surg Br*. 1993;75(3):416-420. doi:10.1302/0301-620X.75B3.8496210
109. Boileau P, Gonzalez JF, Chuinard C, Bicknell R, Walch G. Reverse total shoulder arthroplasty after failed rotator cuff surgery. *J Shoulder Elb Surg*. 2009;18(4):600-606. doi:10.1016/j.jse.2009.03.011
110. Hartzler RU, Steen BM, Hussey MM, et al. Reverse shoulder arthroplasty for massive rotator cuff tear: risk factors for poor functional improvement. *J shoulder Elb Surg*. 2015;24(11):1698-1706. doi:10.1016/J.JSE.2015.04.015
111. Iglesias-Rodríguez S, Domínguez-Prado DM, García-Reza A, et al. Epidemiology of proximal humerus fractures. *J Orthop Surg Res*. 2021;16(1):1-11. doi:10.1186/s13018-021-02551-x
112. Antonios T, Bakti N, Phadkhe A, Gulihar A, Singh B. Outcomes following arthroplasty for proximal humeral fractures. *J Clin Orthop Trauma*. 2020;11:S31-S36. doi:10.1016/j.jcot.2019.07.008
113. Klug A, Gramlich Y, Wincheringer D, Schmidt-Horlohé K, Hoffmann R. Trends in surgical management of proximal humeral fractures in adults: a nationwide study of records in Germany from 2007 to 2016. *Arch Orthop Trauma Surg*. 2019;139(12):1713-1721. doi:10.1007/s00402-019-03252-1
114. Beks RB, Ochen Y, Frima H, et al. Operative versus nonoperative treatment of proximal humeral fractures: a systematic review, meta-analysis, and comparison of observational studies and randomized controlled trials. *J Shoulder Elb Surg*. 2018;27(8):1526-1534. doi:10.1016/j.jse.2018.03.009
115. Murray IR, Amin AK, White TO, Robinson CM. Proximal humeral fractures: Current concepts in classification, treatment and outcomes. *J Bone Jt Surg - Ser B*. 2011;93 B(1):1-11. doi:10.1302/0301-620X.93B1.25702
116. Caffarelli C, Mondanelli N, Crainz E, Giannotti S, Frediani B, Gonnelli S. The Phenotype of Bone Turnover in Patients with Fragility Hip Fracture: Experience in a Fracture Liaison Service Population. *Int J Environ Res Public Health*. 2022;19(12). doi:10.3390/ijerph19127362
117. Pavone V, Vescio A, Denaro R, et al. Use of different plate implants for surgical treatment of proximal humerus fractures in adults: A systematic review. *Acta Biomed*. 2021;92(4). doi:10.23750/abm.v92i4.11394
118. Antonios T, Bakti N, Nzeako O, Mohanlal P, Singh B. Outcomes following fixation for proximal humeral fractures. *J Clin Orthop Trauma*. 2019;10(3):468-473. doi:10.1016/j.jcot.2019.01.029
119. Lopiz Y, García-Fernandez C, Vallejo-Carrasco M, et al. Reverse shoulder arthroplasty for proximal humeral fracture in the elderly. Cemented or uncemented stem? *Int Orthop*. 2022;46(3):635-644. doi:10.1007/s00264-021-05284-y

120. Dines DM, Dines JS. Hemiarthroplasty for Complex Four-Part Fracture of the Proximal Humerus : Technical Considerations and. 2002;(October):29-36.
121. Gupta AK, Harris JD, Erickson BJ, et al. Surgical management of complex proximal humerus fractures - A systematic review of 92 studies including 4500 patients. *J Orthop Trauma*. 2015;29(1):54-59. doi:10.1097/BOT.0000000000000229
122. Jonsson E, Ekholm C, Salomonsson B, et al. Reverse total shoulder arthroplasty provides better shoulder function than hemiarthroplasty for displaced 3- and 4-part proximal humeral fractures in patients aged 70 years or older: a multicenter randomized controlled trial. *J Shoulder Elb Surg*. 2021;30(5):994-1006. doi:10.1016/j.jse.2020.10.037
123. Austin DC, Torchia MT, Cozzolino NH, Jacobowitz LE, Bell JE. Decreased Reoperations and Improved Outcomes with Reverse Total Shoulder Arthroplasty in Comparison to Hemiarthroplasty for Geriatric Proximal Humerus Fractures: A Systematic Review and Meta-Analysis. *J Orthop Trauma*. 2019;33(1):49-57. doi:10.1097/BOT.0000000000001321
124. Gallinet D, Ohl X, Decroocq L, Dib C, Valenti P, Boileau P. Is reverse total shoulder arthroplasty more effective than hemiarthroplasty for treating displaced proximal humerus fractures in older adults? A systematic review and meta-analysis. *Orthop Traumatol Surg Res*. 2018;104(6):759-766. doi:10.1016/j.otsr.2018.04.025
125. Wang J, Zhu Y, Zhang F, Chen W, Tian Y, Zhang Y. Meta-analysis suggests that reverse shoulder arthroplasty in proximal humerus fractures is a better option than hemiarthroplasty in the elderly. *Int Orthop*. 2016;40(3):531-539. doi:10.1007/s00264-015-2811-x
126. Shukla DR, McAnany S, Kim J, Overley S, Parsons BO. Hemiarthroplasty versus reverse shoulder arthroplasty for treatment of proximal humeral fractures: A meta-analysis. *J Shoulder Elb Surg*. 2016;25(2):330-340. doi:10.1016/j.jse.2015.08.030
127. Ceri L, Mondanelli N, Sangaletti R, Bottai V, Muratori F, Giannotti S. Simultaneous bilateral reverse shoulder arthroplasty for bilateral four-part fracture of the proximal humerus in an elderly patient: A case report. *Trauma Case Reports*. 2019;23(August):100242. doi:10.1016/j.tcr.2019.100242
128. Mattei L, Mortera S, Arrigoni C, Castoldi F. Anatomic shoulder arthroplasty: an update on indications,technique, results and complication rates. *joints*. 2015;3((2)):72-77.
129. Jobin CM, Galdi B, Anakwenze OA, Ahmad CS, Levine WN. Reverse shoulder arthroplasty for the management of proximal humerus fractures. *J Am Acad Orthop Surg*. 2015;23(3):190-201. doi:10.5435/JAAOS-D-13-00190
130. Chernchujit B, Prasetia R. The role of teriparatide in tuberosity healing after reverse shoulder arthroplasty in complex proximal humeral fragility fracture. Published online 2018. doi:10.1177/2309499017754104
131. Chun YM, Kim DS, Lee DH, Shin SJ. Reverse shoulder arthroplasty for four-part proximal humerus fracture in elderly patients: can a healed tuberosity improve the functional outcomes? *J Shoulder Elb Surg*. 2017;26(7):1216-1221. doi:10.1016/j.jse.2016.11.034
132. Troiano E, Peri G, Calò I, Colasanti GB, Mondanelli N, Giannotti S. A novel “7 sutures and 8 knots” surgical technique in reverse shoulder arthroplasty for proximal humeral fractures: tuberosity healing improves short-term clinical results. *J Orthop Traumatol*. 2023;24(1). doi:10.1186/S10195-023-00697-4
133. Jain NP, Mannan SS, Dharmarajan R, Rangan A. Tuberosity healing after reverse shoulder arthroplasty for complex proximal humeral fractures in elderly patients—does it improve outcomes? A systematic review and meta-analysis. *J Shoulder Elb Surg*. 2019;28(3):e78-e91. doi:10.1016/j.jse.2018.09.006
134. Boileau P, Alta TD, Decroocq L, et al. Reverse shoulder arthroplasty for acute fractures in the elderly: is it worth reattaching the tuberosities? *J Shoulder Elb Surg*. 2019;28(3):437-

444. doi:10.1016/j.jse.2018.08.025
135. He SK, Liao JP, Guo JH, Huang FG. Fracture-Dedicated Prosthesis Promotes the Healing Rate of Greater Tuberosity in Reverse Shoulder Arthroplasty: A Meta-Analysis. *Front Surg*. 2021;8(December):1-14. doi:10.3389/fsurg.2021.616104
136. Gunst S, Louboutin L, Swan J, Lustig S, Servien E, Nove-Josserand L. Does healing of both greater and lesser tuberosities improve functional outcome after reverse shoulder arthroplasty for fracture? A retrospective study of twenty-eight cases with a computed tomography scan at a minimum of one-year follow-up. *Int Orthop*. 2021;45(3):681-687. doi:10.1007/s00264-020-04928-9
137. Torchia MT, Austin DC, Cozzolino N, Jacobowitz L, Bell JE. Acute versus delayed reverse total shoulder arthroplasty for the treatment of proximal humeral fractures in the elderly population: a systematic review and meta-analysis. *J shoulder Elb Surg*. 2019;28(4):765-773. doi:10.1016/J.JSE.2018.10.004
138. Panagopoulos GN, Pugliese M, Leonidou A, et al. Acute versus delayed reverse total shoulder arthroplasty for proximal humeral fractures: a consecutive cohort study. *J Shoulder Elb Surg*. 2022;31(2):276-285. doi:10.1016/j.jse.2021.07.003
139. Livesey M, Myerson CL, Horneff JG. Reverse shoulder arthroplasty in the revision setting. *JSES Int*. 2025;9(5):1880-1885. doi:10.1016/j.jseint.2025.02.019
140. Farley KX, Wilson JM, Kumar A, et al. Prevalence of Shoulder Arthroplasty in the United States and the Increasing Burden of Revision Shoulder Arthroplasty. *JB JS open access*. 2021;6(3). doi:10.2106/JBJS.OA.20.00156
141. Padegimas EM, Maltenfort M, Lazarus MD, Ramsey ML, Williams GR, Namdari S. Future patient demand for shoulder arthroplasty by younger patients: national projections. *Clin Orthop Relat Res*. 2015;473(6):1860-1867. doi:10.1007/S11999-015-4231-Z
142. Sheth MM, Sholder D, Getz CL, Williams GR, Namdari S. Revision of failed hemiarthroplasty and anatomic total shoulder arthroplasty to reverse total shoulder arthroplasty. *J Shoulder Elb Surg*. 2019;28(6):1074-1081. doi:10.1016/j.jse.2018.10.026
143. Merolla G, Wagner E, Sperling JW, Paladini P, Fabbri E, Porcellini G. Revision of failed shoulder hemiarthroplasty to reverse total arthroplasty: analysis of 157 revision implants. *J Shoulder Elb Surg*. 2018;27(1):75-81. doi:10.1016/j.jse.2017.06.038
144. Boileau P. Complications and revision of reverse total shoulder arthroplasty. *Orthop Traumatol Surg Res*. Published online 2016. doi:10.1016/j.otsr.2015.06.031
145. Peri G, Troiano E, Colasanti GB, Mondanelli N, Giannotti S. Custom-made Glenoid Baseplate and Intra-Operative Navigation in Complex Revision Reverse Shoulder Arthroplasty: A Case Report. *J shoulder Elb Arthroplast*. 2024;8. doi:10.1177/24715492231218183
146. Hao KA, Boschert EN, O'Keefe DS, et al. Comparison of clinical outcomes of revision reverse total shoulder arthroplasty for failed primary anatomic vs. reverse shoulder arthroplasty. *JSES Int*. 2023;7(2):257-263. doi:10.1016/j.jseint.2022.11.003
147. Alentorn-Geli E, Clark NJ, Assenmacher AT, et al. What Are the Complications, Survival, and Outcomes After Revision to Reverse Shoulder Arthroplasty in Patients Older Than 80 Years? *Clin Orthop Relat Res*. 2017;475(11):2744-2751. doi:10.1007/S11999-017-5406-6
148. Boileau P, Watkinson D, Hatzidakis AM, Hovorka I. Neer Award 2005: The Grammont reverse shoulder prosthesis: Results in cuff tear arthritis, fracture sequelae, and revision arthroplasty. *J Shoulder Elb Surg*. 2006;15(5):527-540. doi:10.1016/j.jse.2006.01.003
149. Austin L, Zmistowski B, Chang ES, Williams GR. Is reverse shoulder arthroplasty a reasonable alternative for revision arthroplasty? *Clin Orthop Relat Res*. 2011;469(9):2531-2537. doi:10.1007/S11999-010-1685-X
150. Wall B, Nové-Josserand L, O'Connor DP, Edwards TB, Walch G. Reverse total shoulder

arthroplasty: a review of results according to etiology. *J Bone Joint Surg Am*. 2007;89(7):1476-1485. doi:10.2106/JBJS.F.00666
151. Black EM, Roberts SM, Siegel E, Yannopoulos P, Higgins LD, Warner JJP. Reverse shoulder arthroplasty as salvage for failed prior arthroplasty in patients 65years of age or younger. *J Shoulder Elb Surg*. 2014;23(7):1036-1042. doi:10.1016/j.jse.2014.02.019
152. Shields E, Wiater JM. Patient Outcomes After Revision of Anatomic Total Shoulder Arthroplasty to Reverse Shoulder Arthroplasty for Rotator Cuff Failure or Component Loosening: A Matched Cohort Study. *J Am Acad Orthop Surg*. 2019;27(4):E193-E198. doi:10.5435/JAAOS-D-17-00350
153. Nelson PA, Kwan CC, Tjong VK, Terry MA, Sheth U. Primary Versus Salvage Reverse Total Shoulder Arthroplasty for Displaced Proximal Humerus Fractures in the Elderly: A Systematic Review and Meta-analysis. *J shoulder Elb Arthroplast*. 2020;4. doi:10.1177/2471549220949731
154. Kokkalis ZT, Bavelou A, Papanikos E, Kalavrytinos D, Panagopoulos A. Reverse Shoulder Arthroplasty for Failed Operative Treatment of Proximal Humeral Fractures. *J shoulder Elb Arthroplast*. 2022;6. doi:10.1177/24715492221090742
155. Levy HA, Szeto S, O Starks A, Davis DE. Outcomes after salvage reverse shoulder arthroplasty for failed primary fixation or hemiarthroplasty for proximal humerus fractures: A systematic review. *Shoulder Elb*. 2023;15(3 Suppl):6-18. doi:10.1177/17585732221099200
156. Dezfuli B, King JJ, Farmer KW, Struk AM, Wright TW. Outcomes of reverse total shoulder arthroplasty as primary versus revision procedure for proximal humerus fractures. *J Shoulder Elb Surg*. 2016;25(7):1133-1137. doi:10.1016/j.jse.2015.12.002
157. Walch G, Bacle G, Lädermann A, Nové-Josserand L, Smithers CJ. Do the indications, results, and complications of reverse shoulder arthroplasty change with surgeon's experience? *J Shoulder Elb Surg*. 2012;21(11):1470-1477. doi:10.1016/j.jse.2011.11.010
158. Saltzman BM, Chalmers PN, Gupta AK, Romeo AA, Nicholson GP. Complication rates comparing primary with revision reverse total shoulder arthroplasty. *J Shoulder Elb Surg*. 2014;23(11):1647-1654. doi:10.1016/j.jse.2014.04.015
159. Wierks C, Skolasky RL, Ji JH, McFarland EG. Reverse total shoulder replacement: intraoperative and early postoperative complications. *Clin Orthop Relat Res*. 2009;467(1):225-234. doi:10.1007/S11999-008-0406-1
160. Zumstein MA, Pinedo M, Old J, Boileau P. Problems , complications , reoperations , and revisions in reverse total shoulder arthroplasty : A systematic review. *J Shoulder Elb Surg*. 2011;20(1):146-157. doi:10.1016/j.jse.2010.08.001
161. Ascione F, Domos P, Guarrella V, Chelli M, Boileau P, Walch G. Long-term humeral complications after Grammont-style reverse shoulder arthroplasty. *J Shoulder Elb Surg*. 2018;27(6):1065-1071. doi:10.1016/j.jse.2017.11.028
162. Gallo RA, Gamradt SC, Mattern CJ, et al. Instability after reverse total shoulder replacement. *J Shoulder Elb Surg*. 2011;20(4):584-590. doi:10.1016/j.jse.2010.08.028
163. Teusink MJ, Pappou IP, Schwartz DG, Cottrell BJ, Frankle MA. Results of closed management of acute dislocation after reverse shoulder arthroplasty. *J Shoulder Elb Surg*. 2015;24(4):621-627. doi:10.1016/j.jse.2014.07.015
164. Teusink MJ, Otto RJ, Cottrell BJ, Frankle MA. What is the effect of postoperative scapular fracture on outcomes of reverse shoulder arthroplasty? *J Shoulder Elb Surg*. 2014;23(6):782-790. doi:10.1016/j.jse.2013.09.010
165. Chalmers PN, Rahman Z, Romeo AA, Nicholson GP. Early dislocation after reverse total shoulder arthroplasty. *J Shoulder Elb Surg*. 2014;23(5):737-744. doi:10.1016/j.jse.2013.08.015

166. Gutiérrez S, Keller TS, Levy JC, Lee WE, Luo ZP. Hierarchy of stability factors in reverse shoulder arthroplasty. *Clin Orthop Relat Res*. 2008;466(3):670-676. doi:10.1007/S11999-007-0096-0
167. Stephenson DR, Oh JH, McGarry MH, Rick Hatch GF, Lee TQ. Effect of humeral component version on impingement in reverse total shoulder arthroplasty. *J Shoulder Elb Surg*. 2011;20(4):652-658. doi:10.1016/J.JSE.2010.08.020
168. Edwards TB, Williams MD, Labriola JE, Elkousy HA, Gartsman GM, O'Connor DP. Subscapularis insufficiency and the risk of shoulder dislocation after reverse shoulder arthroplasty. *J Shoulder Elb Surg*. 2009;18(6):892-896. doi:10.1016/j.jse.2008.12.013
169. Gerber C, Pennington SD, Nyffeler RW. Reverse total shoulder arthroplasty. *J Am Acad Orthop Surg*. 2009;17(5):284-295. doi:10.5435/00124635-200905000-00003
170. Shapiro T, McGarry M, Gupta R, Lee Y, Lee T. Biomechanical effects of glenoid retroversion in total shoulder arthroplasty. *J shoulder Elb Surg*. 2007;16(3 Suppl). doi:10.1016/J.JSE.2006.07.010
171. Gerber C, Pennington S, Nyffeler R. Reverse total shoulder arthroplasty. *J Am Acad Orthop Surg*. 2009;17(5):284-295. doi:10.5435/00124635-200905000-00003
172. Barco R, Savvidou OD, Sperling JW, Sanchez-Sotelo J, Cofield RH. Complications in reverse shoulder arthroplasty. *EFORT open Rev*. 2017;1(3):72-80. doi:10.1302/2058-5241.1.160003
173. Simovitch R, Zumstein M, Lohri E, Helmy N, Gerber C. Predictors of scapular notching in patients managed with the Delta III reverse total shoulder replacement. *J Bone Joint Surg Am*. 2007;89(3):588-600. doi:10.2106/JBJS.F.00226
174. Pereira C, Carrapatoso M, Barros LH, Claro R. Glenoid notching after reverse shoulder arthroplasty: The influence of different neck-shaft angles. *Shoulder Elb*. 2024;17(4). doi:10.1177/17585732241262524
175. Roche CP, Stroud NJ, Martin BL, et al. The impact of scapular notching on reverse shoulder glenoid fixation. *J Shoulder Elb Surg*. 2013;22(7):963-970. doi:10.1016/j.jse.2012.10.035
176. Young BL, Cantrell CK, Hamid N. Classifications in brief: The Nerot-sirveaux classification for scapular notching. *Clin Orthop Relat Res*. 2018;476(12):2454-2457. doi:10.1097/CORR.0000000000000442
177. Young BL, Cantrell CK, Hamid N. Classifications in Brief: The Nerot-Sirveaux Classification for Scapular Notching. *Clin Orthop Relat Res*. 2018;476(12):2454-2457. doi:10.1097/CORR.0000000000000442
178. Boileau P, Moineau G, Roussanne Y, O'Shea K. Bony increased-offset reversed shoulder arthroplasty: minimizing scapular impingement while maximizing glenoid fixation. *Clin Orthop Relat Res*. 2011;469(9):2558-2567. doi:10.1007/S11999-011-1775-4
179. Baulot E, Sirveaux F, Boileau P. Grammont's idea: The story of Paul Grammont's functional surgery concept and the development of the reverse principle. *Clin Orthop Relat Res*. 2011;469(9):2425-2431. doi:10.1007/S11999-010-1757-Y
180. Lädermann A, Lübbeke A, Mélis B, et al. Prevalence of neurologic lesions after total shoulder arthroplasty. *J Bone Joint Surg Am*. 2011;93(14):1288-1293. doi:10.2106/JBJS.J.00369
181. Lenoir H, Dagneaux L, Canovas F, Waitzenegger T, Pham TT, Chammas M. Nerve stress during reverse total shoulder arthroplasty: a cadaveric study. *J Shoulder Elb Surg*. 2017;26(2):323-330. doi:10.1016/j.jse.2016.07.020
182. Kennon JC, Lu C, McGee-Lawrence ME, Crosby LA. Scapula fracture incidence in reverse total shoulder arthroplasty using screws above or below metaglene central cage: clinical and biomechanical outcomes. *J Shoulder Elb Surg*. 2017;26(6):1023-1030.

doi:10.1016/j.jse.2016.10.018
183. Otto RJ, Virani NA, Levy JC, Nigro PT, Cuff DJ, Frankle MA. Scapular fractures after reverse shoulder arthroplasty: Evaluation of risk factors and the reliability of a proposed classification. *J Shoulder Elb Surg*. 2013;22(11):1514-1521. doi:10.1016/j.jse.2013.02.007
184. Familiari F, Huri G, Gonzalez-Zapata A, McFarland EG. Scapula fracture and os acromiale after reverse total shoulder arthroplasty. *Orthopedics*. 2014;37(7). doi:10.3928/01477447-20140626-01
185. Favard L, Levigne C, Nerot C, Gerber C, De Wilde L, Mole D. Reverse prostheses in arthropathies with cuff tear: are survivorship and function maintained over time? *Clin Orthop Relat Res*. 2011;469(9):2469-2475. doi:10.1007/S11999-011-1833-Y
186. Wilcox B, Campbell RJ, Low AK, Yeoh T. Management of glenoid bone loss in primary reverse shoulder arthroplasty : a systematic review and meta-analysis. *Bone Joint J*. 2022;104-B(12):1334-1342. doi:10.1302/0301-620X.104B12.BJJ-2022-0819.R1
187. Verborgt O, Vanhees M, Heylen S, Hardy P, Declercq G, Bicknell R. Computer navigation and patient-specific instrumentation in shoulder arthroplasty. *Sports Med Arthrosc*. 2014;22(4):e42-e49. doi:10.1097/JSA.0000000000000045
188. Iannotti JP, Greeson C, Downing D, Sabesan V, Bryan JA. Effect of glenoid deformity on glenoid component placement in primary shoulder arthroplasty. *J Shoulder Elb Surg*. 2012;21(1):48-55. doi:10.1016/j.jse.2011.02.011
189. Jennewine BR, Brolin TJ. Emerging Technologies in Shoulder Arthroplasty: Navigation, Mixed Reality, and Preoperative Planning. *Orthop Clin North Am*. 2023;54(2):209-225. doi:10.1016/j.ocl.2022.11.006
190. Zheng G, Nolte LP. Computer-Assisted Orthopedic Surgery : Current State and Future Perspective. 2015;2(December). doi:10.3389/fsurg.2015.00066
191. Picard F, Deakin AH, Riches PE, Deep K, Baines J. Computer Assisted Orthopaedic Surgery : Past , Present and Future : Published online 2019:55-65.
192. Hernandez D, Garimella R, Eltorai AEM, Daniels AH. Computer-Assisted Orthopaedic Surgery. 2016;(July). doi:10.1111/os.12323
193. Frankle MA, Teramoto A, Luo ZP, Levy JC, Pupello D. Glenoid morphology in reverse shoulder arthroplasty: classification and surgical implications. *J shoulder Elb Surg*. 2009;18(6):874-885. doi:10.1016/J.JSE.2009.02.013
194. Klein SM, Dunning P, Mulieri P, Pupello D, Downes K, Frankle MA. Effects of acquired glenoid bone defects on surgical technique and clinical outcomes in reverse shoulder arthroplasty. *J Bone Joint Surg Am*. 2010;92(5):1144-1154. doi:10.2106/JBJS.I.00778
195. Visotsky J, Basamania C, Seebauer L, Rockwood C, Jensen K. Cuff tear arthropathy: pathogenesis, classification, and algorithm for treatment. *J Bone Jt Surg Am*. 2004;86-A Suppl:35-40.
196. Friedman R, Hawthorne K, Genez B. The use of computerized tomography in the measurement of glenoid version. *J Bone Jt Surg Am*. 1992;Aug;74(7):1032-1037.
197. Gauci MO. Patient-specific guides in orthopedic surgery. *Orthop Traumatol Surg Res*. 2022;108(1). doi:10.1016/j.otsr.2021.103154
198. Moreschini F, Colasanti GB, Cataldi C, Mannelli L, Mondanelli N, Giannotti S. Pre-Operative CT-Based Planning Integrated With Intra-Operative Navigation in Reverse Shoulder Arthroplasty: Data Acquisition and Analysis Protocol, and Preliminary Results of Navigated Versus Conventional Surgery. *Dose-Response*. 2020;18(4):1-11. doi:10.1177/1559325820970832
199. Colasanti GB, Moreschini F, Cataldi C, Mondanelli N, Giannotti S. GPS guided reverse shoulder arthroplasty: An anatomic dissection study. *Acta Biomed*. 2020;91:204-208. doi:10.23750/abm.v91i4-S.9377

200. Gauci MO, Deransart P, Chaoui J, et al. Three-dimensional geometry of the normal shoulder: a software analysis. *J Shoulder Elb Surg*. 2020;29(12):e468-e477. doi:10.1016/j.jse.2020.03.042
201. Bercik MJ, Kruse K, Yalizis M, Gauci MO, Chaoui J, Walch G. A modification to the Walch classification of the glenoid in primary glenohumeral osteoarthritis using three-dimensional imaging. *J Shoulder Elb Surg*. 2016;25(10):1601-1606. doi:10.1016/j.jse.2016.03.010
202. Boileau P, Morin-Salvo N, Gauci MO, et al. Angled BIO-RSA (bony-increased offset–reverse shoulder arthroplasty): a solution for the management of glenoid bone loss and erosion. *J Shoulder Elb Surg*. 2017;26(12):2133-2142. doi:10.1016/j.jse.2017.05.024
203. Donohue KW, Ricchetti ET, Iannotti JP. Surgical management of the biconcave (B2) glenoid. *Curr Rev Musculoskelet Med*. 2016;9(1):30-39. doi:10.1007/S12178-016-9315-1
204. Hsu JE, Ricchetti ET, Huffman GR, Iannotti JP, Glaser DL. Addressing glenoid bone deficiency and asymmetric posterior erosion in shoulder arthroplasty. *J shoulder Elb Surg*. 2013;22(9):1298-1308. doi:10.1016/J.JSE.2013.04.014
205. Sabesan V, Callanan M, Sharma V, Iannotti JP. Correction of acquired glenoid bone loss in osteoarthritis with a standard versus an augmented glenoid component. *J Shoulder Elb Surg*. 2014;23(7):964-973. doi:10.1016/j.jse.2013.09.019
206. Brown CL, Marcaccio S, Mullen JP, et al. Patient Specific Instrumentation in Shoulder Arthroplasty. *Oper Tech Orthop*. 2024;34(4):101152. doi:10.1016/J.OTO.2024.101152
207. Kida H, Momma D, Urita A, et al. PSI and navigation system improve consistency of baseplate placement in reverse shoulder arthroplasty regardless of surgical experience. *J Shoulder Elb Surg*. Published online 2025. doi:10.1016/j.jse.2025.06.022
208. Lee DH, Choi YS, Potter HG, et al. Reverse total shoulder arthroplasty: an imaging overview. *Skeletal Radiol*. 2020;49(1):19-30. doi:10.1007/s00256-019-03275-0
209. Kozak T, Bauer S, Walch G, Al-karawi S, Blakeney W. An update on reverse total shoulder arthroplasty: current indications, new designs, same old problems. *EFORT Open Rev*. 2021;6(3):189-201. doi:10.1302/2058-5241.6.200085
210. Wang AW, Hayes A, Gibbons R, Mackie KE. Computer navigation of the glenoid component in reverse total shoulder arthroplasty: a clinical trial to evaluate the learning curve. *J Shoulder Elb Surg*. 2020;29(3):617-623. doi:10.1016/j.jse.2019.08.012
211. Burns DM, Frank T, Whyne CM, Henry PDG. Glenoid component positioning and guidance techniques in anatomic and reverse total shoulder arthroplasty: A systematic review and meta-analysis. *Shoulder Elb*. 2019;11(2_suppl):16-28. doi:10.1177/1758573218806252
212. Jones RB, Greene AT, Polakovic S V., et al. Accuracy and precision of placement of the glenoid baseplate in reverse total shoulder arthroplasty using a novel computer assisted navigation system combined with preoperative planning: A controlled cadaveric study. *Semin Arthroplast JSES*. 2020;30(1):73-82. doi:10.1053/j.sart.2020.05.004
213. Longo UG, Lalli A, Gobbato B, Nazarian A. Metaverse, virtual reality and augmented reality in total shoulder arthroplasty: a systematic review. *BMC Musculoskelet Disord*. 2024;25(1). doi:10.1186/S12891-024-07436-8
214. Daher M, Ghanimeh J, Otayek J, Ghoul A, Bizdikian AJ, EL Abiad R. Augmented reality and shoulder replacement: a state-of-the-art review article. *JSES Rev Reports, Tech*. 2023;3(3):274-278. doi:10.1016/j.xrrt.2023.01.008
215. Dey Hazra RO, Paksoy A, Imiolczyk JP, Gebauer H, Hayta A, Akgun D. Augmented reality–assisted intraoperative navigation increases precision of glenoid inclination in reverse shoulder arthroplasty. *J Shoulder Elb Surg*. 2025;34(2):577-583. doi:10.1016/j.jse.2024.05.039
216. Mccarthy J. IA-What is artificial intelligence? *Stanford Univ*. Published online 2007:1-15.

http://www-formal.stanford.edu/jmc/
217. Kim HG, Kim SC, Park JH, Kim JS, Kim DY, Yoo JC. Artificial intelligence in shoulder arthroplasty: how smart is it? *JSES Int*. 2025;9(3):988-993. doi:10.1016/J.JSEINT.2024.07.002
218. Maffulli N, Rodriguez HC, Stone IW, et al. Artificial intelligence and machine learning in orthopedic surgery : a systematic review protocol. Published online 2020:1-5.
219. Peng X, Tan F, Hu Y, Pu H, Zou W, Qu C. Artificial intelligence in joint arthroplasty: A bibliometric analysis of global research trends (2001-2025). *Medicine (Baltimore)*. 2025;104(35):e44136. doi:10.1097/MD.0000000000044136
220. Makhni EC, Makhni S, Ramkumar PN. Artificial Intelligence for the Orthopaedic Surgeon: An Overview of Potential Benefits, Limitations, and Clinical Applications. *J Am Acad Orthop Surg*. 2021;29(6):235-243. doi:10.5435/JAAOS-D-20-00846
221. Ramkumar PN, Kunze KN, Haeberle HS, et al. Clinical and Research Medical Applications of Artificial Intelligence. *Arthrosc - J Arthrosc Relat Surg*. 2021;37(5):1694-1697. doi:10.1016/j.arthro.2020.08.009
222. Obermeyer Z, Emanuel EJ. Predicting the Future - Big Data, Machine Learning, and Clinical Medicine. *N Engl J Med*. 2016;375(13):1216-1219. doi:10.1056/NEJMP1606181
223. Schneller T, Kraus M, Schätz J, Moroder P, Scheibel M, Lazaridou A. Machine learning in shoulder arthroplasty: a systematic review of predictive analytics applications. *Bone Jt Open*. 2025;6(2):126. doi:10.1302/2633-1462.62.BJO-2024-0234.R1
224. Yang M, Jun BJ, Owings T, et al. Automated 3D segmentation of rotator cuff muscle and fat from longitudinal CT for shoulder arthroplasty evaluation. *Skeletal Radiol*. 2026;55(1):131-141. doi:10.1007/S00256-025-04991-6
225. Levin JM, Lorentz SG, Hurley ET, et al. Artificial intelligence in shoulder and elbow surgery: overview of current and future applications. *J Shoulder Elb Surg*. 2024;33(7):1633-1641. doi:10.1016/J.JSE.2024.01.033
226. Kumar V, Roche C, Overman S, et al. Using machine learning to predict clinical outcomes after shoulder arthroplasty with a minimal feature set. *J Shoulder Elb Surg*. 2021;30(5):e225-e236. doi:10.1016/j.jse.2020.07.042
227. Karimi AH, Langberg J, Malige A, Rahman O, Abboud JA, Stone MA. Accuracy of machine learning to predict the outcomes of shoulder arthroplasty: a systematic review. *Arthroplast 2024 61*. 2024;6(1):26-. doi:10.1186/S42836-024-00244-4
228. Gupta P, Haeberle HS, Zimmer ZR, Levine WN, Williams RJ, Ramkumar PN. Artificial intelligence-based applications in shoulder surgery leaves much to be desired: a systematic review. *JSES Rev Reports, Tech*. 2023;3(2):189-200. doi:10.1016/j.xrrt.2022.12.006
229. Baumgarten KM. Accuracy of Blueprint software in predicting range of motion 1 year after reverse total shoulder arthroplasty. *J Shoulder Elb Surg*. 2023;32(5):1088-1094. doi:10.1016/j.jse.2022.12.009
230. Michener LA, McClure PW, Sennett BJ. American Shoulder and Elbow Surgeons Standardized Shoulder Assessment Form, patient self-report section: Reliability, validity, and responsiveness. *J Shoulder Elb Surg*. 2002;11(6):587-594. doi:10.1067/mse.2002.127096
231. Constant CR, Gerber C, Emery RJH, Søjbjerg JO, Gohlke F, Boileau P. A review of the Constant score: Modifications and guidelines for its use. *J Shoulder Elb Surg*. 2008;17(2):355-361. doi:10.1016/j.jse.2007.06.022
232. Rudin C. Stop Explaining Black Box Machine Learning Models for High Stakes Decisions and Use Interpretable Models Instead. *Nat Mach Intell*. 2019;1(5):206. doi:10.1038/S42256-019-0048-X

233. Mehta N, Nicholson GP. Management of Glenoid Bone Loss in Primary Reverse Total Shoulder Arthroplasty. *Curr Rev Musculoskelet Med*. 2023;16(8):358. doi:10.1007/S12178-023-09845-Z
234. Walch G, Badet R, Boulahia A, Khoury A. Morphologic study of the glenoid in primary glenohumeral osteoarthritis. *J Arthroplasty*. 1999;14(6):756-760. doi:10.1016/S0883-5403(99)90232-2
235. Kandemir U, Allaire RB, Jolly JT, Debski RE, McMahon PJ. The relationship between the orientation of the glenoid and tears of the rotator cuff. *J Bone Joint Surg Br*. 2006;88(8):1105-1109. doi:10.1302/0301-620X.88B8.17732
236. Hughes RE, Bryant CR, Hall JM, et al. Glenoid inclination is associated with full-thickness rotator cuff tears. *Clin Orthop Relat Res*. 2003;407(407):86-91. doi:10.1097/00003086-200302000-00016
237. TM. Gregory, A. Sankey, B. Augereau, E. Vandenbussche, A. Amis, R. Emery UH. Accuracy of glenoid component placement in total shoulder arthroplasty and its effect on clinical and radiological outcome in a retrospective, longitudinal, monocentric open study. *PLoS One*. 2013;8(10). doi:10.1371/JOURNAL.PONE.0075791
238. Iannotti JP, Jun BJ, Patterson TE, Ricchetti ET. Quantitative Measurement of Osseous Pathology in Advanced Glenohumeral Osteoarthritis. *J Bone Joint Surg Am*. 2017;99(17):1460-1468. doi:10.2106/JBJS.16.00869
239. Caprili G, Calamita AG, Novi M, Campanacci DA, Nicoletti S. Assessing the accuracy of a machine learning prediction for 2 different shoulder prostheses: an external validation study. *JSES Int*. 2025;9(4):1352-1356. doi:10.1016/j.jseint.2025.04.024
240. Puckett CD, Gwilt MS, Collon KW, Waterman BR. Baseplate coverage in reverse total shoulder arthroplasty: a systematic review. *JSES Rev Reports, Tech*. 2025;5(3):460-468. doi:10.1016/j.xrrt.2025.02.010
241. Kumar V, Roche C, Overman S, et al. What Is the Accuracy of Three Different Machine Learning Techniques to Predict Clinical Outcomes After Shoulder Arthroplasty? *Clin Orthop Relat Res*. 2020;478(10):2351-2363. doi:10.1097/CORR.0000000000001263
242. Parsons M, Greene A, Polakovic S, et al. Intersurgeon and intrasurgeon variability in preoperative planning of anatomic total shoulder arthroplasty: a quantitative comparison of 49 cases planned by 9 surgeons. *J Shoulder Elb Surg*. 2020;29(12):2610-2618. doi:10.1016/j.jse.2020.04.010
243. da Rocha Motta Filho G, Amaral MVG, Nascimento LGP, et al. Assessment of Inter- and Intrasurgeon Variability in Preoperative Planning of Reverse Shoulder Arthroplasty: A Multicenter Evaluation. *Rev Bras Ortop*. 2024;59(6):e950-e957. doi:10.1055/S-0044-1788783
244. Varady NH, Bram JT, Chow J, et al. Inconsistencies in measuring glenoid version in shoulder arthroplasty: a systematic review. *J Shoulder Elb Surg*. 2025;34(2):639-649. doi:10.1016/j.jse.2024.08.020
245. Reid JJ, Kunkle BF, Greene AT, Eichinger JK, Friedman RJ. Variability and reliability of 2-dimensional vs. 3-dimensional glenoid version measurements with 3-dimensional preoperative planning software. *J Shoulder Elb Surg*. 2022;31(2):302-309. doi:10.1016/j.jse.2021.07.011
246. Tashjian RZ, Hung M, Keener JD, et al. Determining the minimal clinically important difference for the American Shoulder and Elbow Surgeons score, Simple Shoulder Test, and visual analog scale (VAS) measuring pain after shoulder arthroplasty. *J shoulder Elb Surg*. 2017;26(1):144-148. doi:10.1016/J.JSE.2016.06.007
247. Simovitch R, Flurin PH, Wright T, Zuckerman JD, Roche CP. Quantifying success after total shoulder arthroplasty: the minimal clinically important difference. *J Shoulder Elb*

Surg. 2018;27(2):298-305. doi:10.1016/j.jse.2017.09.013
248. Simovitch RW, Elwell J, Colasanti CA, et al. Stratification of the minimal clinically important difference, substantial clinical benefit, and patient acceptable symptomatic state after total shoulder arthroplasty by implant type, preoperative diagnosis, and sex. *J Shoulder Elb Surg*. 2024;33(9):e492-e506. doi:10.1016/j.jse.2024.01.040
249. Aleem AW, Chamberlain AM, Keener JD. The functional internal rotation scale: a novel shoulder arthroplasty outcome measure. *JSES Int*. 2020;4(1):202-206. doi:10.1016/j.jses.2019.10.002
250. Mclendon PB, Christmas KN, Simon P, et al. Machine Learning Can Predict Level of Improvement in Shoulder Arthroplasty. *JBJS Open Access*. 2021;6(1):e20.00128. doi:10.2106/JBJS.OA.20.00128
251. Walker D, Matsuki K, Struk AM, Wright TW, Banks SA. Scapulohumeral rhythm in shoulders with reverse shoulder arthroplasty. *J Shoulder Elb Surg*. 2015;24(7):1129-1134. doi:10.1016/j.jse.2014.11.043
252. Codsi MJ, Iannotti JP. The effect of screw position on the initial fixation of a reverse total shoulder prosthesis in a glenoid with a cavitary bone defect. *J Shoulder Elb Surg*. 2008;17(3):479-486. doi:10.1016/j.jse.2007.09.002
253. Harman M, Frankle M, Vasey M, Banks S. Initial glenoid component fixation in “reverse” total shoulder arthroplasty: a biomechanical evaluation. *J shoulder Elb Surg*. 2005;14(1 Suppl S):S162-S167. doi:10.1016/J.JSE.2004.09.030
254. Hoenig MP, Loeffler B, Brown S, et al. Reverse glenoid component fixation: Is a posterior screw necessary? *J Shoulder Elb Surg*. 2010;19(4):544-549. doi:10.1016/j.jse.2009.10.006
255. Dharia MA, Bischoff JE, Schneider D. Impact of Modeling Assumptions on Stability Predictions in Reverse Total Shoulder Arthroplasty. *Front Physiol*. 2018;9(AUG). doi:10.3389/FPHYS.2018.01116
256. Roche C, DiGeorgio C, Yegres J, et al. Impact of screw length and screw quantity on reverse total shoulder arthroplasty glenoid fixation for 2 different sizes of glenoid baseplates. *JSES Open Access*. 2019;3(4):296-303. doi:10.1016/j.jses.2019.08.006
257. James J, Allison MA, Werner FW, et al. Reverse shoulder arthroplasty glenoid fixation: Is there a benefit in using four instead of two screws? *J Shoulder Elb Surg*. 2013;22(8):1030-1036. doi:10.1016/j.jse.2012.11.006
258. Lung TS, Cruickshank D, Grant HJ, Rainbow MJ, Bryant TJ, Bicknell RT. Factors contributing to glenoid baseplate micromotion in reverse shoulder arthroplasty: a biomechanical study. *J shoulder Elb Surg*. 2019;28(4):648-653. doi:10.1016/J.JSE.2018.09.012
259. Oh JH, Jeong HJ, Won YS. Implant selection for successful reverse total shoulder arthroplasty. *Clin shoulder Elb*. 2023;26(1):93-106. doi:10.5397/CISE.2022.01193
260. Saraglis G, Singh H, Charfare Z, et al. Mid-term Results Following Reverse Shoulder Arthroplasty and the Role of Navigation in the Management of Glenoid Bone Loss. *Cureus*. 2024;16(2). doi:10.7759/CUREUS.54633
261. Kida H, Urita A, Momma D, et al. Implications of navigation system use for glenoid component placement in reverse shoulder arthroplasty. *Sci Rep*. 2022;12(1):1-9. doi:10.1038/s41598-022-25833-8
262. Velasquez Garcia A, Abdo G. Does computer-assisted navigation improve baseplate screw configuration in reverse shoulder arthroplasty? A systematic review and meta-analysis of comparative studies. *J Orthop*. 2022;36:29-35. doi:10.1016/J.JOR.2022.12.008
263. Gaj E, Pagnotta SM, Berlinberg EJ, et al. Intraoperative navigation system use increases accuracy of glenoid component inclination but not functional outcomes in reverse total shoulder arthroplasty: a prospective comparative study. *Arch Orthop Trauma Surg*.

2024;144(1):91-102. doi:10.1007/S00402-023-05038-Y
264. Nashikkar PS, Scholes CJ, Haber MD. Role of intraoperative navigation in the fixation of the glenoid component in reverse total shoulder arthroplasty: a clinical case-control study. *J Shoulder Elb Surg*. 2019;28(9):1685-1691. doi:10.1016/j.jse.2019.03.013
265. Hones KM, King JJ, Schoch BS, Struk AM, Farmer KW, Wright TW. The in vivo impact of computer navigation on screw number and length in reverse total shoulder arthroplasty. *J Shoulder Elb Surg*. 2021;30(10):e629-e635. doi:10.1016/j.jse.2021.01.017
266. Iannotti JP, Jun BJ, Patterson TE, Ricchetti ET. Quantitative Measurement of Osseous Pathology in Advanced Glenohumeral Osteoarthritis. *J Bone Joint Surg Am*. 2017;99(17):1460-1468. doi:10.2106/JBJS.16.00869
267. De Falco L, Troiano E, Cesari M, et al. Intra-operative local plus systemic tranexamic acid significantly decreases post-operative bleeding and the need for allogeneic blood transfusion in total knee arthroplasty. *Med Glas (Zenica)*. 2021;18(1):1-6. doi:10.17392/1327-21
268. Katolik LI, Romeo AA, Cole BJ, Verma NN, Hayden JK, Bach BR. Normalization of the Constant score. *J Shoulder Elb Surg*. 2005;14(3):279-285. doi:10.1016/j.jse.2004.10.009
269. Fabre T, Piton C, Leclouerec G, Gervais-Delion F, Durandeau A. Entrapment of the suprascapular nerve. *J Bone Joint Surg Br*. 1999;81(3):414-419. doi:10.1302/0301-620X.81B3.9113
270. Gummesson C., Ward MM AI. The shortened disabilities of the arm, shoulder and hand questionnaire (QuickDASH): validity and reliability based on responses within the full-length DASH. *BMC Musculoskelet Disord*. 2006;7. doi:10.1186/1471-2474-7-44
271. Rockwood Jr C, Jensen K. X-ray evaluation of shoulder problems. In: *Rockwood Jr CA, Matsen III FA, Wirth MA, Harryman DT, Eds. The Shoulder. 2nd Ed. Philadelphia: WB Saunders; 1998:199-231.*
272. Tashjian RZ, Beck L, Stertz I, Chalmers PN. Preoperative three-dimensional computer planning for reverse total shoulder arthroplasty and bone grafting for severe glenoid deformity. *Shoulder Elb*. 2021;13(5):492-501. doi:10.1177/1758573220908903
273. Guareschi AS, Gannon ST, Welsh ME, et al. Outcomes following humeral head autograft glenoid reconstruction in primary reverse total shoulder arthroplasty. *J shoulder Elb Surg*. 2025;34(4). doi:10.1016/J.JSE.2024.06.031
274. Merolla G, Giorgini A, Bonfatti R, et al. BIO-RSA vs. metal-augmented baseplate in shoulder osteoarthritis with multiplanar glenoid deformity: a comparative study of radiographic findings and patient outcomes. *J shoulder Elb Surg*. 2023;32(11):2264-2275. doi:10.1016/J.JSE.2023.04.028
275. Pastor MF, Kieckbusch M, Kaufmann M, Ettinger M, Wellmann M, Smith T. Reverse shoulder arthroplasty for fracture sequelae: Clinical outcome and prognostic factors. *J Orthop Sci*. 2019;24(2):237-242. doi:10.1016/j.jos.2018.09.016
276. Baker HP, Gutbrod J, Cahill M, Shi L. Optimal Treatment of Proximal Humeral Fractures in the Elderly: Risks and Management Challenges. *Orthop Res Rev*. 2023;15(June):129-137. doi:10.2147/ORR.S340536
277. Sasanuma H, Iijima Y, Saito T, et al. Clinical results of reverse shoulder arthroplasty for comminuted proximal humerus fractures in elderly patients: a comparison between nonporous stems versus trabecular metal stems. *JSES Int*. 2020;4(4):952-958. doi:10.1016/j.jseint.2020.08.010
278. Morea V, Polizzi A, Niccoli G, Zattoni G, Andriollo L. Reverse Shoulder Megaprosthesis for Massive Proximal Humeral Bone Loss in Fracture Outcome Settings: A Report of Two Cases and Literature Review. *Cureus*. 2024;16(2). doi:10.7759/CUREUS.54276
279. Holzgrefe RE, Hao KA, Panther EJ, et al. Early clinical outcomes following navigation-

assisted baseplate fixation in reverse total shoulder arthroplasty: a matched cohort study. *J Shoulder Elb Surg*. Published online 2022. doi:10.1016/j.jse.2022.07.007

280. Boufadel P, Lopez R, Fares MY, et al. Intraoperative Navigation in Reverse Shoulder Arthroplasty: Advantages and Future Prospects. *Clin Orthop Surg*. 2024;16(5). doi:10.4055/CIOS23407
281. Giorgini A, Tarallo L, Novi M, Porcellini G. Computer-Assisted Surgery in Reverse Shoulder Arthroplasty: Early Experience. *Indian J Orthop*. 2021;55(4):1003-1008. doi:10.1007/s43465-020-00344-8
282. Sprowls GR, Wilson CD, Stewart W, et al. Intraoperative navigation and preoperative templating software are associated with increased glenoid baseplate screw length and use of augmented baseplates in reverse total shoulder arthroplasty. *JSES Int*. 2020;5(1):102-108. doi:10.1016/J.JSEINT.2020.09.003
283. Velasquez Garcia A, Abdo G, Sanchez-Sotelo J, Morrey ME. The Value of Computer-Assisted Navigation for Glenoid Baseplate Implantation in Reverse Shoulder Arthroplasty: A Systematic Review and Meta-Analysis. *JBJS Rev*. 2023;11(8). doi:10.2106/JBJS.RVW.23.00038
284. Rosenthal Y, Rettig SA, Virk MS, Zuckerman JD. Impact of preoperative 3-dimensional planning and intraoperative navigation of shoulder arthroplasty on implant selection and operative time: a single surgeon's experience. *J shoulder Elb Surg*. 2020;29(12):2564-2570. doi:10.1016/J.JSE.2020.03.041
285. Youderian AR, Greene AT, Polakovic S V., et al. Two-year clinical outcomes and complication rates in anatomic and reverse shoulder arthroplasty implanted with Exactech GPS intraoperative navigation. *J shoulder Elb Surg*. 2023;32(12):2519-2532. doi:10.1016/J.JSE.2023.05.021